BAW-10146
October 1980

DETERMINATION OF MINIMUM REQUIRED TUBE WALL THICKNESS FOR 177-FA ONCE-THROUGH STEAM GENERATORS

BABCOCK & WILCOX
Nuclear Power Group
Nuclear Power Generation Division
P. O. Box 1260
Lynchburg, Virginia 24505

Babcock & Wilcox

Babcock & Wilcox
Nuclear Power Group
Nuclear Power Generation Division
Lynchburg, Virginia

Report BAW-10146

October 1980

Determination of Minimum Required Tube Wall Thickness for 177-FA Once-Through Steam Generators

Key Words: Steam Generator Tubes, Tube Plugging Criteria, Reg. Guide 1.121

ABSTRACT

This report describes the analytical and experimental justification for establishing a minimum acceptable steam generator tube wall thickness for B&W 177-FA nuclear steam systems (NSS) in accordance with the guidelines in NRC draft Regulatory Guide 1.121, "Bases for Plugging Degraded PWR Steam Generator Tubes." The experimental justification is based on axial pull, burst, and collapse tests performed by B&W and Battelle Pacific Northwest Laboratories. Degradation allowances (defect growth rates and NDT measurement error) and crack sizes to meet technical specification leakage limits are also covered by the draft Regulatory Guide but are not addressed as a part of this report.

The results of this program indicate that a wall thickness of 0.0116 inch meets the minimum requirements of the NRC draft Regulatory Guide 1.121. This is equivalent to a 69% through-wall defect, which must be reduced by the degradation allowance in order to establish the plugging criteria. To preclude crack propagation due to flow-induced vibration and to minimize the possibility of primary-to-secondary leakage, it is recommended that any lane tube with a detectable circumferential crack in the upper span be removed from service.

CONTENTS

CONTENTS (Cont'd)

List of Tables

Tables (Cont'd)

List of Figures

Figures (Cont'd)

1. EXECUTIVE SUMMARY

This report includes the analytical and experimental justification for establishing a minimum acceptable steam generator tube wall thickness for B&W 177-FA nuclear steam systems (NSS) in accordance with the guidelines in NRC draft Regulatory Guide 1.121. Degradation allowances (defect growth rates and NDT measurement error) and crack sizes to meet Technical Specification leakage limits are also covered by the draft Reg. Guide but are not addressed in this report. This report is applicable to the following B&W 177-FA plants:

Utility	Plant
Duke Power Company	Oconee Units 1, 2, and 3
General Public Utilities	Three Mile Island Units 1 and 2
Arkansas Power & Light Company	Arkansas Nuclear One, Unit 1
Sacramento Municipal Utility District	Rancho Seco
Florida Power Corporation	Crystal River Unit 3
Consumers Power Company	Midland Nuclear Units 1 and 2
Toledo Edison Company	Davis-Besse Unit 1

An initial step in establishing a minimum required wall thickness was characterizing the types of degradation that have been experienced in B&W operating plants. Four types of OD tube damage (with more than superficial wall thinning) have been identified:

1. Circumferential cracks in lane tubes (i.e., tubes adjacent to the untubed inspection lane) at the upper tubesheet (UTS) and the 15th tube support plate (TSP).
2. Localized metal removal (commonly referred to as erosion/corrosion), primarily at the 14th TSP but also at other TSP locations in the upper half of the OTSG.
3. Localized wear in lane tubes at the 15th TSP caused by tube/TSP contact.
4. Manufacturing defects not related to operating service.

Degradation types 1, 2, and 3 have been detected at some but not all B&W plants. Circumferential cracks at the UTS and the 15th TSP have been found only in lane tubes at the ANO-1 and Oconee sites. Wear at the 15th TSP has been reported only in lane tubes at Rancho Seco, TMI-1, and Oconee. The 14th TSP erosion/corrosion type defects have been isolated in the Oconee 1 generators. Manufacturing defects have been confirmed to exist in the TMI-2 OTSGs. Indications between tube support plates have been reported in other units and are thought to be manufacturing defects.

All failures due to circumferential cracking have been confined to lane tubes. Destructive examinations of tube samples from the Oconee plants have revealed that circumferential cracks develop on the tube OD, proceed through the wall, and then propagate symmetrically around the tube. These examinations further indicated that after development of the through-wall crack, the circumferential crack propagation was due to low-stress, high-cycle fatigue. The most probable high-cycle fatigue mechanism is flow-induced vibration (FIV). If a crack large enough for FIV propagation should occur, a primary-to-secondary leak would probably develop rather quickly. Therefore, any lane tube with a detectable circumferential crack in the upper span (i.e., between the 15th TSP and the UTS) should be removed from service.

Investigators have examined three tubes from Oconee 1 which contain the 14th TSP erosion/corrosion type defects. Damaged areas are enveloped by an area approximately 0.75 inch long and 45° around the tube. All wear marks have the approximate dimensions of TSP land areas, 1.5 inches long and 22° around the circumference. Various shapes and sizes of manufacturing defects have been discovered, including tube mill "scab" defects and shallow "grind" marks. All examined erosion/corrosion, wear/fretting and manufacturing defects are bounded by an area 1.5 inches long and 45° around the tube circumference.

Tube loadings were calculated for normal operating and faulted conditions. The faulted conditions considered were a safe shutdown earthquake (SSE) in combination with either a loss of coolant accident (LOCA), a main steam line break (MSLB), or a feedwater line break (FWLB). These loadings were used in conjunction with the postulated bounding defect area (1.5 in. by 45°) to determine the minimum acceptable wall thicknesses for degraded tubes in accordance with the guidelines of NRC draft Reg. Guide 1.121 and Section III of the ASME Code. Appendix F of the ASME Code, which establishes the Code

acceptance criteria for faulted conditions, prescribes stress limits only for primary stresses; therefore, an additional limit was developed to ensure that a tensile failure would not be caused by differential thermal expansion (secondary stresses) between the tubes and shell during an accident condition. This limit was based on B&W tensile tests in which tubes with machined defects were pulled to failure.

Minimum wall thicknesses were calculated for a total of eight different acceptance criteria. The results of these calculations are summarized in Table 1-1. The limiting criterion is the requirement that primary membrane stresses be limited to 70% of the material's ultimate stress during accident conditions. For the postulated bounding defect, this limit results in a required wall thickness of 0.0116 inch or 31% of a nominal 0.0375-inch tube wall; therefore, the maximum allowable defect size is 69%.

While the 69% limit is conservative for manufacturing defects, these defects are inherently of a different nature than the actively growing defects. They can be characterized from eddy-current data as relatively small, with no similar defects in the area, not at a location examined previously and found to be "clean," and away from support plates and known areas of tube degradation. It is judged that these indications can be safely excluded from normal Technical Specification requirements and that a 69% plugging criterion is conservatively applicable to this type of indication.

The primary conclusions resulting from this program are summarized as follows:

1. Any lane tube with a detectable circumferential crack in the upper span should be removed from service due to the growth mechanism of this type of defect.
2. For all other identified defects, limiting the defect depths to 69% of the tube wall thickness meets the requirements of draft Reg. Guide 1.121 and the ASME Code. This depth does not include an allowance for defect growth rate nor inspection technique inaccuracies.
3. A 69% plugging limit is conservatively applicable for manufacturing defects.

Table 1-1. Allowable Depths for OTSG Defects

Criterion	Minimum thickness, in.	Defect depth, % of wall in 0.0375-in. tube	Critical accident condition
Normal Operation			
$P_m \leq S_y$	0.0114	70	--
$3\Delta p \leq P_b$	0.0103	73	--
$\left\{\begin{array}{l}\Delta(P_m + P_b + Q) \leq 3S_m \\ \text{usage factor} \leq 1.0\end{array}\right\}$	<0.0079	>79	--
Faulted Conditions			
$P_m \leq 2.4S_m,\ 0.7S_u$	0.0116	69	FWLB
$\Delta p \leq P_b$	0.0046	88	FWLB
$\Delta p \leq 0.9p_c$	<0.0050	>85	LOCA
$P_m + P_b \leq 3.6S_m$	<0.0079	>79	FWLB + SSE
Primary Plus Thermal			
$\left(\frac{\Delta p}{P_b}\right)^2 + \left(\frac{P_{ax}}{P_u}\right)^2 \leq 1$	<0.0114	>70	MSLB

Note: See section 6 for discussion of criteria and minimum wall thickness calculations. Nomenclature not specifically defined in section 6 is taken from the ASME Boiler and Pressure Vessel Code.

2. INTRODUCTION

This report includes the analytical and experimental justification for th establishment of a minimum acceptable steam generator tube wall thickne for B&W 177-fuel assembly nuclear steam systems (NSS) in accordance with the guidelines in NRC draft Regulatory Guide 1.121. The expe imental justification is based on axial, burst, and collapse tests performed by B&W and the Battelle Pacific Northwest Laboratories. Degradation allowances (defect growth rates and NDT measurement error) and crack sizes to meet Technical Specification leakage limits are also covered by the draft Reg. Guide but are not addressed in this report.

2.1. Description of B&W 177-FA Once-Through Steam Generator

The B&W 177-FA utilizes two once-through steam generators (OTSGs). Each unit is a straight-tube, straight-shell heat exchanger as shown in Figure 2-1. Heated reactor coolant enters each OTSG through a single 36-inch-ID vertical nozzle in the upper head, flows downward through more than 15,000 tubes 0.625 inch in OD, transfers heat to the secondary water, and exits through two 28-inch-ID outlet nozzles in the lower head. The tubes are arranged in a triangular pattern distributed over the entire cross section of the OTSG. In the 177-FA OTSGs, half of row 76 was left untubed and is referred to as the "open tube lane" (see Figure 2-2).

On the secondary side, feedwater enters a 14-inch-ID toroidal header and is distributed through 32 nozzles, which spray the water downward into an annular feedwater heating chamber between the lower shroud and shell. The feedwater is heated to saturation by direct contact condensation of steam aspirated from the tube bundle through bleed ports in the shroud. The saturated feedwater flows downward in the annulus, entering the tube bundle through ports in the lower shroud. The water begins to boil immediately as it flows upward, becoming saturated steam and then superheated steam before exiting the tube bundle in the upper tube span, which is located between the

15th TSP and the UTS. The superheated steam is routed downward in the annulus between the upper shroud and the shell, finally exiting through two 24-inch-ID steam outlet nozzles.

2.2. Reactor Coolant System Loop Arrangement

The loop arrangement for all of the 177-FA plants except Davis-Besse 1 is shown in Figure 2-3. In this arrangement, the elevation of the bottom of the OTSG is lower than that of the reactor vessel. In the loop arrangement for the Toledo Edison Company's (TECO) Davis-Besse Unit 1, the OTSGs are elevated relative to the reactor vessel as shown in Figure 2-4. Since the OTSGs are of the same design in both loop arrangements, this report includes consideration of all plants listed below.

2.3. Applicability

This report is applicable to the following B&W 177-FA plants:

Utility	Plant
Duke Power Company	Oconee Units 1, 2, and 3
General Public Utilities	Three Mile Island Units 1 and 2
Arkansas Power & Light Company	Arkansas Nuclear One, Unit 1
Sacramento Municipal Utility District	Rancho Seco
Florida Power Corporation	Crystal River Unit 3
Consumers Power Company	Midland Nuclear Units 1 and 2
Toledo Edison Company	Davis-Besse Unit 1

Figure 2-1. B&W's 177-FA Nuclear Once-Through Steam Generator

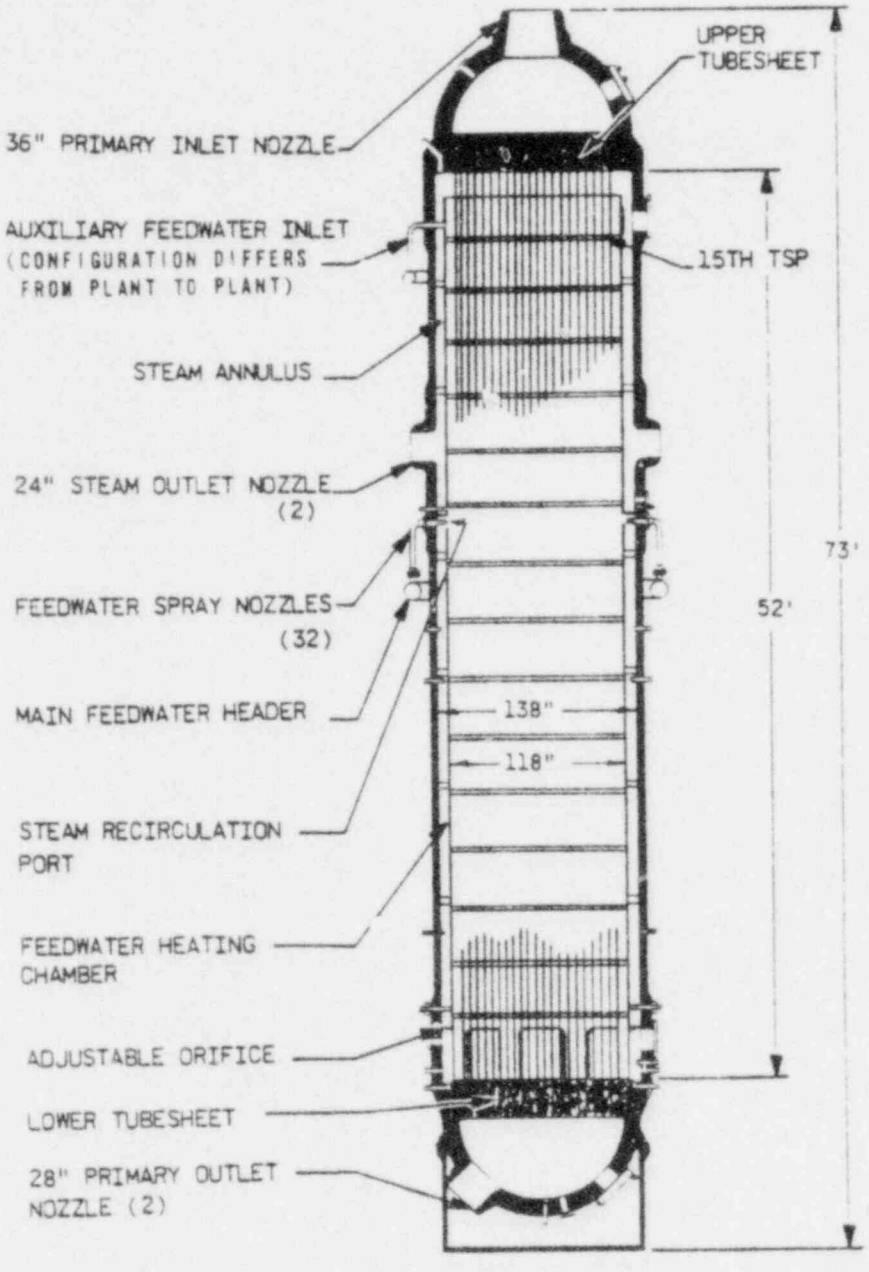

Figure 2-2. 177-FA OTSG, Tube Bundle Cross Section

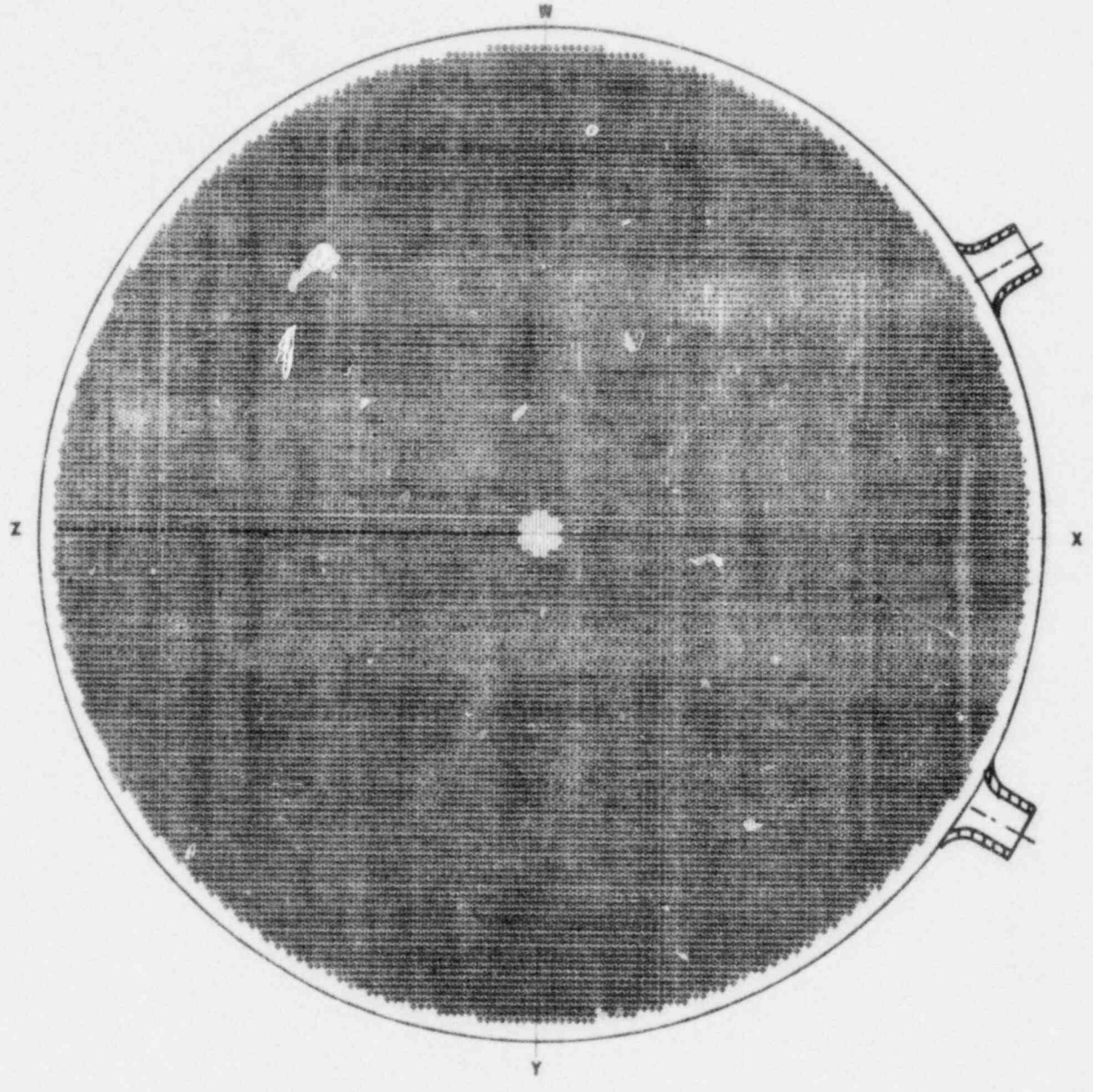

○ Tube

● Untubed Inspection Lane

Figure 2-3. Lowered-Loop Reactor Coolant System Arrangement, Elevation View

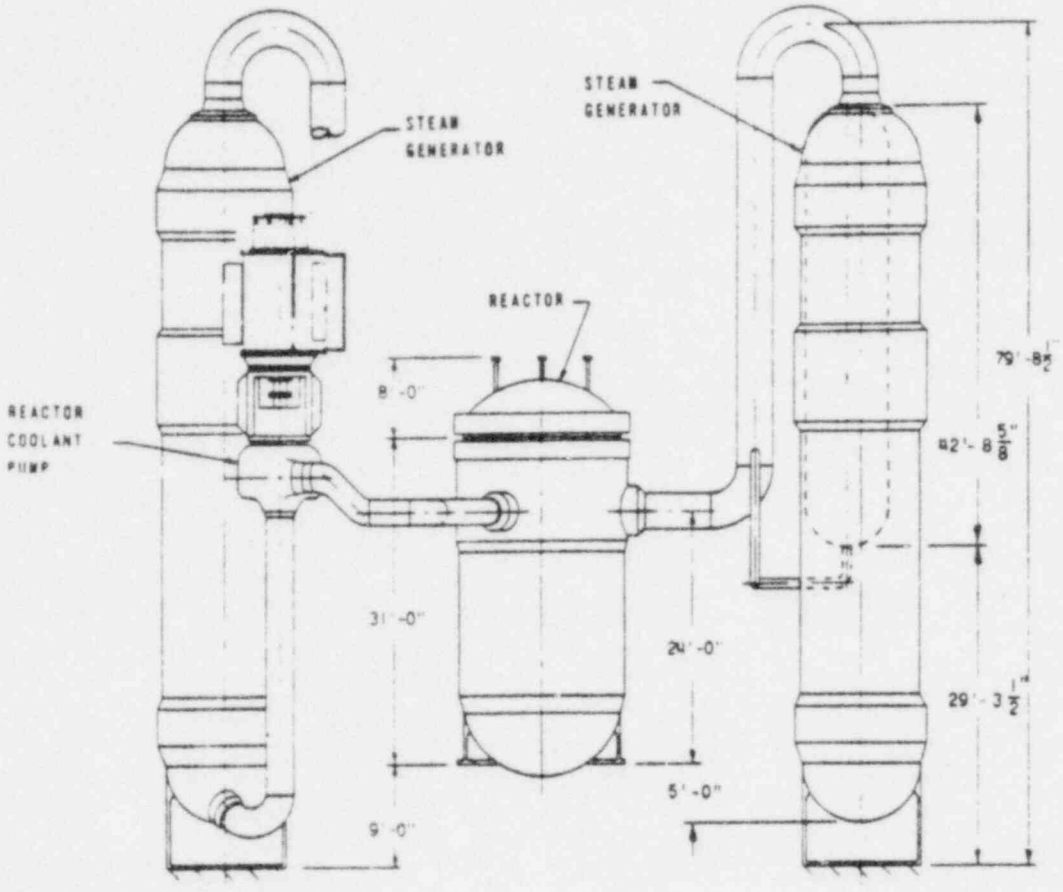

Figure 2-4. Raised-Loop Reactor Coolant System Arrangement, Elevation View

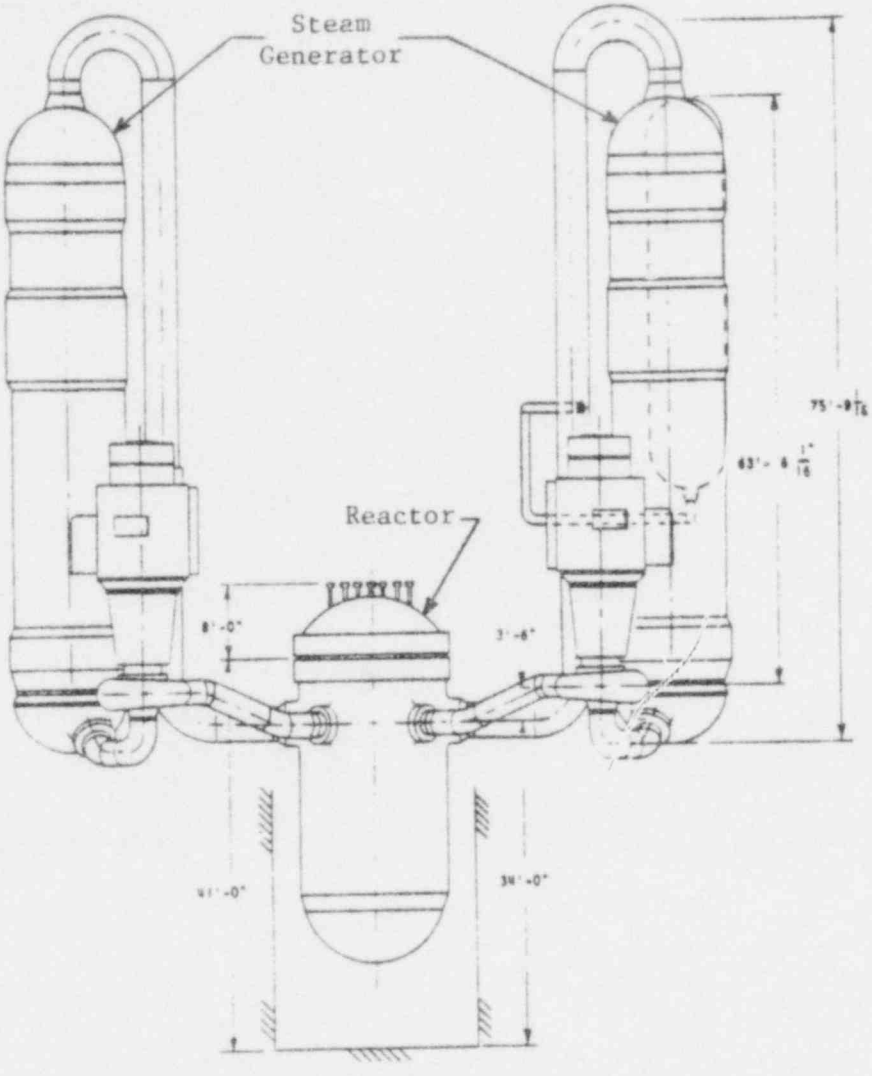

3. HYDRAULIC FORCING FUNCTIONS

This section presents the analyses performed to calculate the hydraulically induced loadings on the OTSG and the thermal response of its tubes and shell to an assumed LOCA, an MSLB, and an FWLB.

3.1. Primary Side Break (LOCA)

Transient pipe reaction forces, which are hydraulically induced structural loadings on the reactor coolant system due to the time rate of change of momentum of the primary system coolant, were generated for full-area guillotine breaks at the OTSG primary inlet and outlet. The reaction forces were calculated using the CRAFT2 computer code[1] and analytical methodology as set forth in reference 2.

3.1.1. FORCE2 Subroutine

B&W developed the FORCE2 computer subroutine to calculate the pipe reaction hydraulic loadings on the reactor coolant loop during both normal operation and accident transients, such as LOCA. FORCE2, using CRAFT2 results as input data, calculates the two-dimensional structural pipe reaction forces around the coolant loop by solving the fluid momentum equation.[2] These forces, when combined in an analysis with the deadweight, thermal, and seismic loadings acting on the NSS coolant loop, establish the structural loading requirements for the coolant loop and its supports and restraints.

FORCE2 is available as a subroutine in the CRAFT2 code; its relationship with the CRAFT2 routines is illustrated in Figure 3-1. The pipe reaction force methodology used for the analysis reported herein is identical to that of reference 2, which provides a more detailed description.

3.1.2. CRAFT2 Computer Code

B&W uses the CRAFT2 computer program as the basic analytical tool for predicting the transient thermal-hydraulic blowdown behavior of a PWR in the unlikely occurrence of a LOCA. As indicated in Figure 3-1, these CRAFT2

blowdown data are used as input to the FORCE2 subroutine to determine the transient pipe reaction forces.

3.1.3. CRAFT2 Modeling

Figure 3-2 shows the node-flow diagram used in generating the LOCA forcing functions, and Table 3-1 provides a list and a description of the reaction force paths. The reaction force CRAFT2 model contains the following assumptions:

1. 100% power (2568 MWt) — This assumption is appropriate for a generic analysis of all B&W operating plants.
2. Moody discharge model with $C_D = 1.21$.
3. Heat transfer in the piping is negligible during the period of interest (0 to 500 milliseconds).
4. Reaction forces in straight, constant area paths (except for the OTSG tubes) are neglected.

These assumptions are identical with the pipe reaction force methodology presented in reference 2. In reference 3 the NRC has approved the analytical methods presented in reference 2.

3.1.4. Analysis/Results

Transient pipe reaction forces were generated for two break locations — the OTSG primary inlet (hot leg break) and outlet (lower cold leg break). The breaks are considered to occur in the "A" loop and are assumed to linearly open to full-area guillotine breaks in 10 milliseconds.

The results of the calculations are sets of transient pipe reaction forces (one set per break location for each CRAFT2 flow path listed in Table 3-1). These reaction forces are combined analytically with the remaining reactor coolant system (RCS) loads, such as deadweight, thermal, and seismic, to obtain the resultant OTSG loading state.

Figure 5-7 in reference 2 is illustrative of the reaction forces calculated in this analysis. Figures 3-3 through 3-6 and 3-7 through 3-10 show the OTSG primary side transient node pressures for the outlet and inlet breaks, respectively. Table 3-2 provides additional documentary information on these two breaks.

3.1.5. Shell and Tube Temperature Calculations

To calculate the tube and shell temperatures resulting from a LOCA, CRAFT2 was used with the modeling described in reference 4. The most severe transient, which occurred for the double-ended rupture of a 36-inch-ID hot leg pipe, includes the cooling attributable to auxiliary feedwater.

The CRAFT2 results were extended by hand calculations to determine the minimum tube temperature. The maximum tube-to-shell temperature differential was calculated to occur approximately 5 minutes after the break, with the average tube temperature at about 250F. The lower part of the shell was estimated to cool from 538 to 530F in this same period of time, while the upper part of the shell was assumed to remain at its initial temperature.

3.2. Secondary Side Breaks (MSLB and FWLB)

The OTSG shown in Figure 2-1 is typical of OTSGs in all B&W 177-FA plants. Upon investigation of each utility's OTSG and steam and feedwater line piping, several differences were identified. In developing a generic model of the OTSG to generate hydrodynamic loadings, the obvious design differences were investigated. The differences between the units and the generic model are shown in Table 3-3.

Once the feasibility of developing a generic model was confirmed, a model that envelopes all of the 177-FA plants was developed. The generic model is an open-loop system of 127 control volumes and 199 flow paths developed for use in the CRAFT2 code. Diagrams of the model are shown in Figures 3-11 through 3-16. To resolve the design differences among the generators, the following assumptions were made:

1. Since the majority of plants have 15,531 tubes, that number was assumed for the generic model. This parameter choice will not affect the analysis significantly.
2. The angle between the OTSG steam outlet nozzles was chosen to be 100°. This value will produce more conservative results (higher loads) than would the case with the nozzles separated by 126°.
3. An 18-inch upper shroud opening was assumed in the generic model. However, the sensitivity of the crossflow velocities to a 13.125-inch shroud opening was investigated and is discussed below.

In addition to the assumptions listed, the fluid conditions chosen were selected as a representative set of fluid conditions for clean tubes, but a set that maximizes the total secondary pressure differential in the OTSG, thereby producing the highest loads on the OTSG shroud. This selection of fluid conditions is presented in Table 3-4.

The break fluid discharge model used for the MSLB and FWLB was the Zaloudek-Moody discharge model. However, for an MSLB, the Zaloudek part of the model is not used because of the fluid quality conditions. A discharge coefficient (C_D) of 1.0 was used for all breaks. For calculating loads, a break opening time (BOT) of 10 milliseconds was used for steam line breaks, and 1 millisecond was used for the FWLB. Reference 5 states that 1 millisecond should be used unless a longer time can be justified. B&W's primary piping calculations, based on pipe IDs larger than 2 feet, demonstrate that 10 milliseconds is a conservative representation of the actual BOT required to achieve a full-area steam line break.

The heat transfer between the primary and secondary sides of the OTSG was simulated by modified use of the option 1 OTSG model in the CRAFT2 code. In this option, the primary side temperatures were input as constants, and a normalized heat transfer coefficient determines the heat flow. The heat transfer is proportional to the temperature difference between the secondary side temperature and the fixed primary side temperatures. Sensitivity studies were performed to study the effects of the heat transfer modeling. These studies showed that using a more realistic heat transfer model would produce crossflow velocities 5% higher than those originally calculated. Because of the potential impact of these higher velocities, the crossflow velocities shown in Tables 3-5 and 3-6 include the factor of 5%.

3.2.1. CRAFT2 and Auxiliary Code Descriptions

The hydraulic forcing functions are calculated in a two-step process. The CRAFT2 code is used to generate pressure and flow time histories, which are used as input into the INTFCE code[6] to calculate hydraulic forces on the OTSG shroud. CRAFT2 is a digital computer program for calculating local fluid pressure, flow, and density transients that occur in reactor coolant systems during a postulated LOCA. The code solves the conservation equation for each node and the momentum equation for each flow path between nodes. The

explicit solution technique was used for calculating secondary side blowdown loads.

The INTFCE code computes the resultant forces on each component at several pres-specified points from the pressure data calculated by CRAFT2. The resultant forces are then summed to obtain the total combined forces and associated moments.

3.2.2. Hydraulic Forcing Functions

The decompression process that occurs after a postulated break initiates at the break location in the OTSG secondary side inlet or outlet piping. Depending on flow passage geometry, a decompression wave propagates in all directions within the coolant at the local speed of sound. Wave reflections lead to a complex pressure distribution within the OTSG. The resultant pressure differences between regions induce loadings on the OTSG and its internal structures. The lateral forces acting on the interior of the OTSG and on the internal structures can be determined by vectorially summing the products of the fluid pressures and the surface areas on which the pressures act over the entire length of the OTSG. The developed model must exhibit sufficient spatial detail to define the loadings on the OTSG shroud.

3.2.3. Break Description

For this analysis, three pipe break cases were considered:

1. Double-ended guillotine rupture in a single steam line located at the OTSG nozzle-piping interface.
2. Double-ended guillotine rupture in both steam lines simultaneously at their point of connection. The steam line piping plans in all the the 177-FA Owners Group plants are not identical. Close examination of these piping plans indicated that the steam lines join at varying distances from the OTSG.

   The most severe loads on the OTSG would occur as a result of a break in both steam lines at the connection point nearest the OTSG; the closest connection point was found to be 60 feet from the OTSG. Therefore, the break considered was a double-ended guillotine break in both steam lines 60 feet from the OTSG shell.
3. Double-ended guillotine rupture in a single feedwater line. This was simulated by assuming shearing off half of the feedwater header.

3.2.4. Results of Hydraulic Forcing Function Analysis

The MSLB and FWLB were analyzed to determine pertinent loads and crossflow velocities through the OTSG upper tube region. To calculate such velocities,

the peak (with respect to time) spatial average crossflow velocity ($\bar{V}$) at the OTSG tube bundle periphery were deduced from the CRAFT2 results. The velocity is termed average in that it is a representative velocity of flow crossing a surface of finite area as opposed to a velocity at a specific point in space.

The CRAFT2 crossflow velocity is also an average in the sense that the CRAFT2 model does not distinguish between the three tube pattern arrangements (TPAs): the open tube lane, the 60° TPA, and the 30° TPA. Each of the three TPAs presents a different cross section to the flow, which results in three corresponding resistances to fluid flow. Consequently, each region has a different crossflow velocity. Details of the correlation between the TPAs and crossflow velocities are presented in Figure 3-17. Hence, the peak average CRAFT2 crossflow velocity must be further refined in order to represent the three different TPAs.

Using Oconee 1 data, B&W has estimated the crossflow velocities between the upper tubesheet and the 15th TSP from the center of the tube bundle to its outer edge for the three TPAs. Similarly, the axial (direction perpendicular to the W-Z plane in Figure 3-17) crossflow velocity profile at the tube bundle periphery has been estimated for the open tube lane and the 30° TPA. Based on these estimates, multipliers were constructed at the tube bundle periphery to apply to the peak average CRAFT2 crossflow velocity in order to obtain the peak (with respect to time) average crossflow velocities ($\bar{V}_{peak}$) for the three TPAs. These data are shown in Tables 3-5 and 3-6. From the estimated axial crossflow velocity profiles at the tube bundle periphery, a multiplier was constructed to apply to $\bar{V}_{peak}$ in order to obtain the maximum (with respect to both time and axial distance) crossflow velocities (V_{max}) for the three TPAs (see Tables 3-5 and 3-6). The maximum velocity occurs at an elevation slightly above the top of the shroud.

Figures 3-18 and 3-19 are plots of the lateral loads on the OTSG shroud for the single and double steam line breaks, respectively. The double steam line break case produced the highest crossflow velocities, while the single steam line break produced the highest lateral loads on the OTSG shroud.

Assumption 3 in section 3.2 refers to the effect of shroud opening height on the calculation of crossflow velocities. For this analysis, a shroud opening height of 18 inches was assumed. However, some of the 177-FA Owners Group

plants, i.e., Oconee 3, TMI-2, Rancho Seco, Midland 1 and 2, and Davis-Besse 1, have a 13.125-inch shroud opening. Estimates of the crossflow velocities were made for the 13.125-inch opening. It was concluded that the crossflow velocities for the 13.125-inch shroud underestimated the crossflow velocities through the 18-inch shroud opening by a factor of 1.37. Therefore, to predict crossflow velocities through the 13.125-inch opening, the crossflow velocities given in Tables 3-5 and 3-6 should be multiplied by 1.37.

The single FWLB case produced loads and crossflow velocities of insignificant magnitude compared to the MSLB cases and as a result, those loads and velocities are not included in this report.

3.2.5. Shell and Tube Temperature Calculations

To calculate the long-term cooling of the OTSG tubes and shell, a simplified model of the OTSG was generated for the TRAP2 computer code[7]; the model was used for both MSLBs and FWLBs. The model of the NSS is shown in Figure 3-20, and its control volumes and flow paths are described in Tables 3-7 and 3-8.

3.2.5.1. Main Steam Line Break (MSLB)

The MSLB rupture path is modeled near the highest point of the tube section of the OTSG secondary side. The rupture can be considered to occur at the OTSG exit nozzle since no modeling or steam piping is provided between the OTSG and the rupture on the affected OTSG.

Two cases were run, considering the double-ended rupture of a 36-inch main steam line, to assess the impact of auxiliary feedwater flow on the affected OTSG temperatures. Although some plants have 24-inch main steam lines from the OTSG connecting directly to the turbine without headering into a common larger pipe, the rupture of a 36-inch steam line was chosen to represent a bounding condition for all plants. It was assumed that a low steam line pressure signal would close the main feedwater valves and an ESFAS signal would actuate both high-pressure injection pumps.

For one case the auxiliary feedwater was assumed to feed the affected OTSG at its maximum runout flow rate of 1650 gpm. At 20 minutes, auxiliary feedwater was assumed to be terminated by the operator. This very conservative set of assumptions resulted in a calculated average tube temperature of about 235F at 20 minutes. The lower part of the shell below the feedwater header

was calculated to cool to about 520F while the upper part cooled very little.

Some plants have logic that prevents auxiliary feedwater from entering the affected generator if the steam line pressure is less than some low pressure, typically 600 psig. The other case that was analyzed took credit for this logic. This analysis shows that the OTSG tubes undergo a much less severe thermal transient, with the tube temperature falling to 473F. As with the other case, there was little cooling of the shell. Both of the conditions analyzed put the OTSG tubes in tension.

3.2.5.2. Feedwater Line Break (FWLB)

The double-ended rupture of the main feedwater piping can be considered to occur at the feedwater inlet nozzles or along the main piping since no piping is modeled between the break and the steam generator inlet nozzles. The FWLB causes the reactor coolant system and the tubes to heat up. The maximum calculated average tube temperature, 625F, occurs approximately one minute into the transient. The shell temperature is assumed to stay at its initial value. The FWLB thermal transient results in a compressive loading on the OTSG tubes.

Table 3-1. List of CRAFT Flow Paths Considered in Pipe Reaction Force Calculations

Order No.(a)	Flow path No.(b)	Reactor coolant system
1	1	RV
2	2	RV
3	5	OTSG A inlet
4	6	OTSG A
5	7	OTSG A
6	8	OTSG B
7	9	OTSG A
8	11	Lower cold leg A2
9	13	Upper cold leg A1
10	15	Upper cold leg A2
11	17	OTSG A
12	19	Lower cold leg A1
13	21	Upper cold leg A2
14	23	Upper cold leg A1
15	29	OTSG B inlet
16	30	OTSG B
17	31	OTSG B
18	32	OTSG A
19	33	OTSG B
20	35	Lower cold leg B2
21	37	Upper cold leg B2
22	39	Upper cold leg B2
23	41	OTSG B
24	43	Lower cold leg B1
25	45	Upper cold leg B1
26	47	Upper cold leg B1
27	52	Surge line
28	55	Surge line
29	58	Surge line
30	62	Surge line
31	65	Surge line
32	66	Pressurizer nozzle
33	68	RV outlet to A loop
34	69	Hot leg A
35	71	Hot leg A
36	72	Lower cold leg A2
37	73	Upper cold leg A2
38	74	Lower Cold leg A1
39	75	Upper cold leg A1
40	76	Hot leg B
41	78	Hot leg B
42	79	Lower cold leg B2
43	80	Upper cold leg B2
44	81	Lower cold leg B1
45	82	Upper cold leg B1
46	83	RV outlet to B loop
47	84	RV head
48	85	RV

Table 3-1. (Cont'd)

Order No.[a]	Flow path No.[b]	Reactor coolant system
49	86	RV inlet from A2
50	87	RV inlet from A1
51	88	RV inlet from B2
52	89	RV inlet from B1
53	90	Pump A2
54	91	Pump A1
55	92	Pump B2
56	93	Pump B1
57	94	Pressurizer nozzle
58	107	Surge line nozzle
59	108	Surge line nozzle
60	109	Hot leg A
61	110	RV head

(a) Relates to the order in which data are placed on the magnetic computer tape.

(b) Relates to the flow path numbering scheme shown in Figure 2-2.

Table 3-2. CRAFT Pipe Reaction Force Runs, Descriptive Information

LOCA case	Break loc'n	Break type	Opening area, A	Opening time, ms	FORCE2 tape (label)	CRAFT2 tape (label)	Program name, version	Version date
LCL5GIV	OTSG outlet nozzle	Guillotine	2A	10	2794 (ANTOUN2)	2927 (ANTOUN1)	CRAFT2, 9.7	10/19/77
HTL6GFA	OTSG inlet nozzle	Guillotine	2A	10	1904 (ANTOUN2)	1898 (ANTOUN1)	CRAFT2, 9.7	10/19/77

Note: A = pipe internal cross-sectional area,
= 4.276 ft^2 for the lower cold leg,
= 7.069 ft^2 for the hot leg.

Table 3-3. 177-FA Owners Group OTSG Differences and Generic Model

Plant	Total No. of tubes	Angle between steam outlet nozzles, °	Aux FW inlet nozzles, No./size, in.	Upper shroud opening, in.
Oconee 1	15,531	100	7/3	18
Oconee 2	15,531	100	7/3	18
Oconee 3	15,531	100	1/6	13.125
TMI-1	15,531	126	7/3	18
TMI-2	15,531	126	1/6	13.125
CR-3	15,531	126	7/3	18
ANO-1	15,531	126	7/3	18
Rancho Seco	15,457	126	1/6	13.125
Midland 1	15,457	100	1/6	13.125
Midland 2	15,457	100	1/6	13.125
DB-1	15,531	100	1/6	13.125
Generic	15,531	100	Not considered in model	18

Table 3-4. Generic OTSG Model Data and Dimensions

Primary coolant flow, 10^6 lbm/h	68.95
Steam flow, 10^6 lbm/h	6.125
Aspirator bleed flow, 10^6 lbm/h	0.8269
Coolant inlet temperature, F	608.60
Coolant outlet temperature, F	555.40
Primary pressure drop, psi	43.44
Primary operating pressure, psi	2200
Feedwater temperature, F	461.3
Secondary steam outlet pressure, psi	925
Tube OD, in.	0.625
Tube wall thickness (min/nom.), in.	0.034/0.0375

Table 3-5. Single MSLB Crossflow Velocities

Reference: Runs SGSL1PI and SGSL1LA, single MSLB at OTSG.

Tube bank location	$\bar{V}_{peak}$, fps	V_{max}, fps
Open lane	467	864
30° TPA	282	523
60° TPA	231	427

$V_{choking}$ = 1740 fps

$\bar{V}_{crossflow}$ = 256 fps

Table 3-6. Double MSLB Crossflow Velocities

Reference: Runs SGSL2JF and SGSL2RG, double MSLB at WYE.

Tube bank location	$\bar{V}_{peak}$, fps	V_{max}, fps
Open lane	518	958
30° TPA	313	579
60° TPA	256	474

$V_{choking}$ = 1660 fps

$\bar{V}_{crossflow}$ = 285 fps

Table 3-7. TRAP2 Nodal Description for MSLB and FWLB Models

Node No.	Description
1	Reactor vessel, lower plenum, cold legs
2	Core and hot legs
3	Upper half, primary side of OTSG tube region
4	Lower half, primary side of OTSG tube region
5	Upper half, primary side of OTSG tube region
6	Lower half, primary side of OTSG tube region
7	Lower half, secondary side of OTSG tube region
8	Upper half, secondary side of OTSG tube region
9	Lower half, secondary side of OTSG tube region
10	Upper half, secondary side of OTSG tube region
11	Pressurizer
12	Main steam line piping
13	Main feedwater piping
14	Main feedwater piping
15	Turbine

Table 3-8. TRAP2 Flow Path Description for MSLB and FWLB Models

Flow path No.	Description
1	Core heat generation
2	Hot leg
3	Hot leg
4	Affected OTSG primary side
5	Unaffected OTSG primary side
6	Cold legs
7	Cold legs
8	Affected OTSG secondary side
9	Unaffected OTSG secondary side
10	Pressurizer surge line
11	Main steam piping
12	Main steam piping
13	Turbine stop valves
14	Turbine stop valves
15	HPI flow
16	Auxiliary feedwater flow
17	Auxiliary feedwater flow
18	Main feedwater pumps
19	Main feedwater pumps
20	Main feedwater flow
21	Main feedwater flow

Figure 3-1. CRAFT2-FORCE2 Computer Code Interface

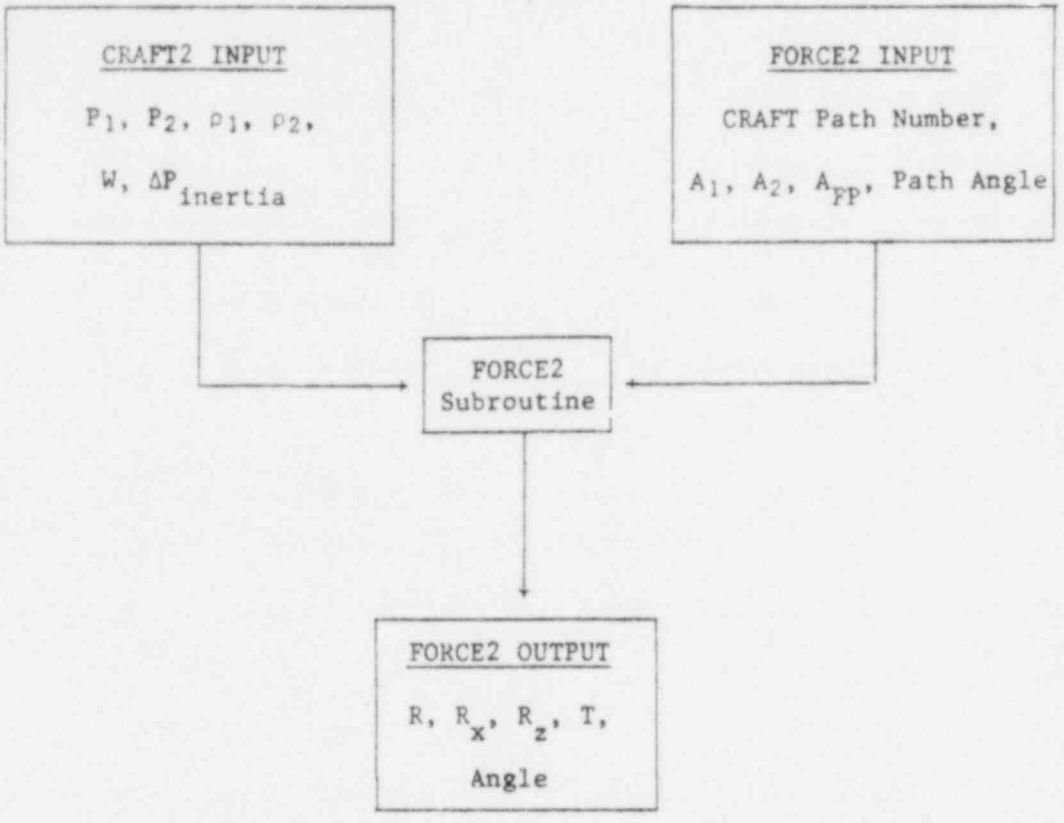

Variables

P — Pressure
ρ — Density
W — Flow
A — Path Area
R — Reaction Force
T — Thrust
Angle = $Tan^{-1}[R_z/R_x]$

Subscripts

1 — Inlet
2 — Outlet
FP — Flow Path
x — X Direction
z — Z Direction

Figure 3-2. NSS Primary Coolant Loop – FORCE2 Program Nodal Representation

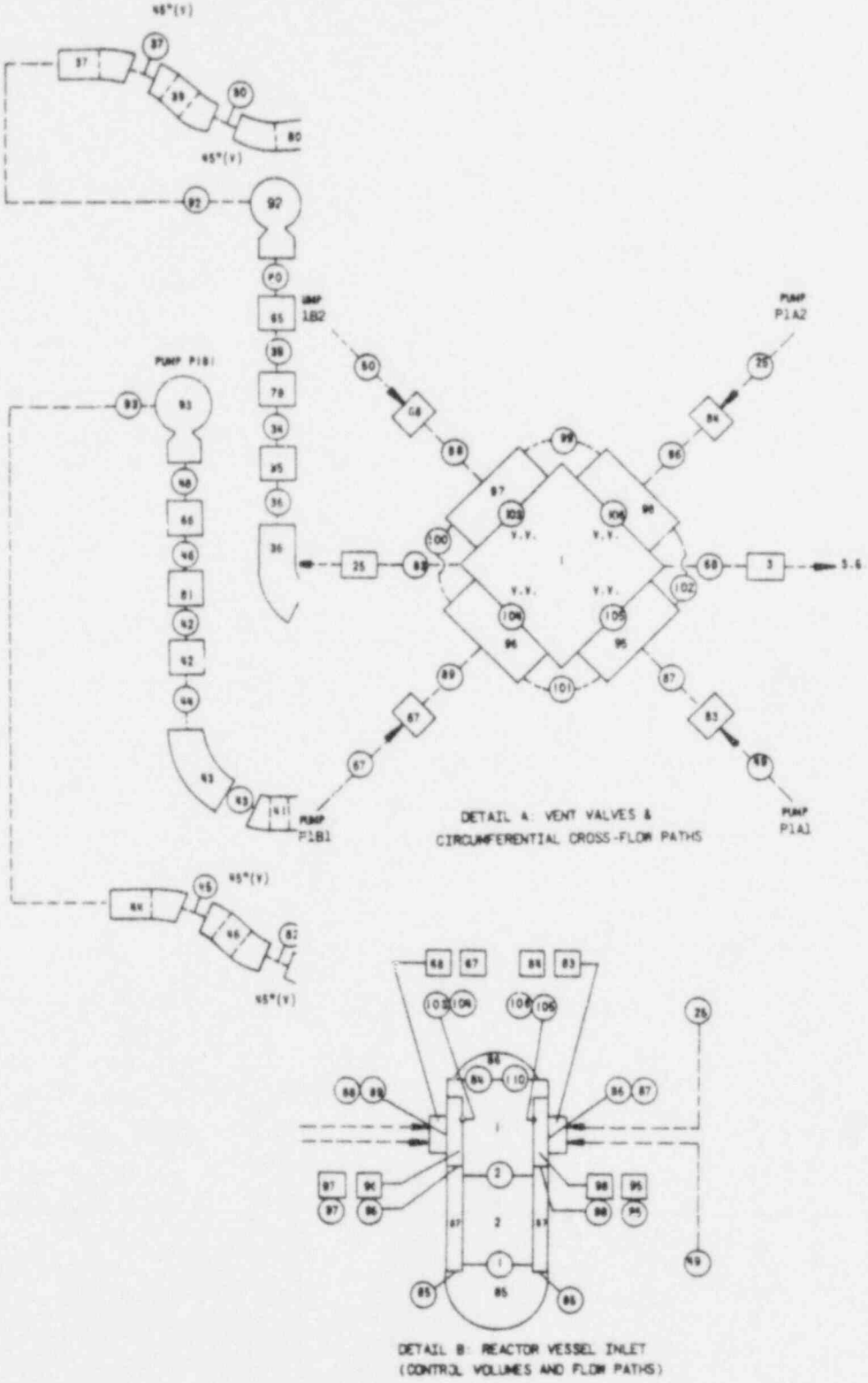

Figure 3-3. Primary Side Pressure Vs Time for the "A" Loop Steam Generator, Node 29 for Cold Leg Break

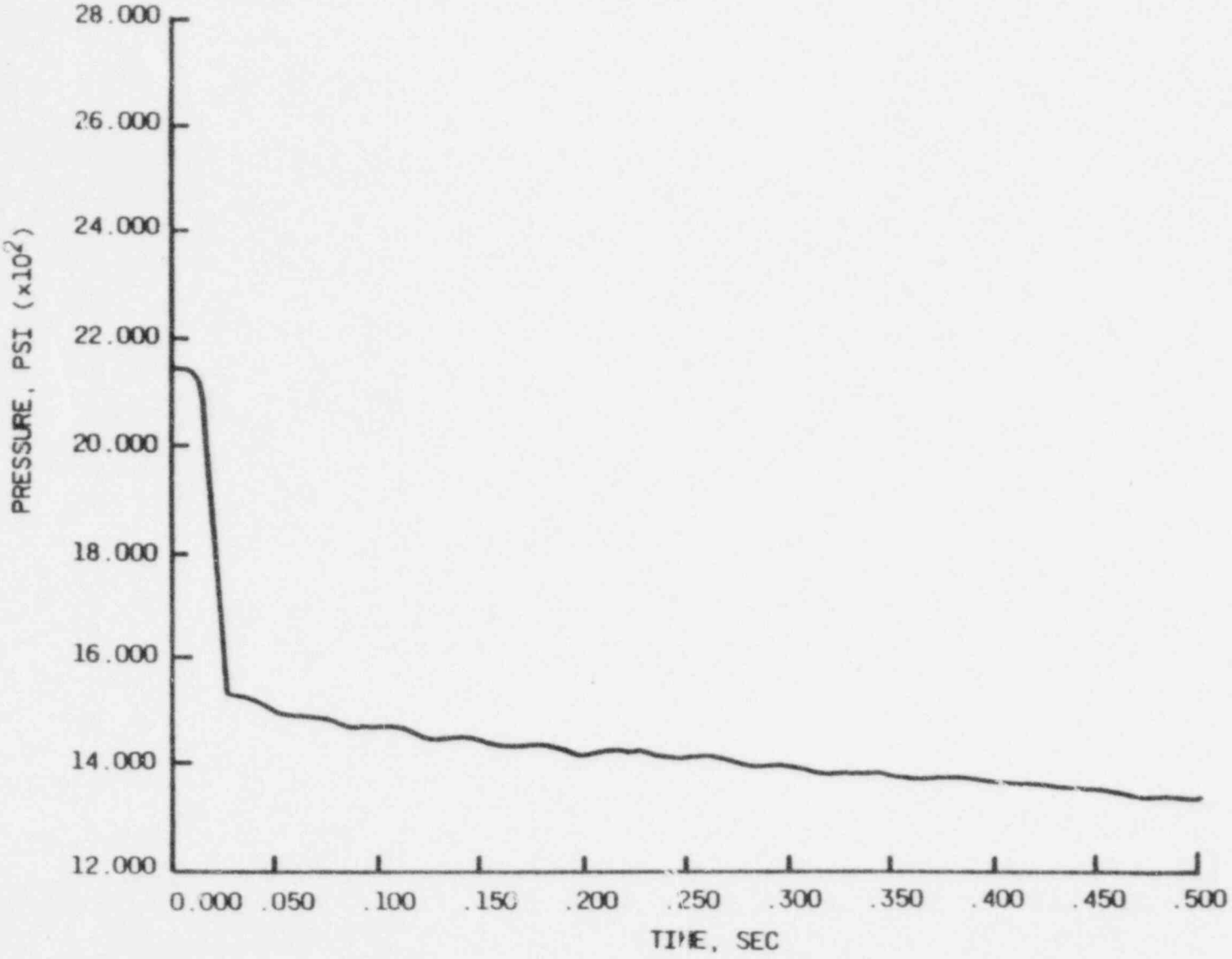

Figure 3-4. Transient Primary Side Pressure for The "A" Loop Steam Generator, Node 8 for Cold Leg Break

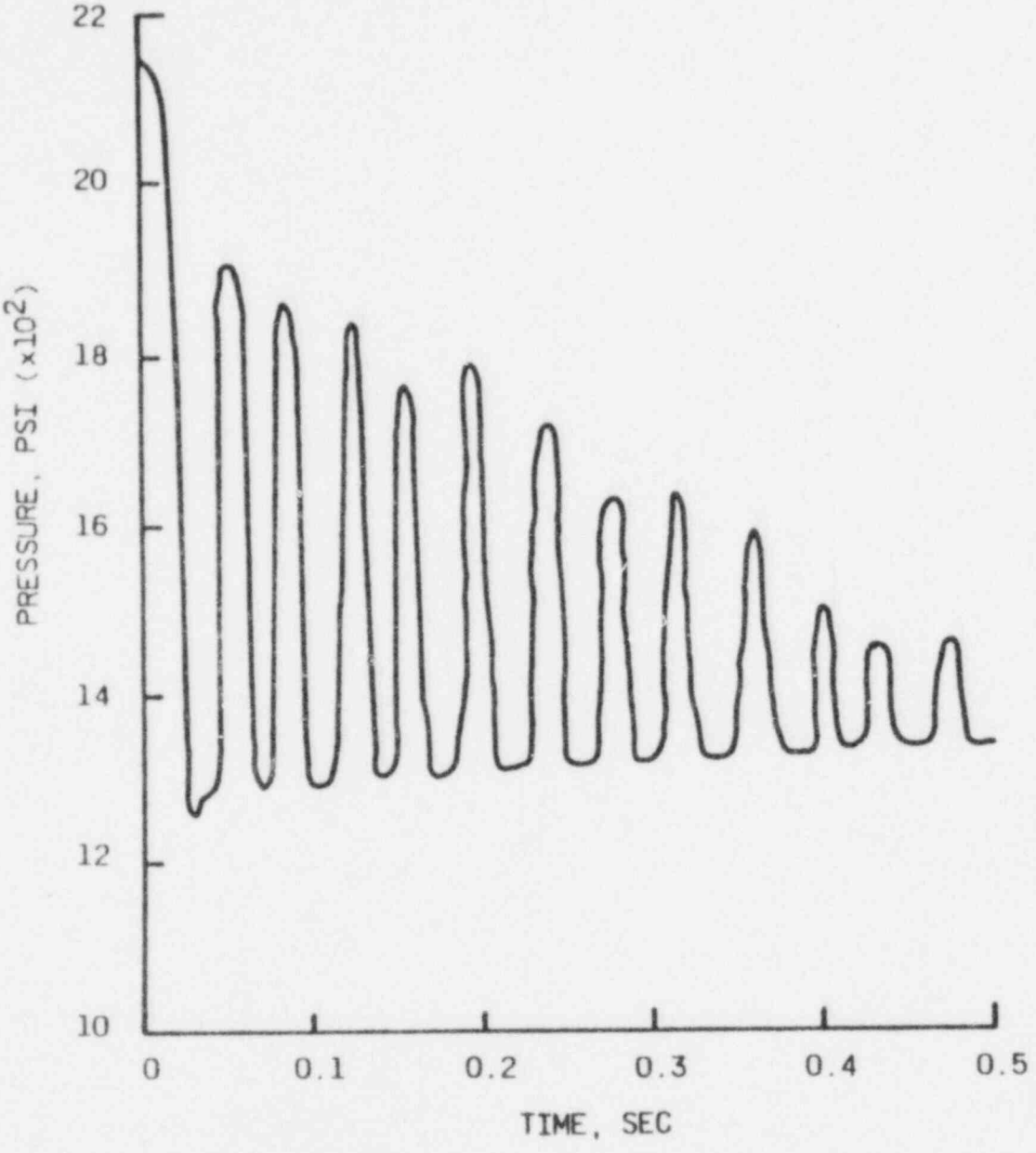

Figure 3-5. Transient Primary Side Pressure for The "A" Loop Steam Generator, Node 9 for Cold Leg Break

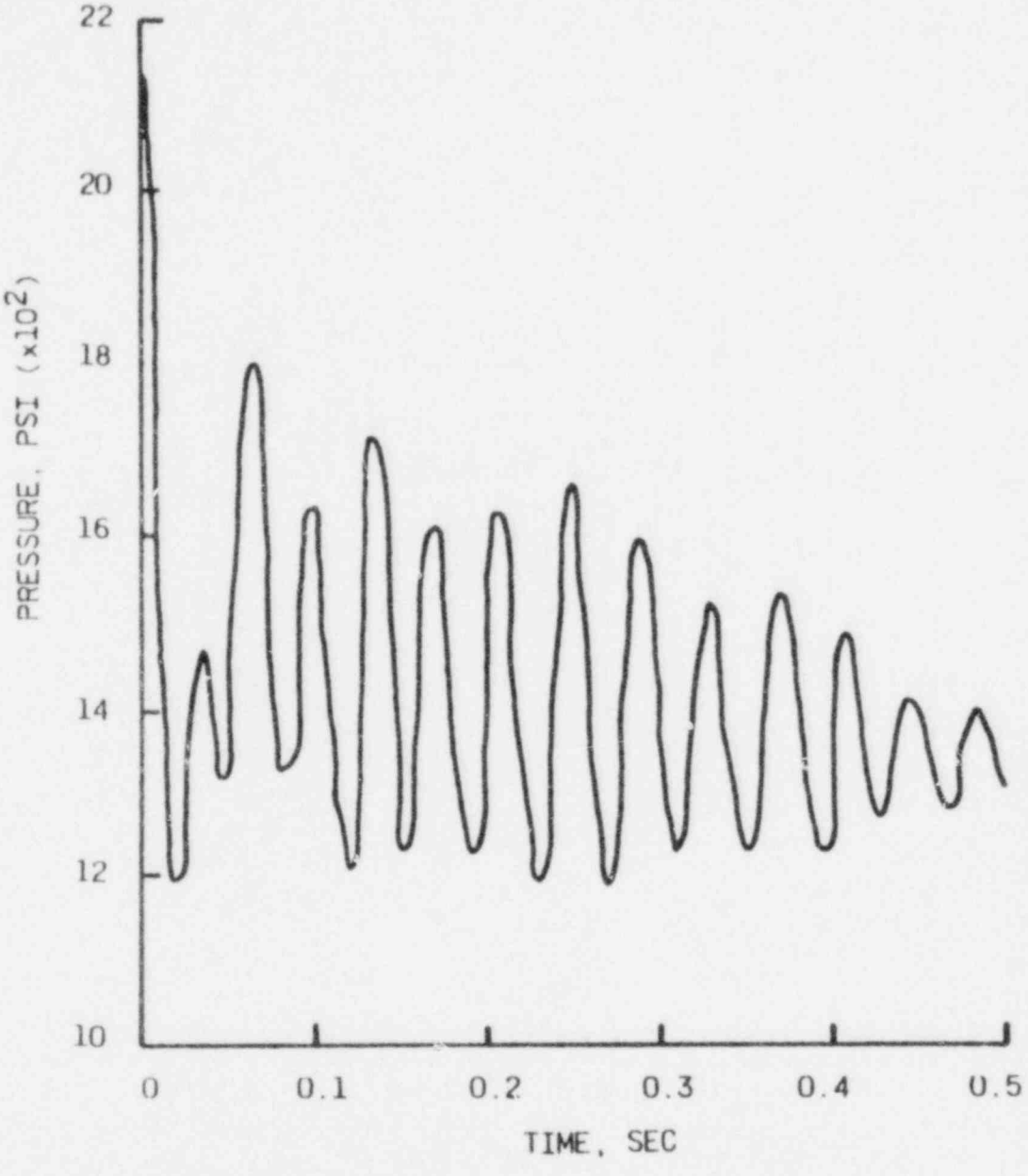

Figure 3-6. Transient Primary Side Pressure for The "A" Loop Steam Generator, Node 10 for Cold Leg Break

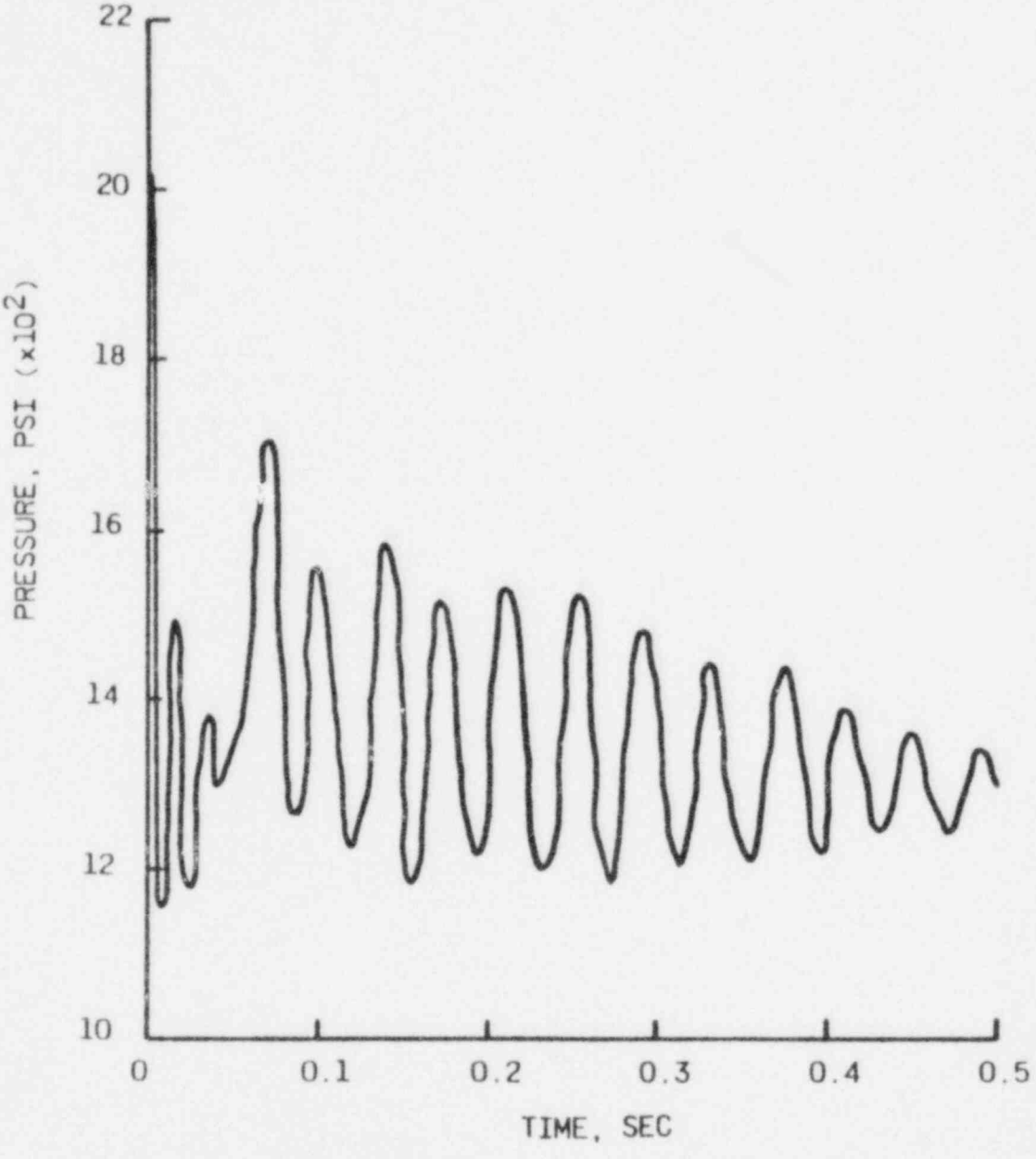

Figure 3-7. Primary Side Pressure Vs Time for the "A" Loop Steam Generator, Node 29 for Hot Leg Break

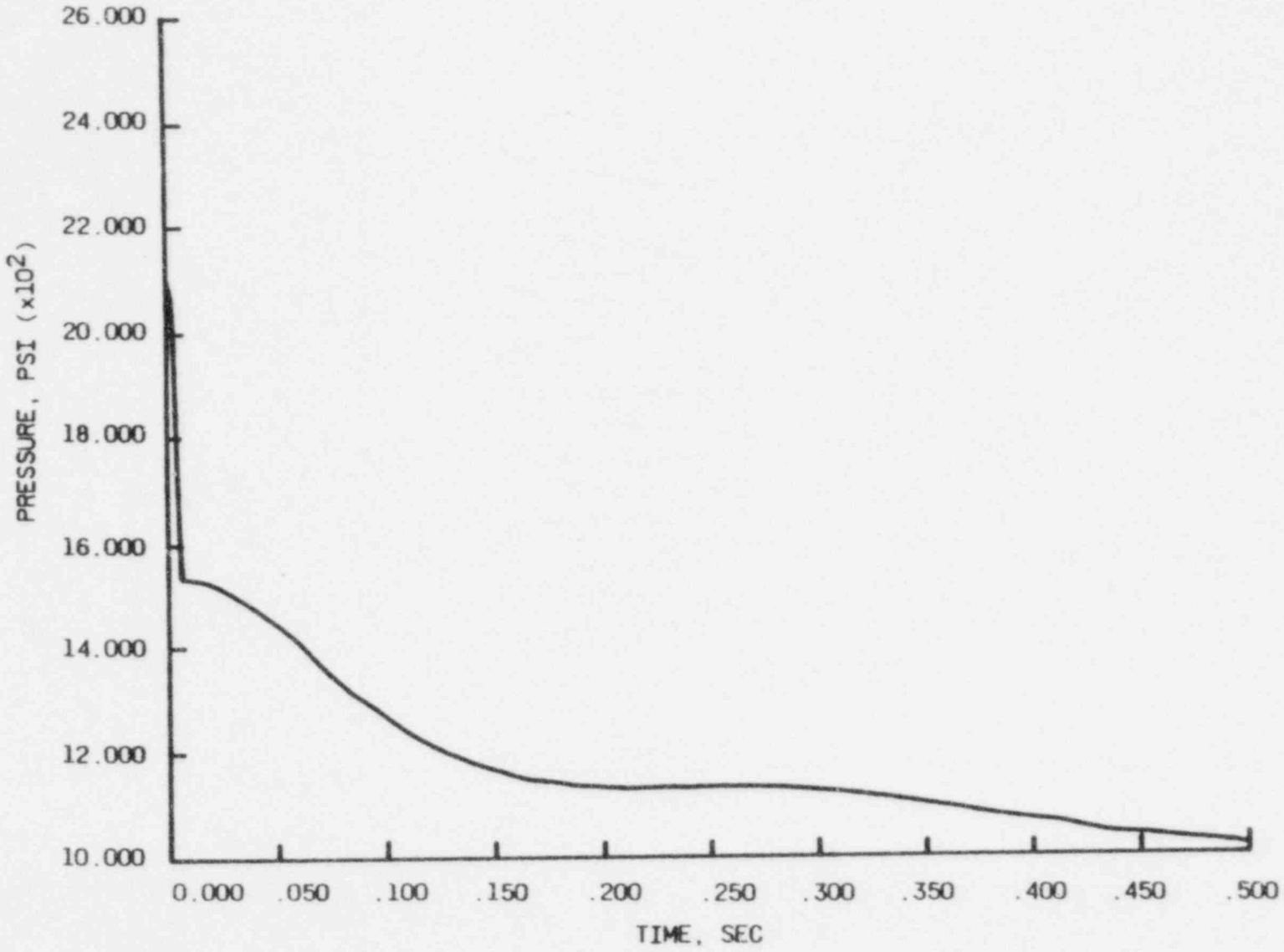

Figure 3-8. Transient Primary Side Pressure for The "A" Loop Steam Generator, Node 8 for Hot Leg Break

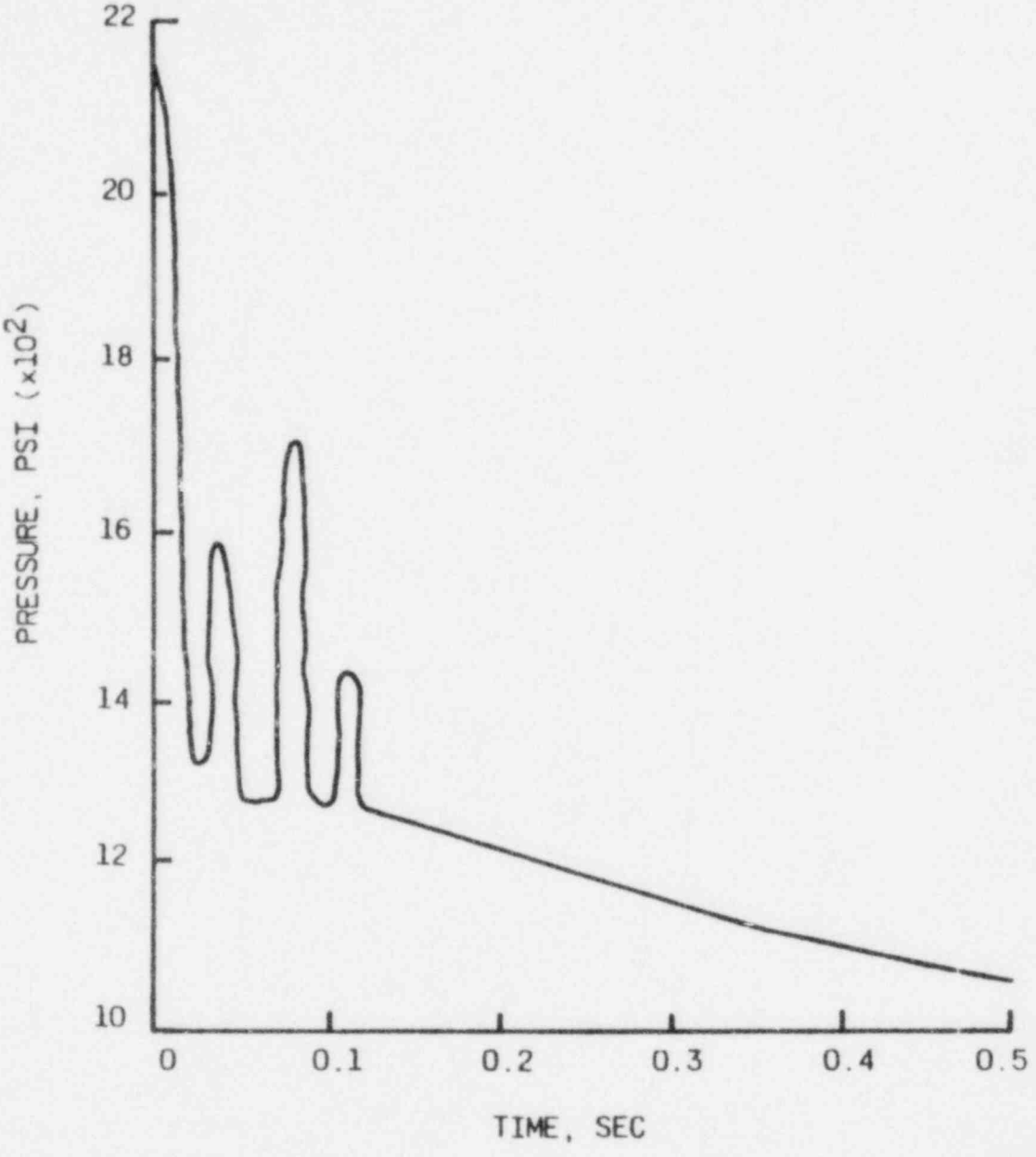

Figure 3-9. Transient Primary Side Pressure for The "A" Loop Steam Generator, Node 9 for Hot Leg Break

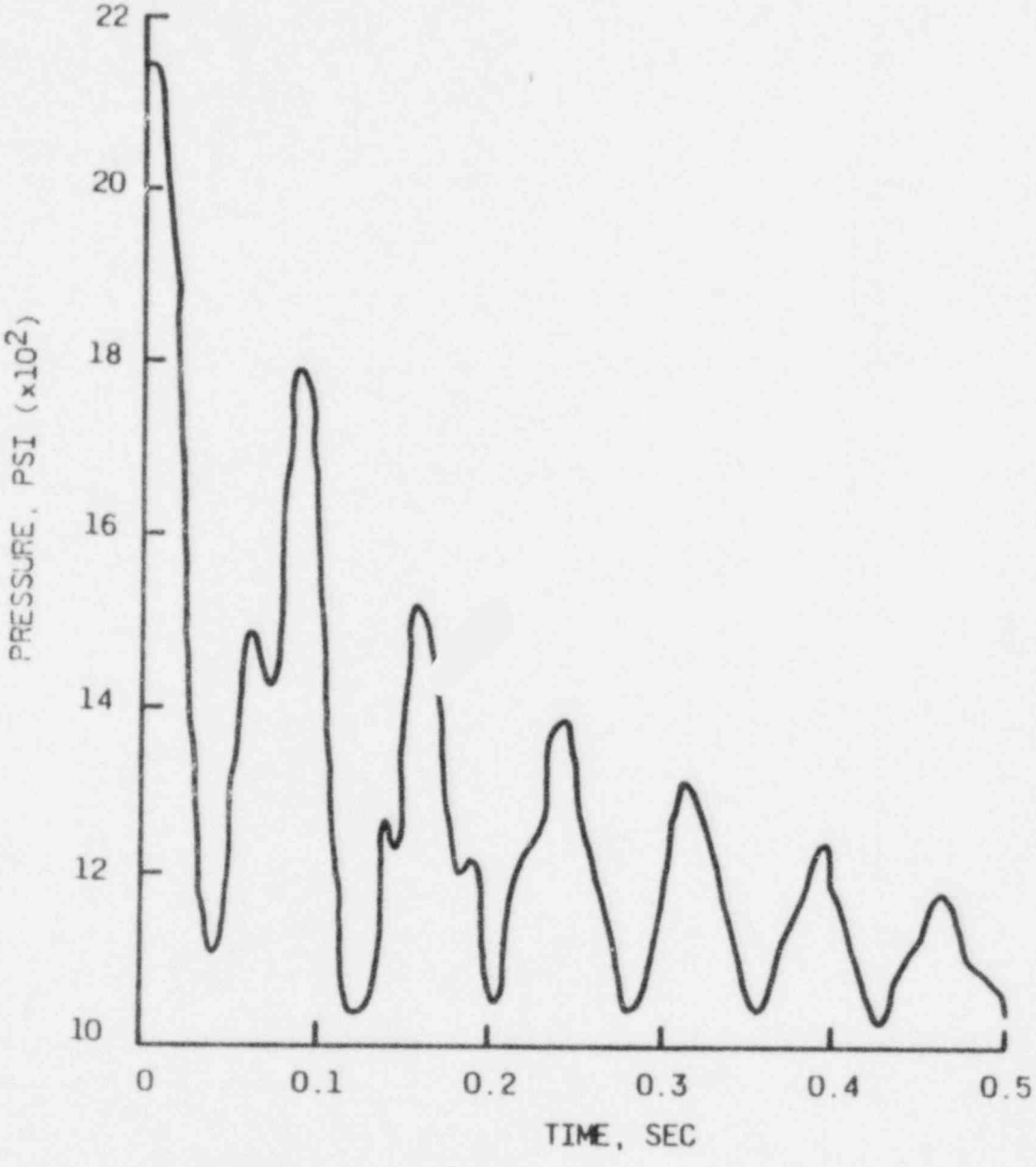

Figure 3-10. Transient Primary Side Pressure for The "A" Loop Steam Generator, Node 10 for Hot Leg Break

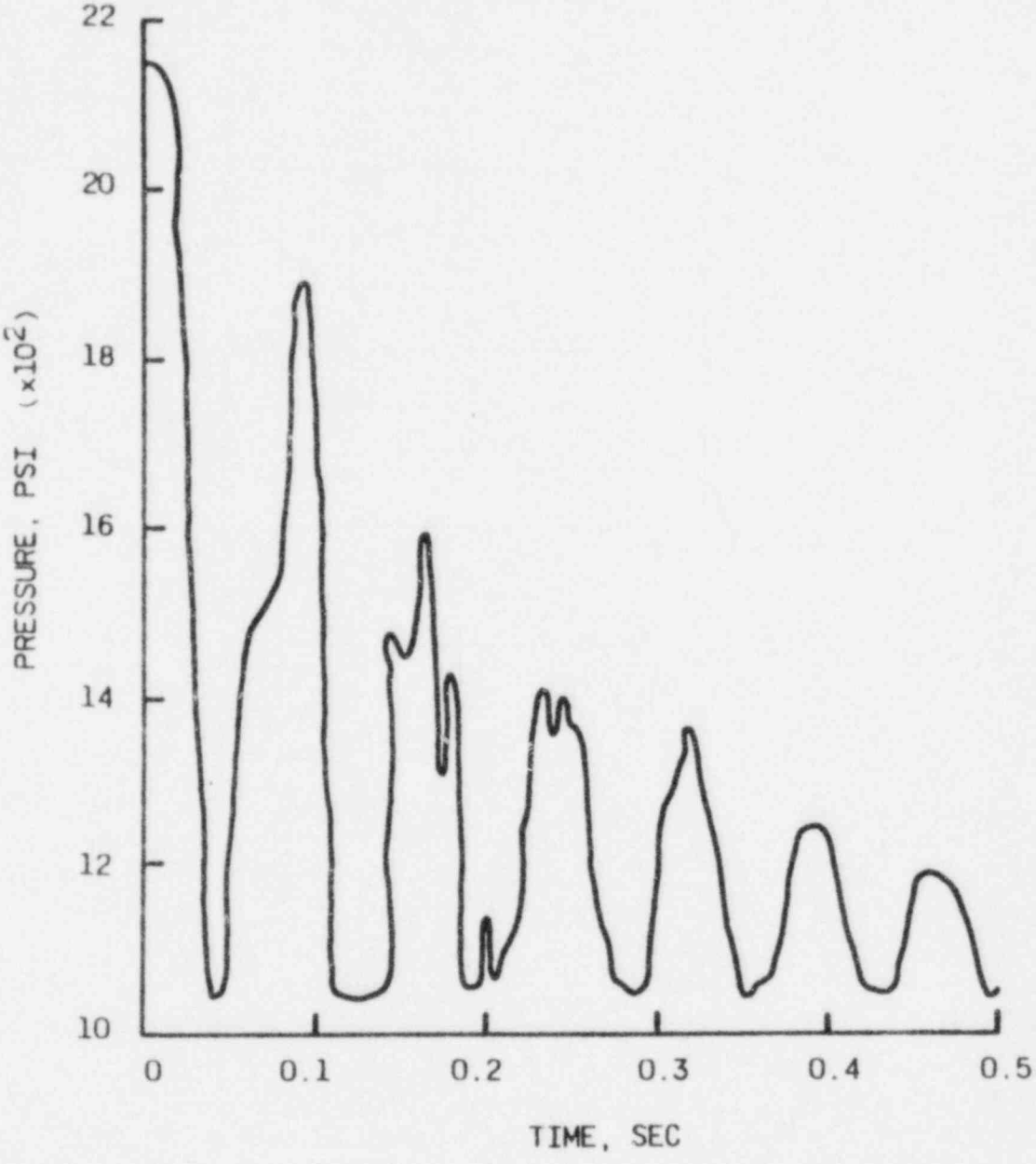

Figure 3-11. OTSG Noding Diagram

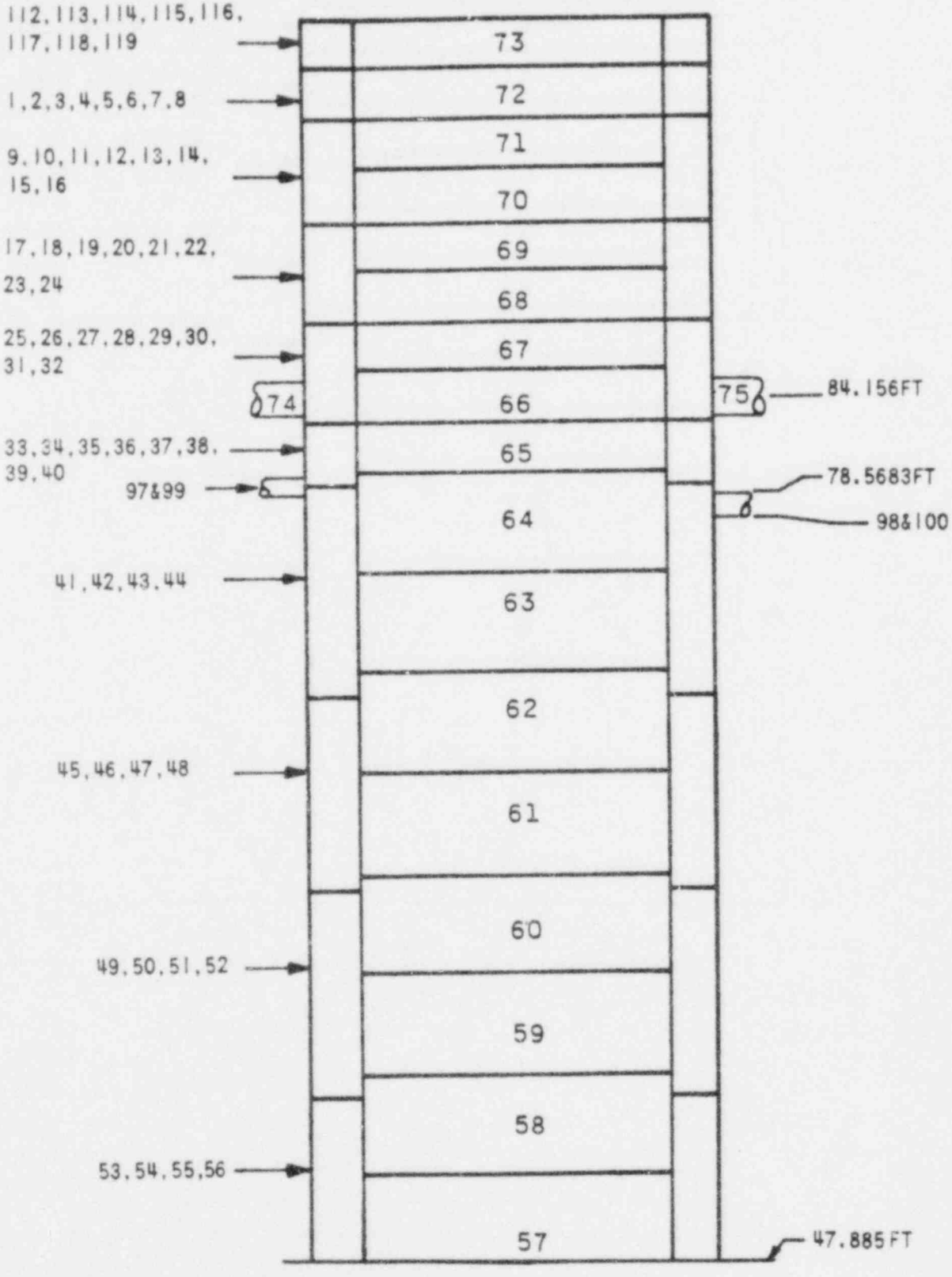

Figure 3-12. Developed View of Steam and Feedwater Annuli

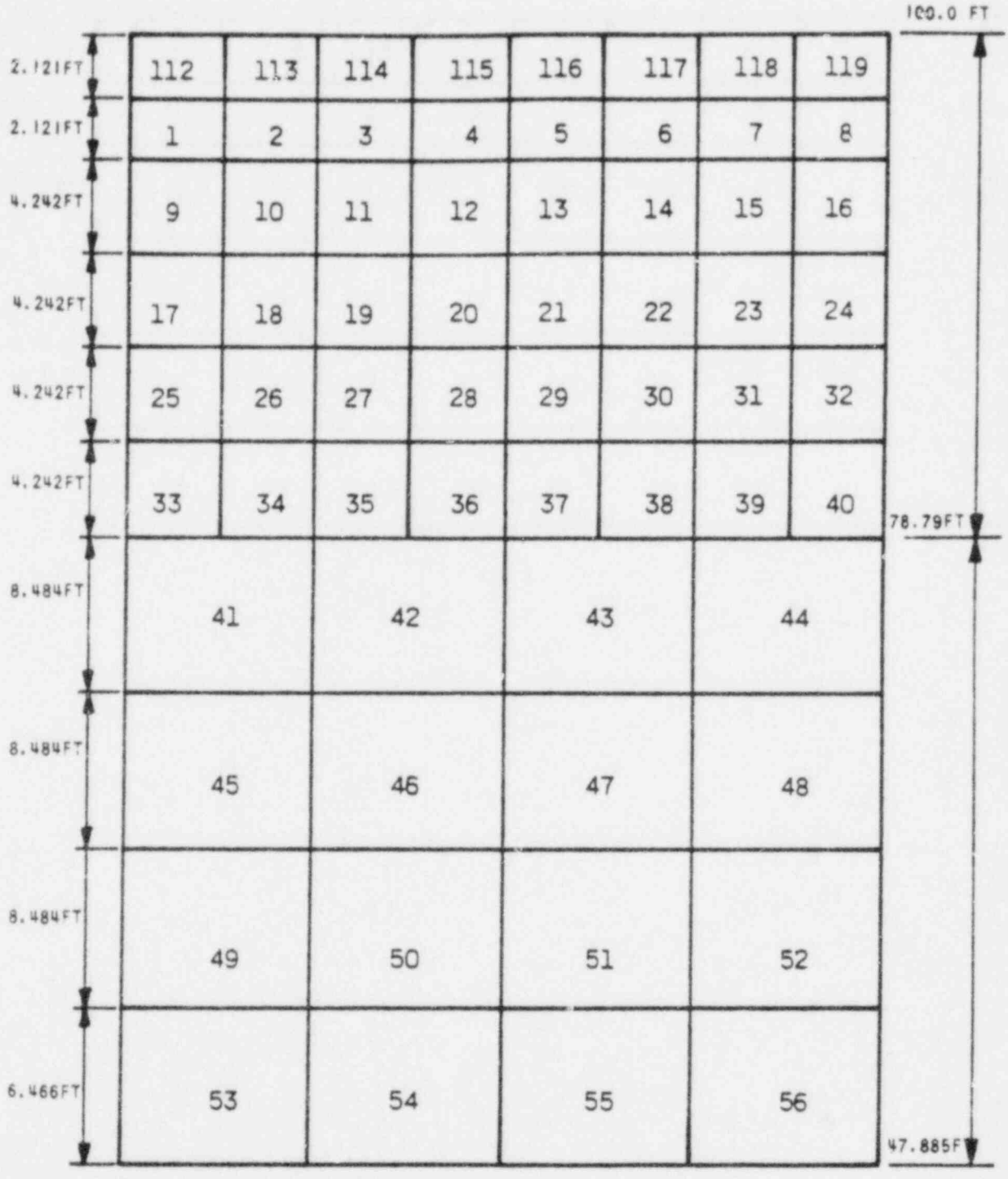

Figure 3-13. Top View of OTSG

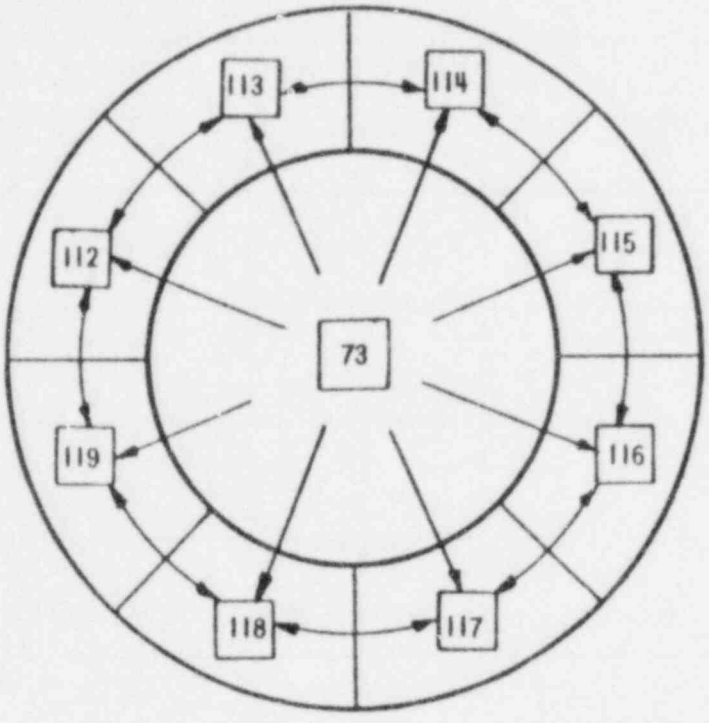

Figure 3-14. Cross Section of Feedwater/Steam Outlet Diagram

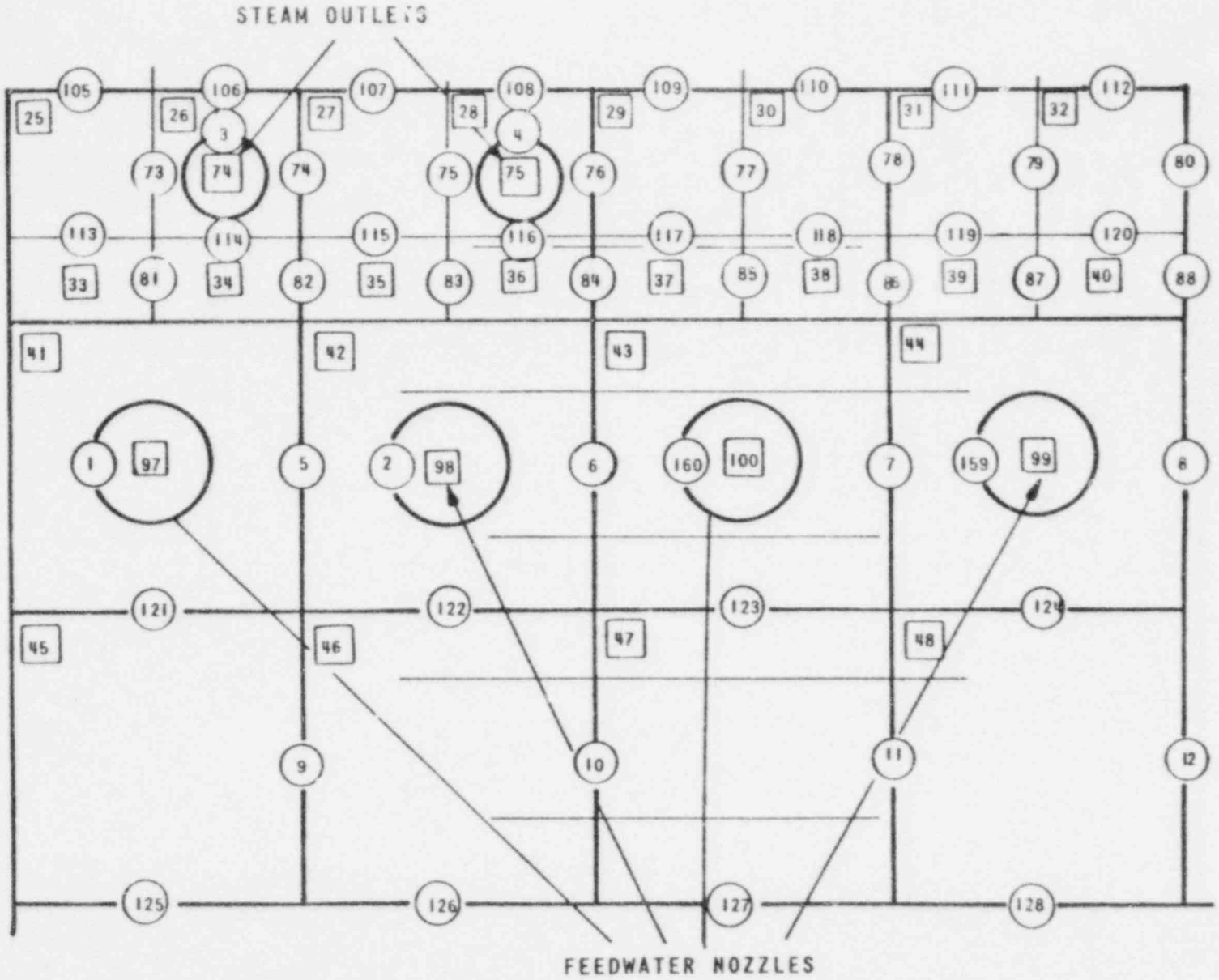

Figure 3-15. Steam Line Noding Diagram

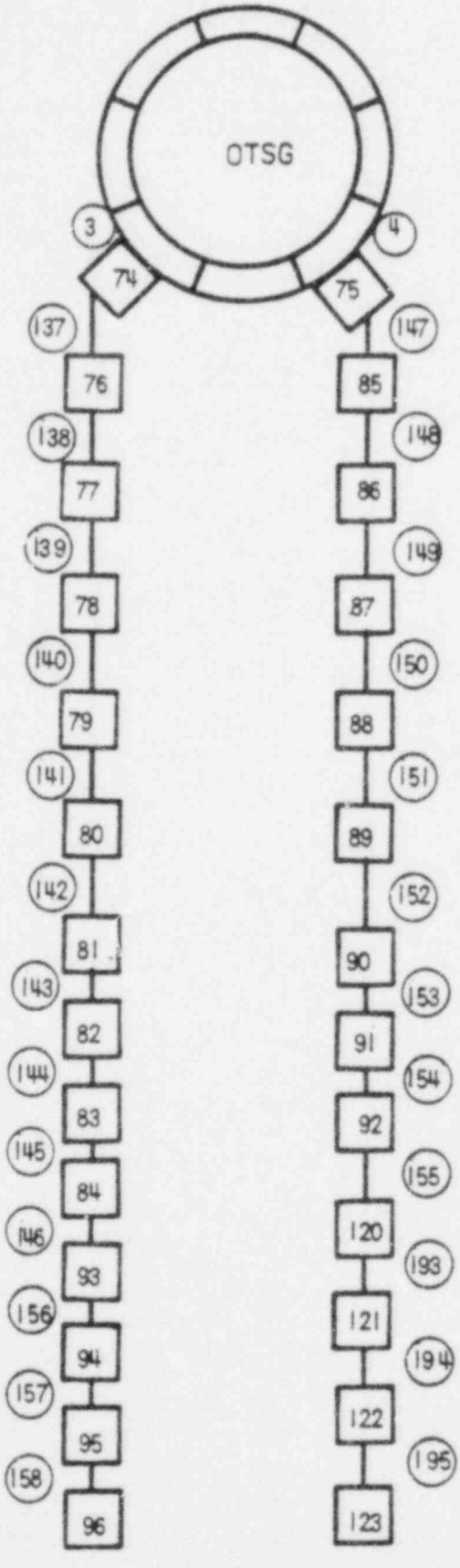

Figure 3-16. Feedwater Line Noding Diagram, Model No. 2

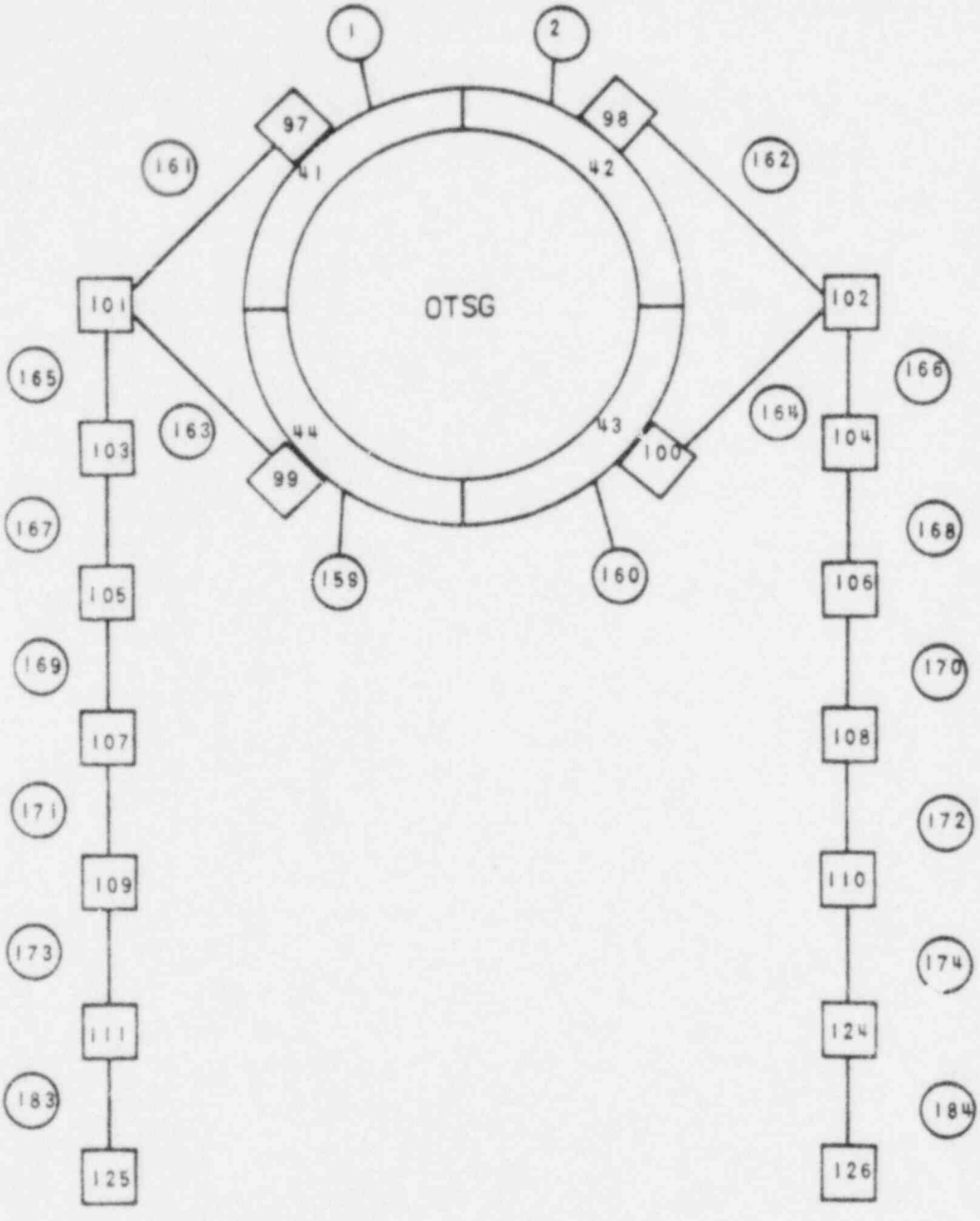

Figure 3-17. OTSG Tube Pattern Arrangements

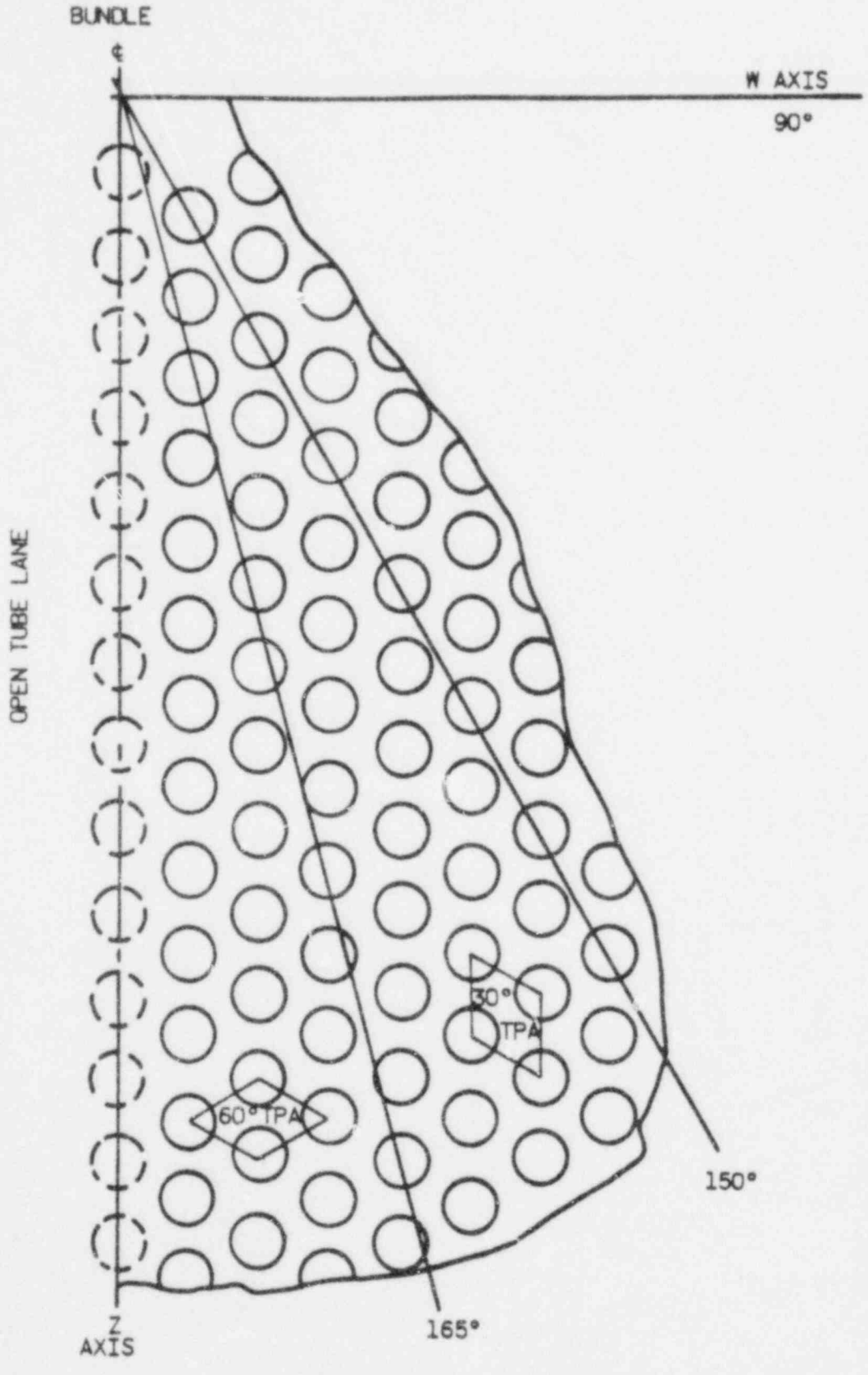

Figure 3-18. Load on OTSG Shroud for Single MSLB

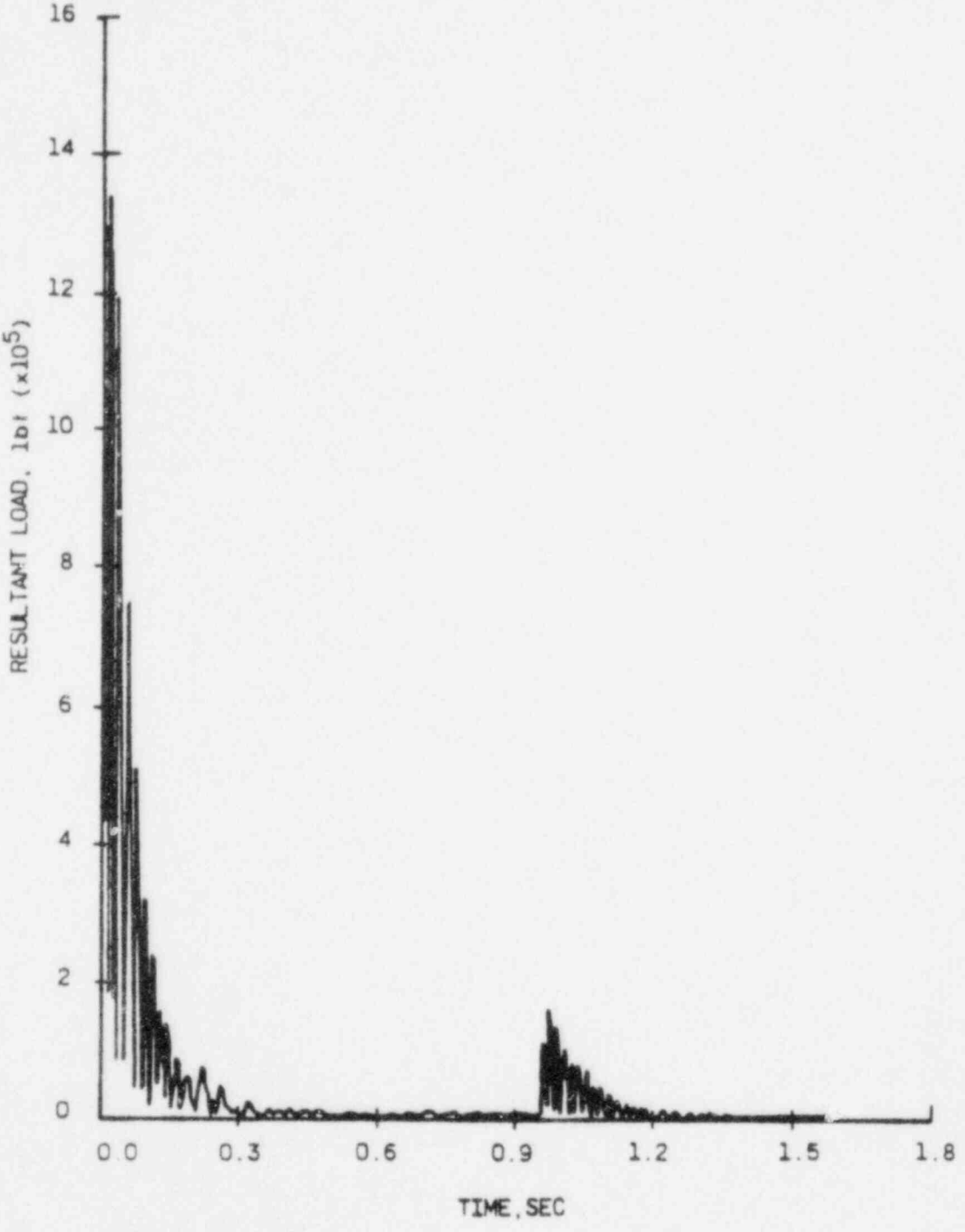

Figure 3-19. Load on OTSG Shroud for Double MSLB

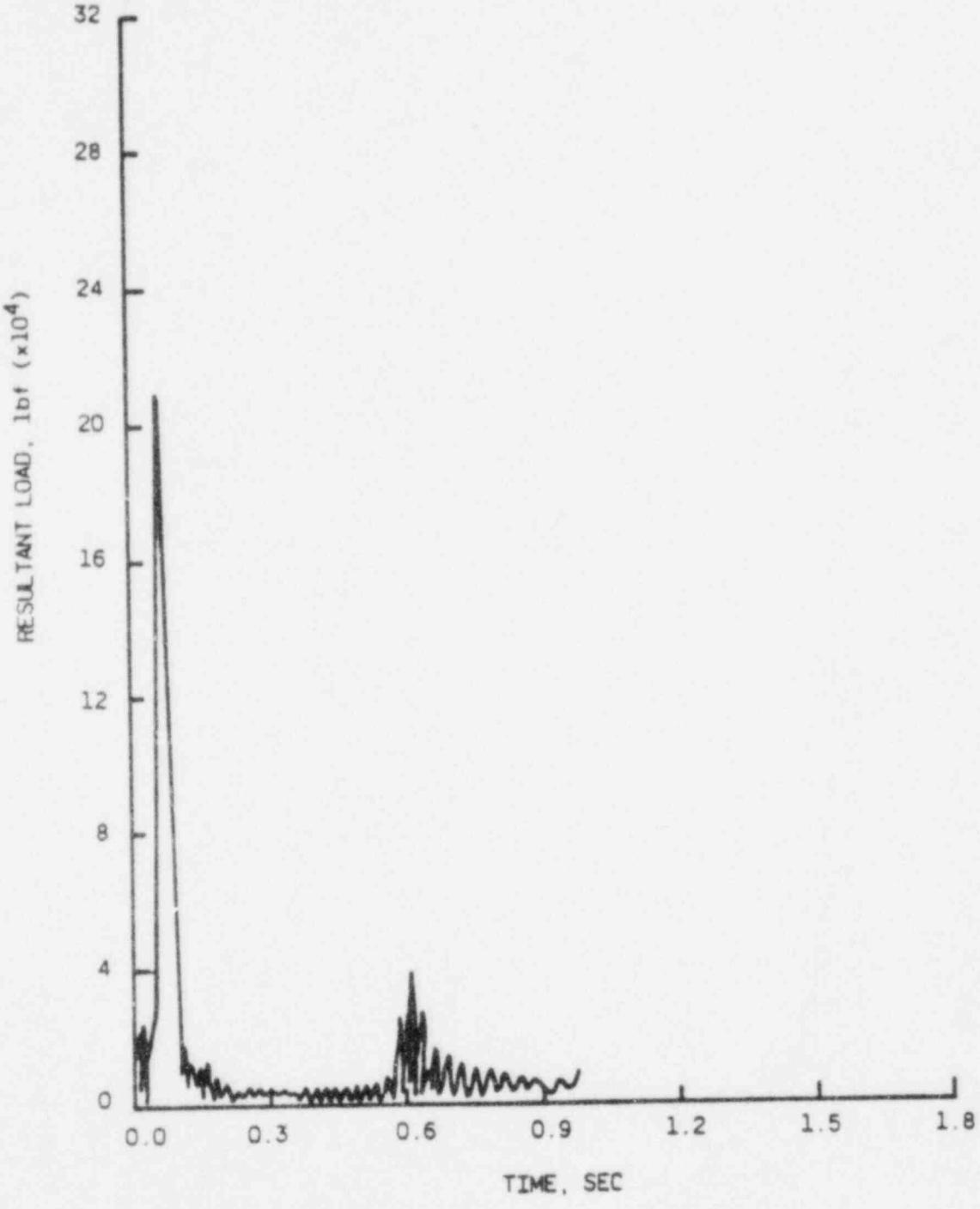

Figure 3-20. TRAP2 Model of NSS

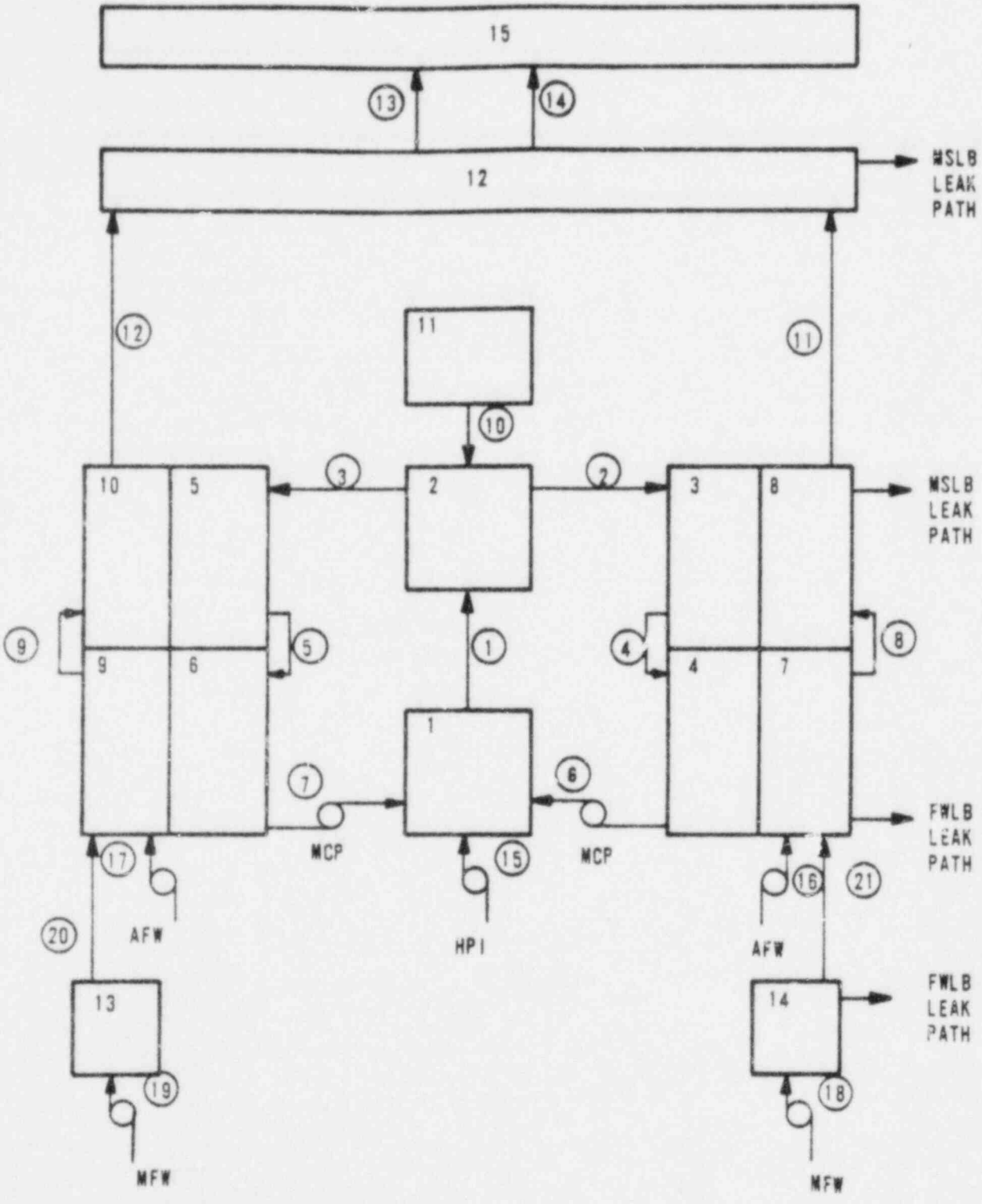

4. DYNAMIC STRUCTURAL RESPONSE

Draft Regulatory Guide 1.121[8] states the position that the minimum acceptable tube wall thickness for steam generator tube plugging criteria should be based in part on ensuring tube integrity during postulated design basis accidents. This section addresses the dynamic structural response of the OTSG components and supports to a safe shutdown earthquake, a primary piping LOCA, main steam line breaks, and feedwater line breaks. The results from this section are used in section 5 to calculate the stresses caused by these design basis accidents. It was convenient to provide these results in some cases as displacement profiles and in other cases as forces.

All of the dynamic structural analyses supporting the operating licenses of the B&W 177-FA operating plants were performed before the development of the analytical methods used today.[9] Two dynamic structural analyses of 177-FA reactor coolant systems (Midland and Davis-Besse) using current methodology were in progress concurrently with the work performed for this report, but neither contained the conservatism desired for an Owners Group generic approach.

It was anticipated that the dynamic loads on the OTSG tube bundle from postulated design basis accidents would play a minor role in defining the minimum acceptable tube wall thickness. Therefore, it was possible to draw from the data base of 205- and 145-FA analyses to estimate tube loads. Table 4-1 lists the specific analyses used. The loads were estimated in a manner that ensured that a detailed analysis of operating OTSGs would produce lower loads. The results of the stress analysis later demonstrated that a detailed dynamic structural analysis would provide no significant benefit since the dynamic loads are relatively small compared to the thermal loads.

In order to use the dynamic structural response of a different OTSG analysis in estimating 177-FA OTSG loads, several points must be shown: the similarity of the OTSGs, the conservatism of the seismic spectra used to calculate the

SSE response, and the conservatism of the forcing functions used to calculate responses to LOCA, MSLB, and FWLB.

4.1. Similarity of OTSG Designs

All three OTSG designs, whether for 145-, 177-, or 205-FA systems, have similar basic dimensions as shown in Figure 4-1. The support and restraint schemes are similar, with [redacted] support provided at the upper belt and at the base, and vertical su[redacted]he base. Primary piping inlet and outlet locations are practically [redacted]. The configurations of the OTSG internals are similar, with all hav[redacted]dle of straight-through tubes welded at each end to massive tubesheets, [redacted]rted laterally at intermediate elevations by broached support plates and enclosed by a shroud. The shroud is fixed to the outer shell at the steam-feedwater separation and supported laterally at intermediate elevations by alignment pins from the shell. Figure 4-2 illustrates the structural model of a 145-FA OTSG, which was a readily available and suitable model of OTSG internals. All OTSG designs are similar in that the support plate and alignment pin placements leave only short free-span lengths for the shroud and tube bundle. This is significant in limiting the dynamic response of the tubes.

The fact that the 177-FA OTSG has a middle elevation steam and feedwater nozzle belt that differs from the lower elevation (integral economizer) design of the 145- and 205-FA OTSGs serves to stiffen the shell between the upper and lower tubesheets. The effect of this difference on MSLB results will be discussed later. The location of the OTSG with respect to the rest of the RCS leads to the nomenclature of a "raised-loop" plant when the OTSG is elevated so that the reactor coolant (RC) pumps are near the OTSG base, and a "lowered loop" plant when the OTSG is lowered so that the RC pumps are near the middle of the OTSG. Regardless of the arrangement, comparison of LOCA results between the two types has shown that the similarity of primary piping inlet and outlet locations controls the results for the OTSG. SSE results depend on the spectral excitation of the OTSG itself, and if the spectra used in the design case envelop spectra from both raised- and lowered-loop plants, the elevation of the OTSG is not significant.

4.2. Conservatism of Seismic Spectra

The spectra used in calculating seismic response were derived from the floor response spectra that were developed specifically for the B&W standard plant (Std-205). As described in the standard safety analysis report, these spectra are selected to encompass 60 to 75% of the United States.[10] Comparison of the horizontal spectra in Figures 4-3 and 4-4 illutrates the degree of conservatism involved in this approach for the Owners Group of operating plants. The peak acceleration level used is approximately four times that of the highest operating plant (Rancho Seco), and the ground acceleration level is approximately two times higher. Vertical spectra compare similarly.

4.3. Conservatism of Forcing Functions

The forcing functions used to calculate LOCA response are those of a 205-FA reactor coolant system. Examination of OTSG loads due to all LOCA cases demonstrated that the controlling cases for OTSG loads are those designated HTL-5, HTL-6, HTL-7, and LCL-6 as shown in Figure 4-5. These are the cases that cause the worst lateral and longitudinal excitation of the OTSG, principally by thrust. The other LOCA forcing functions calculated for the Owners Group OTSGs were compared to the 205-FA forcing functions used in the Std-205 LOCA analysis. The peak forces affecting the tubes and the associated dynamics of the forcing functions indicated that the Std-205 results could be used in lieu of a unique 177-FA LOCA analysis.

The MSLB and FWLB had not been analyzed previously for structural response. Therefore, a special analysis was performed using forcing functions for a 177-FA OTSG with a middle elevation steam and feedwater nozzle beat.

Since the basis for the conservative estimate of dynamic structural response for all 177-FA OTSG tubes has already been described, the remainder of this section states the analytical assumptions, describes the computer codes used in the analyses, and reports the results from SSE, LOCA, MSLB, and FWLB.

4.4. Assumptions

The following assumptions have been used in estimating the dynamic structural response:

1. There is enough conservatism in the analytical approach to allow for differences in OTSG configuration, support stiffness, and mathematical modeling techniques.

2. Differences in tube axial LOCA loads due to different blowdown characteristics of the 177-FA versus the 205-FA RCS are negligible. This assumption refers to the fact that the hot leg temperature of the 177-FA RCS is lower than that of the 205-FA RCS and causes higher vertical loads in the 177-FA OTSG for HTL-7.

3. The RCS and OTSG internals behave in a linear, elastic fashion for such relatively large-displacement events as the design basis accidents discussed here.

4.5. Computer Codes

The following computer codes were employed in calculating the dynamic structural response:

ST3DS, LUMS – These codes form a combination describing the static and dynamic behavior of structural systems that can be modeled with beam and lumped mass finite elements. ST3DS performs a flexibility and static load analysis of the system, while LUMS performs a dynamic analysis of the system subjected to time-dependent loading or acceleration spectra excitation. These codes, which have been accepted by the NRC, operate in the sequence illustrated in Figure 4-6.

The following pre- and post-processor codes were also used:

STDEC – This is a multipurpose data card image manipulator in its pre-processor role. As a post-processor, it combines data from ST3DS and LUMS and provides modal composite damping spectra interpolation, force-time history resolution, and modal response combinations for closely spaced modes.

INTFCE – Converts pressure-time history data into force-time history data for structural loading application.

4.6. Seismic Results

Dynamic structural response to SSE excitation was calculated by the response spectra method using the Std-205 RCS model and spectra. The RCS model did not have enough detail to show the OTSG tube response specifically; therefore, it was necessary to correlate the RCS results with 205- and 145-FA OTSG substructure models as follows:

1. The mode shapes of the various OTSG components in the substructure models were examined. The modes contributing the most to tube displacement were found to be the first two system modes, each of which had the same mode shape in orthogonal lateral directions and was approximately equal to the first vibrational mode of a fixed-fixed beam between the upper and lower tubesheets. Furthermore, the tubes, shroud, and shell were displacing in unison.

2. Since the results from the RCS model represent the total OTSG behavior, the relative displacements from upper tubesheet, middle elevation, and lower tubesheet were used to define the magnitude of an OTSG tube's peak displacement in the shape described previously.

3. Axial tube forces from both RCS and substructure models were calculated to be of comparable magnitude and were taken directly from the substructure model for convenience. The calculated value was multiplied by a factor of 1.2 to allow for modeling differences that could affect the results.

The RCS displacements used were calculated using Rosenbluth's weighted double-sum method for all modes. This fact, combined with the applied factor of 1.2, introduced additional conservatism for the assumed displacement profile. The maximum differential displacements between the tubesheets and the middle elevation for each of two orthogonal horizontal directions were then combined using a root mean square approach to obtain the peak tube displacement. Rotations of the tubesheets were examined and found to be negligible.

The response of the entire tube bundle was calculated, and the results for the SSE event were reported as an OTSG tube with the displacement profile of a fixed-fixed beam and a peak midspan displacement of 1.827 inches. The peak axial force per tube was 63 pounds.

4.7. LOCA Results

Dynamic structural response to LOCA events was calculated by the time history method using the Std-205 RCS model and forcing functions. The approach taken for reporting SSE results, that of a peak displacement and a displacement profile, was also taken for LOCA results. The computer codes and methodology are shown in Figure 4-6.

Of the four LOCA events mentioned previously as causing high OTSG responses, LCL-6 (the outlet nozzle guillotine) causes the highest differential displacement between the OTSG midspan and the upper or lower tubesheets. HTL-7, the inlet nozzle guillotine, causes the highest axial tube loads. Conservatism in the reported results arises from combining the worst effects of two independent LOCA events and from an applied factor of 1.2.

The LOCA analysis was performed on the RCS model; therefore, the portion of OTSG axial load carried by the tubes had to be hand calculated. This was done by simply considering the stiffness of the OTSG shell compared to that of the tube bundle and distributing the load appropriately. The shroud is not attached to the upper and lower tubesheets and thus does not bear axial load. The results for the LOCA event were reported as a peak midspan displacement of 0.1225 inch and a peak axial force per tube of 274 pounds.

4.8. MSL/FWL Break Results

The analyses for the MSLB and FWLB were performed using the 145-FA OTSG substructure model (because it was applicable and readily available) and blowdown pressure-time histories from a 177-FA OTSG with mid-elevation steam and feedwater nozzles. The forces due to the blowdown were applied to the 145-FA OTSG model as if the MSL and FWL nozzles were at the middle elevation of the 177-FA OTSG without compensating for the generally smaller OTSG. Although the internal configurations of the two OTSGs are different, the tube bundle loads depend mainly on the points of load application and the load distribution by stiffness paths. The application of peak pressure differentials at the midspan produces larger displacements than would have been produced by applying them nearer the end. The ratio of shell-to-tube bundle bending stiffnesses was calculated for both 145- and 177-FA OTSGs. The ratios are both on the order of 10^4 magnitude, with the 177-FA OTSG shell providing a stiffer load path in relation to its tubes than the 145-FA OTSG. Therefore, the loads calculated for the 145-FA bundle are higher than they would have been if the shell-to-tube bundle stiffness had been the same as that of the 177-FA OTSG.

Blowdown pressure-time histories were provided for three secondary side break cases: a single MSL OTSG nozzle guillotine, a guillotine of the MSL downstream from the Y-connection of the two OTSG MSL piping runs, and a guillotine of a FWL nozzle at the feedwater header. The pressure-time histories were converted to force-time histories on various OTSG internal components by

integrating the pressure from each node of the hydrodynamic model over the associated area of the internal component. The force-time histories for the three breaks were then compared, and it was found that the single MSL OTSG nozzle guillotine break produced peak forces at least an order of magnitude greater than the FWL guillotine break and approximately the same as the other MSL guillotine break. The single MSL OTSG nozzle guillotine break forces were used to calculate the dynamic structural response of the OTSG internals.

The peak differential displacement between the tubesheets and the tube bundle due to the MSLB was 0.0525 inch. Since this is only 3% of the combined SSE and LOCA results, and it is the worst secondary break case for internals pressure loading, no further calculations of secondary break structural dynamic response were deemed necessary.

4.9. Summary

Conservative estimates of the dynamic structural response of a 177-FA OTSG to a concurrent SSE and LOCA were developed for use in the stress analysis of the OTSG tubes. MSLB and FWLB accidents were considered and found to produce negligible responses compared to the combined SSE and LOCA response. SSE results were reported as a 1.827-inch peak midspan differential displacement of the tube as a fixed-fixed beam and an axial load of 63 pounds per tube. LOCA results were reported as 0.1225 inch and 274 pounds. The combined SSE plus LOCA results are a displacement of 1.95 inches and an axial load of 337 pounds.

Table 4-1. Data Base for Estimating Loads

Results	Source analysis	Remarks	
Seismic	STD-205	STD-205	structural RCS model
		STD-205	isolated structural OTGS model
		STD-205	seismic spectra
LOCA	STD-205	STD-205	structural RCS model
		STD-205	forcing functions
MSL/FWL breaks	Unique for Owners Group	145-FA	isolated structural OTSG model
		177-FA	OTSG forcing function

Figure 4-1. OTSG Comparison

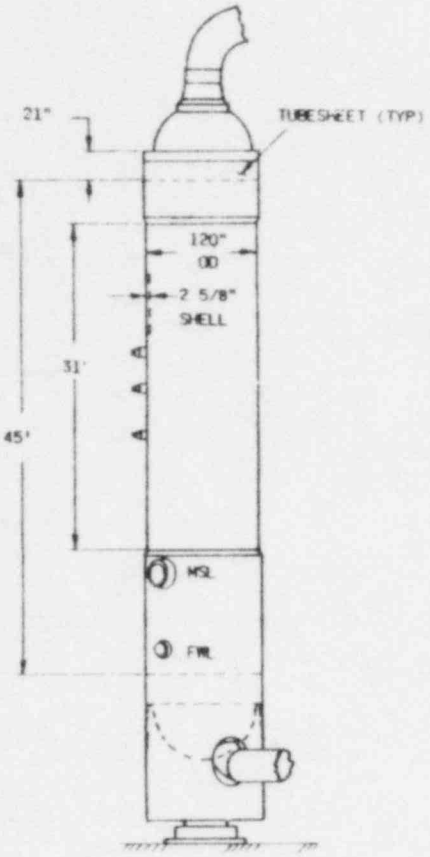

145 FA OTSG

OPERATING WEIGHT = 670 KIP

TOTAL # OF TUBES = 10030

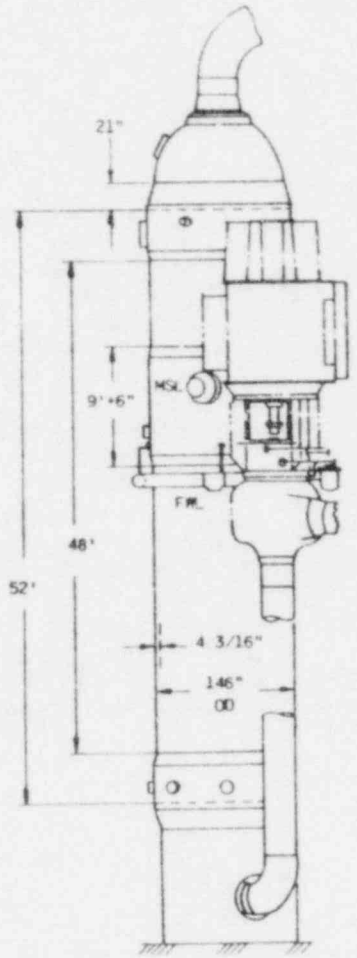

177 FA OTSG (LOWERED LOOP)

OPERATING WEIGHT = 1310 KIP

TOTAL # OF TUBES = 15457

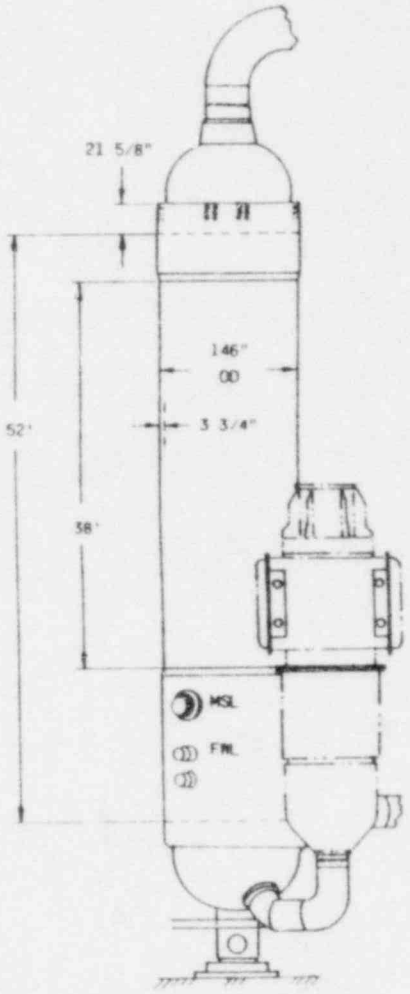

205 FA OTSG (RAISED LOOP)

OPERATING WEIGHT = 1560 KIP

TOTAL # OF TUBES = 16000

ALL TUBES, OD = 0.6250", ID = 0.5570"

Figure 4-2. Structural Model of 145-FA OTSG

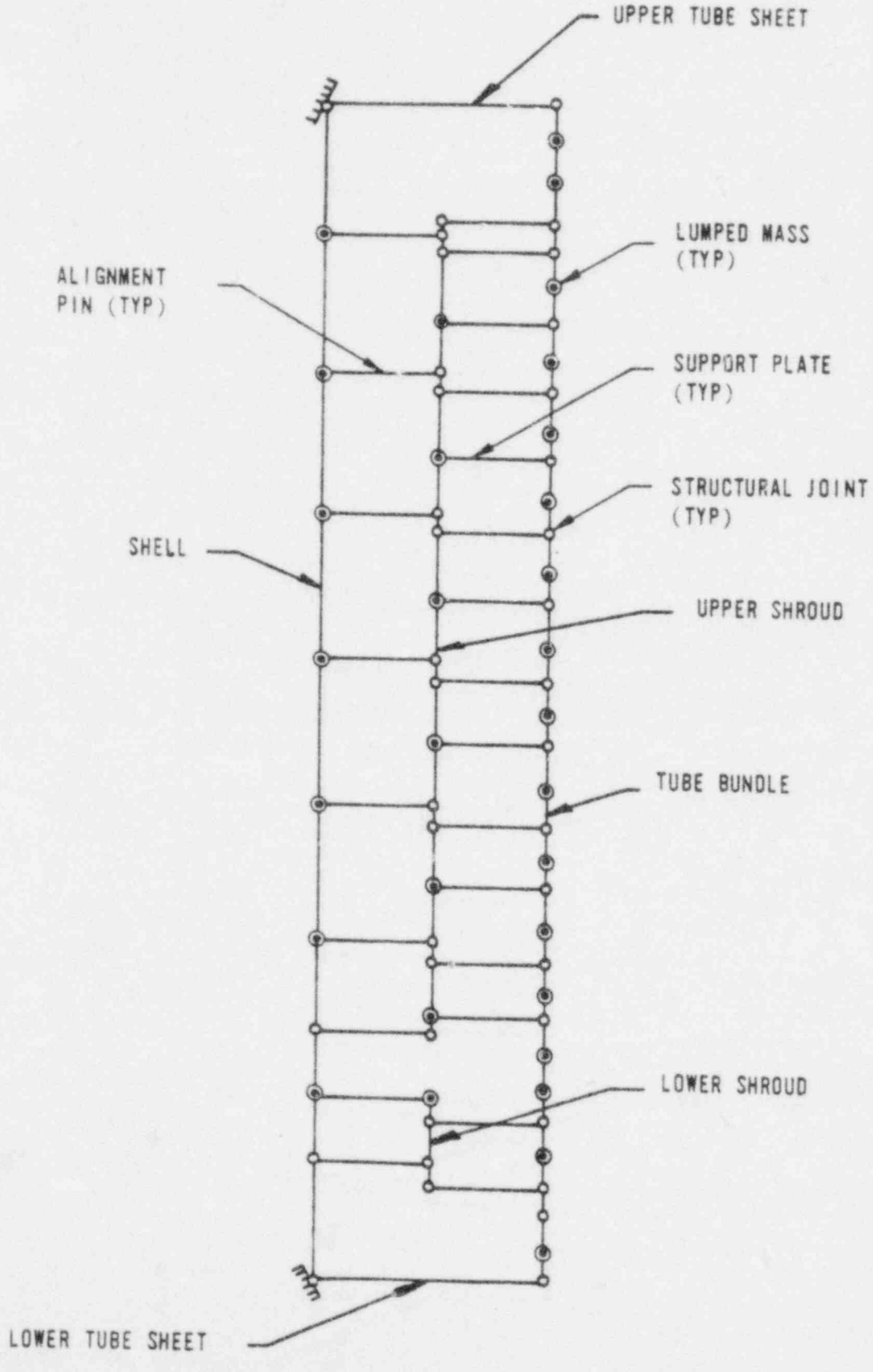

Figure 4-3. Horizontal Spectra for SSE — B-SAR-205

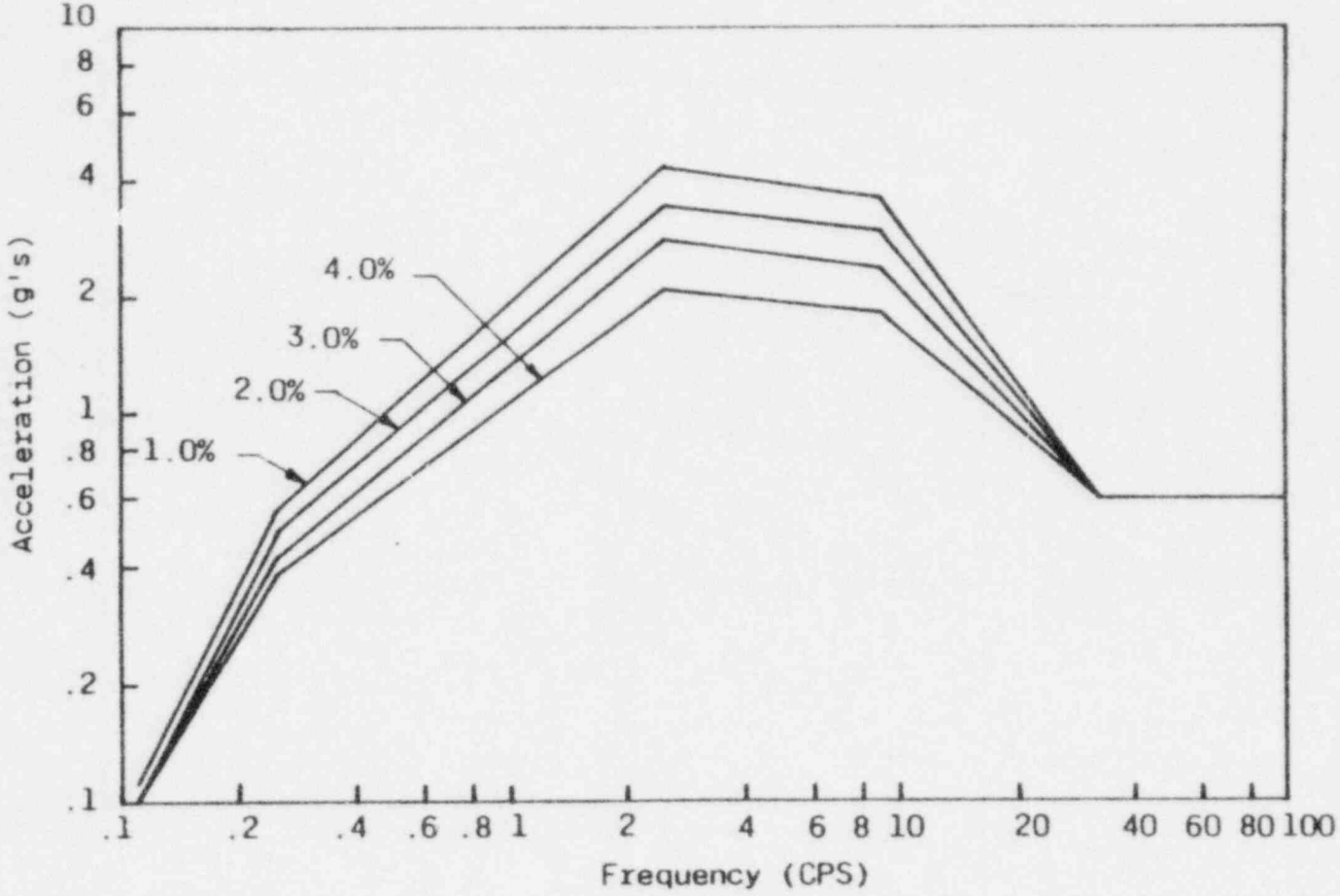

Figure 4-4. Horizontal Spectra for SSE — Rancho Seco

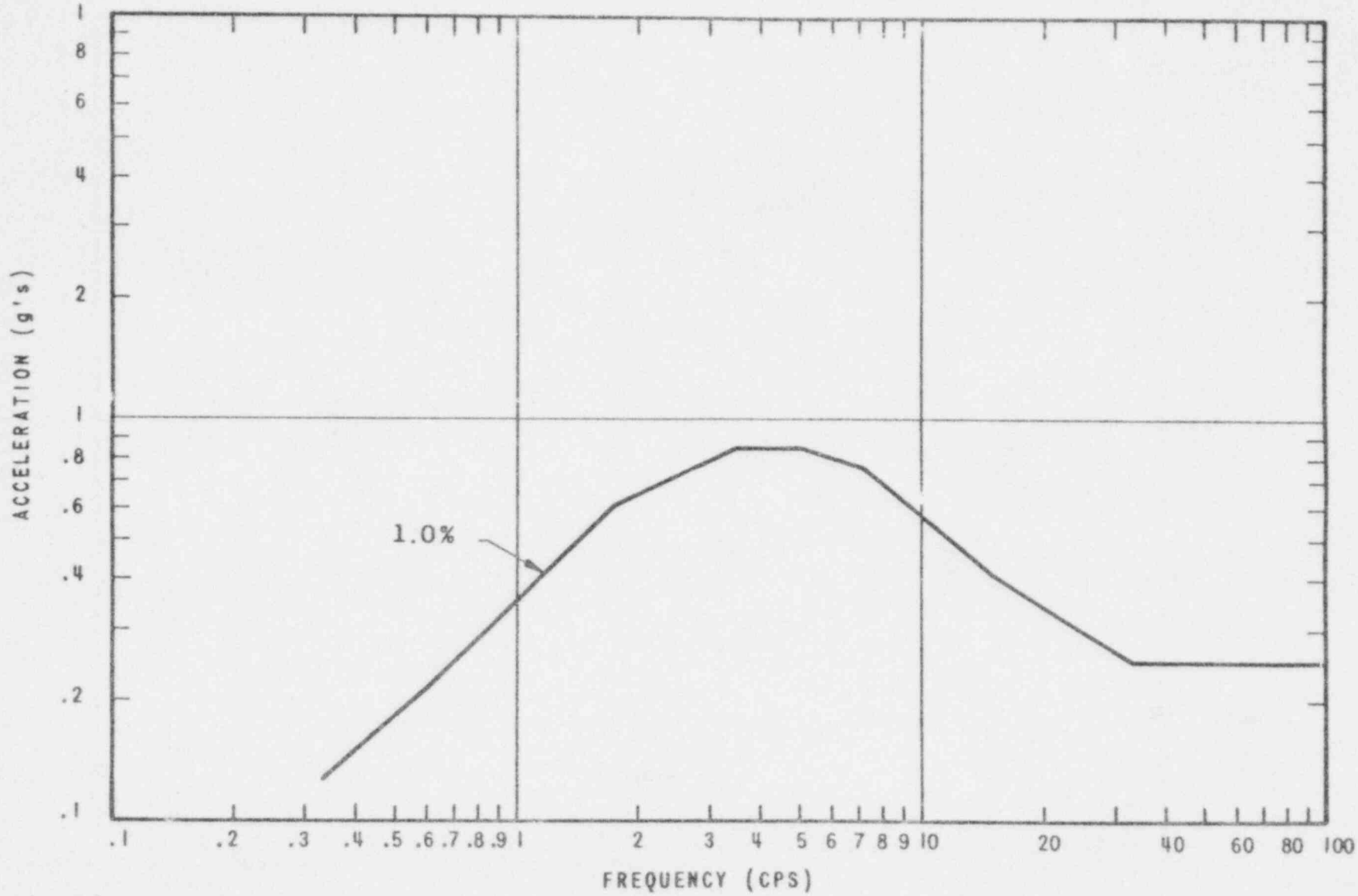

Figure 4-5. LOCA Designation

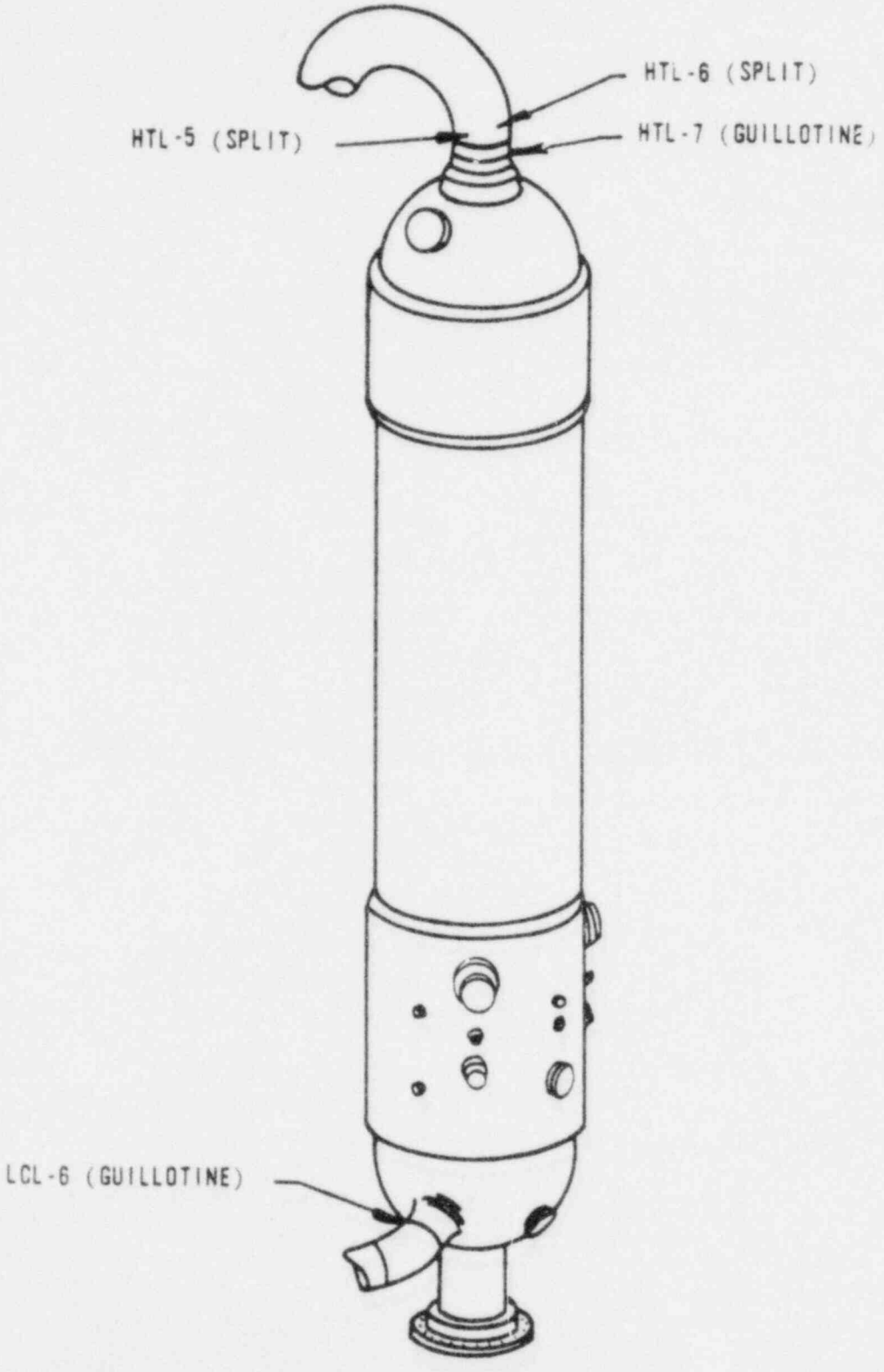

5. OTSG TUBE LOADS

Tube loads were calculated for normal operating and faulted conditions. Normal operating tube loads were determined using design operating transients and are combined with the tube geometry in section 6.2 to calculate minimum allowable tube wall thicknesses that satisfy the acceptance criteria of Draft Reg. Guide 1.121.[8] Faulted condition tube loads are those arising from a safe shutdown earthquake (SSE), a loss of coolant accident (LOCA), a main steam line break (MSLB) and and a feedwater line break (FWLB); loads were determined using the pressures, temperatures, and displacements presented in sections 3 and 4. These loads were used in Section 6.3 to calculate minimum wall thicknesses based on the limits of draft Reg. Guide 1.121[8] and Appendix F of the ASME Code, Section III.[11]

Flow-induced vibration loads (in the form of tube bending moments) were calculated from data obtained during an OTSG field measurement program. Dynamic loads were calculated from a "worst-case" deformation mode shape for the combined LOCA and SSE accident condition. Axial tube loads resulting from OTSG pressure and thermal loading conditions were determined using the MSC/NASTRAN computer program[12] and representative finite element models. Section 5.1 describes the finite element models used to calculate these axial tube loads.

5.1. Description of Models

Three basic models were used in the process of determining tube loads once primary and secondary OTSG fluid pressures and temperatures were established. The first, a three-dimensional thermal model, was employed to obtain equivalent axisymmetric convection film coefficients at the outer edge of the tubesheet. These coefficients were input to a second model, an axisymmetric OTSG thermal model, and used to simulate heat transfer between fluid and structure for both steady-state and transient operating conditions. The third, an axisymmetric OTSG structural model which accepts thermal loadings (in the form of metal temperatures) and fluid pressure loadings, was used to obtain tube loads. The following paragraphs describe each of these models in more detail.

5.1.1. Thermal Model for Head-Tubesheet-Shell

Heat transfer through the tubesheets is a three-dimensional phenomenon. In order to include the tubesheets in an axisymmetric heat transfer model of the overall OTSG, it was necessary to represent the tubesheets as solid plates and assume approximate temperature distributions. It was anticipated that the tubesheets could be assumed to be at the temperature of the primary fluid passing through them. Such a uniform temperature distribution was particularly appropriate for steady-state operating conditions and moderate transients, e.g., heatup and cooldown. Two questions then arose:

1. At what radius ($\bar{R}$) should the assumed uniform temperature distribution of the tubesheet terminate?

2. What equivalent convective surface heat transfer coefficients could be used at this assumed outer tubesheet radius to approximate the axial variation of temperature outside $\bar{R}$ assuming that the volume inside $\bar{R}$ is filled with primary fluid?

A three-dimensional heat transfer analysis was performed to address these questions. The model used included the outer peripheral region of the tubesheet and short segments of the adjoining head and shell. The objective of the analysis was to follow the transition from three-dimensional to axisymmetric heat transfer.

Figure 5-1 is an axisymmetric view of the complete three-dimensional model. The tubesheet portion of the model begins at the inside radius of the head and extends inward to include about four tube holes. The model consists of twelve identical 2-inch layers of five- and six-sided elements. A typical tubesheet layer is shown in Figure 5-2. The remaining portion of the three-dimensional model characterizes the thermal characteristics of the head, tubesheet outer ring, and shell using a single depth of elements. It is expected that any non-axisymmetric temperature distribution extending into this portion of the model can easily be accommodated by these three-dimensional elements.

Applying normal steady-state design conditions to the three-dimensional thermal model, it was determined that the effective perforated plate radius used in structural analysis may be conveniently used for the assumed outer tubesheet radius ($\bar{R}$) in an axisymmetric thermal analysis. This radius (designated by R* in structural analysis) is a quarter of a tubesheet hole diameter beyond the radius of the outermost tubesheet hole center. Using average temperatures

and heat fluxes at (or near) $\bar{R}$ for each of the 12 layers of tubesheet elements, equivalent film coefficients were computed for use in the axisymmetric thermal analysis where the temperature within $\bar{R}$ was taken to be that of the primary fluid temperature. The equivalent film coefficients were found by dividing the heat flux (Btu/h-in.^{2}) by the difference between the primary fluid temperature and the average metal temperature at $\bar{R}$.

5.1.2. Axisymmetric OTSG Thermal Model

For known primary and secondary fluid temperatures, OTSG metal temperatures were found using the axisymmetric finite element thermal model illustrated in Figure 5-3 Included in this model were the upper and lower spherical heads, upper and lower tubesheet rings, cylindrical shell, and support skirt. The temperatures of the tubesheets inside the tubesheet rings were assumed to be the same as that of the primary fluid passing through them. The model comprised trapezoidal and triangular ring elements for volumetric heat transfer and conical surface elements for convective heat transfer at the primary and secondary surfaces. The exterior surface of the OTSG was assumed to be perfectly insulated.

5.1.3. Axisymmetric OTSG Structural Model

The geometry of the structural model was very similar to that of the axisymmetric thermal model. The structural model consisted of trapezoidal ring, triangular ring, and truss-type rod elements. The ring elements were used to model the upper and lower spherical heads, upper and lower tubesheets and tubesheet rings, cylindrical shell, and support skirt. Rod elements were used to model the tubes between tubesheets. This was done by dividing the tube bundle into twelve concentric annular regions and calculating the axial stiffness of each group of tubes. Each region was then represented by a single rod element with an equivalent stiffness. These rod elements were also used to simulate tube preload and tube contraction due to internal pressure (Poisson's effect).

Figure 5-4 is an overview of the complete axisymmetric structural model, and Figure 5-5 shows the upper head and tubesheet in more detail. The finite element simulation of the tubesheets was based on an attempt to realistically represent tubesheet stiffness with the fewest number of elements as possible. The placement of grid points dictated the location of the rod elements

representing the tube bundle and thus the manner in which the tube bundle was broken up into 12 concentric annular regions. Figure 5-6 illustrates the arrangement of the rod elements and their attachment points to the upper and lower tubesheets. The boundaries of the 12 tube bundle regions are also noted.

Effectively, the axisymmetric model was constrained only at the base of the support skirt (in the axial and radial directions).

The following static loads were applied to the structural model:

1. Thermal loads in the form of grid point temperatures.
2. Pressure loads on primary and secondary surfaces.
3. Tube loads due to pressure differential (Poisson's effect).
4. Tube preload.

5.2. Tube Loads for Normal Operation

Tube loads were determined for significant operating transients and for flow-induced vibration from steam cross flow in the generator upper span.

5.2.1. Operating Transients Loads

The transients listed in Table 5-1 were selected for inclusion in the study to assess the cyclic life of degraded tubes. Of particular interest were the following transients:

Transient No.	Transient description	Design cycles
1A	Heatup to 15% power	240
1B	Cooldown from 15% power	240
2A	Power change: 0 to 15% power	1,440
2B	Power change: 15 to 0% power	1,440
3	Power loading: 8 to 100% power	48,000
4	Power unloading: 100 to 8% power	48,000

Worst-case tube loads were first determined for each of these transients. The following procedure was used:

1. Perform a steady-state initial condition heat transfer analysis to determine the temperature distribution throughout the OTSG at the beginning of a transient.

2. Perform a transient heat transfer analysis, and determine the critical time during the transient for tube load based on the difference between the average tube and shell temperatures.

3. Perfrom a static structural analysis applying the grid point temperature thermal load, pressure loads, and tube preload.

Figures 5-7 through 5-11 present the transient curves used in the normal operation analysis which were obtained from the functional specification of the OTSG. Table 5-2 lists the times at maximum tube-to-shell ΔT for the transients along with the tube-to-shell temperature difference and the primary and secondary pressures at these times. Tables 5-3 and 5-4 show the results of the axisymmetric structural analysis NASTRAN runs for normal operation. Tube loads were calculated at the center of the tubesheet and at the grid point nearest the outermost tube.

5.2.2. Flow-Induced Vibration Loads

Upper span tube displacements were obtained for transient and steady-state conditions during a field measurement program of lane tubes in the Oconee 2B OTSG. The maximum reported displacement, at 1/4 span from the upper tubesheet, was 55 mils peak-to-peak in the fundamental mode shape, which was associated with frequencies in the 60-Hz range. This was for one of four tube samples at approximately 75% power during a transient in which one of the four RC pumps was tripped. The maximum tube vibration determined from preliminalry data of a second, more extensively instrumented plant (TMI-2) was less than 30 mils peak-to-peak at approximately the same axial location. Representing the upper span by a fixed-pinned beam, 46.375 inches long, the maximum measured deflection would produce a maximum upper span bending moment of 53 in.-lb (at the lower surface of the upper tubesheet).

5.3. Tube Loads for Faulted Conditions

Tube loads were calculated for MSLB, LOCA, and FWLB accident conditions considering thermal and pressure loads on the generator. Dynamic loads were determined for these three accidents as well as for a safe shutdown earthquake (SSE). Flow-induced vibration loads were determined for the MSLB accident.

5.3.1. Thermal and Pressure Loads

OTSG temperatures and pressures for accident conditions were determined in section 3. The data (at the time of maximum tube-to-shell ΔTs) used to generate tube loads are summarized below.

Accident cond.	Time, min.	Temperature, F			Pressure, psi	
		Down-comer	Steam annulus	Tube	Pri.	Sec.
MSLB	20	521	575	235	2500	0
LOCA	5	530	575	248	0	925
FWLB	1	536	575	625	2566*	24

Since metal temperatures were already know, no heat transfer analysis was necessary. However, it was convenient to do so merely to generate grid point temperature data for use as input to the structural analysis model. Primary, saturation, and steam ambient temperatures were taken to be equal to the corresponding metal temperatures.

Tables 5-5 and 5-6 present results of the axisymmetric structural analysis NASTRAN runs for accident conditions. Tube loads were calculated at the center of the tubesheet and at the grid point nearest to the outermost tube.

5.3.2. Dynamic Loads

Section 4 shows that the dynamic effects of secondary side pipe breaks (MSLB and FWLB accidents) are negligible. For a combined LOCA and SSE accident, there is a moment load derived from a full-length tube bent into a cosine mode shape with a mid-deflection of 1.95 inches.

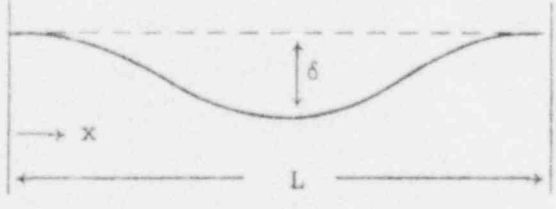

δ = 1.95 in. = mid span deflection

L = 625.375 in. = tube length between tubesheets

I = 0.002765 $in.^4$ = moment of inertia

x = distance from secondary face of tubesheet

---

*The maximum primary pressure of 2696 psi occurs earlier, 40 seconds into the transient.

The moment for such a modeshape is

$$M(x) = \frac{\delta}{2} EI \frac{d^2}{dx^2} \left(1 - \cos \frac{2\pi x}{L}\right)$$

$$= \frac{\delta}{2} EI \left(\frac{2\pi}{L}\right)^2 \cos \frac{2\pi x}{L} .$$

Letting E be 31.7×10^6 psi, and assuming an amplification factor of 2.0 to account for the dynamic response of the tube, the maximum moment is 18 in.-lb. The axial tube load during a combined LOCA and SSE accident is 337 pounds.

5.3.3. Flow-Induced Vibration Loads

Steam cross flow through the upper span of the tube bundle during an MSLB accident could be expected to reach velocities of the order of 1000 fps (section 3). This is far above even the least conservative estimate of Conner's critical velocity for instability in an OTSG. Therefore, it is assumed that the tubes will make contact with one another during a MSLB accident.

Using the assumed flow-induced vibration mode shape of section 5.2.2, the maximum bending moment that could exist in the upper tube span for a maximum displacement of 0.125 inch during tube-to-tube contact is 104 in.-lb.

5.4. Summary of Results

The results of this section, which will be used in the stress analysis in section 6, are summarized in Table 5-7.

Table 5-1. Transients Selected for Normal Operation Analysis

Transient No.	Transient description	Design cycles[a][b]
1A	Heatup to 15% power	240
1B	Cooldown from 15% power	240
2	Power change: 0 to 15% and 15 to 0%	1,440
3	Power loading: 8 to 100% power	48,000
4	Power unloading: 100 to 8% power	48,000
5	10% step load increase	8,000
6	10% step load decrease	8,000
7	Step load reduction (100% to 8% pwr)	310
8	Reactor trip	288
9	Rapid depressuration	40
11	Rod withdrawal accident	40
14	Control rod drop	40
15	Loss of station power	40
17A	Loss of FW to one SG	20
17B	Stuck-open turbine bypass valve	10

[a] For life of plant.

[b] For a specific plant, these are listed in the FSAR; e.g., Table 3.9-2 of the Midland FSAR or Table 5.1-9 of the TMI-2 FSAR.

Table 5-2. Transient Analysis: Critical Times

Transient No.	Critical time, h	ΔT, F	Primary pressure, psi	Secondary pressure, psi
1A	4.725	65	2200	900
1B	2.025	-142	0[b]	0[b]
2A	0.3333	49	2250	900
2B	0.3333	-13	2200	900
3	0.1667	39	2225	885
4	0.3000	10	2200	900

[a] Tube-to-shell temperature difference ($T_{tube} - T_{shell}$).

[b] This conservatively assumes no primary-to-secondary pressure differential. If the actual pressure difference is included, the critical time would occur slightly later, but the stress intesnity would be lower than that reported in Table 5.2.3-1.

Table 5-3. Normal Operation Mechanical Tube Loads

Transient No.	Table temp, F	Tube E, 10^6 psi	δ_d, in.[a]	T-S center δ, in.[b]	T-S center Load, lb[c]	Outermost tube δ, in.[d]	Outermost tube Load, lb[c]
1A	579	29.284	0.100414	-0.068837	87	0.052217	419
1B	350	30.25	0.0336	-0.19448	40	0.010717	65
2A	582	29.272	0.103238	-0.071819	86	0.053230	429
2B	532	29.472	0.099961	-0.068129	88	0.052422	421
3	582	29.272	0.102783	-0.071653	85	0.052461	426
4	558.5	29.366	0.100186	-0.068521	87	0.052557	420

[a] Negative of rod element deformation loading.

[b] Relative displacement between tubesheets at center.

[c] Tube load = $\frac{EA}{L}(\delta + \delta_d)$ where A = 0.063127 in.^{2} and L = 673.375 in.

[d] Relative displacement between tubesheets at outer tubes.

Table 5-4. Normal Operation Total Tube Loads, Mechanical + Thermal

Transient No.	Temp, F	ΔT,[a] F	E, 10^6 psi	α, $10^{-6}/°F$	δ_d,[b] in.	δ,[c] in.	Load,[d] lb	δ,[e] in.	Load[d] lb
1A	579	509	29.284	7.879	0.100414	2.35610	-670	2.31763	-775
1B	350	280	30.25	7.63	0.0336	1.63392	649	1.79519	1107
2A	582	512	29.272	7.882	0.103238	2.43278	-498	2.42292	-525
2B	532	462	29.472	7.832	0.099961	2.31288	-65	2.38819	143
3	582	512	29.272	7.882	0.102783	2.45912	-427	2.46202	-419
4	558.5	488.5	29.366	7.858	0.100186	2.40626	-216	2.44822	-100

(a) Temperature increase above 70F.

(b) Negative of rod element deformation loading.

(c) Relative displacement between tubesheets at center.

(d) Tube load = $EA\left(\frac{\delta+\delta_d}{L} - \alpha\Delta T\right)$ where A = 0.0663127 in.^{2} and L = 673.375 in.

(e) elative displacement between tubesheets at outer tubes.

Table 5-5. Accident Condition Mechanical Tube Loads

Accident condition	Tube temp, F	Tube E, 10^6 psi	δ_d,[a] in.	T/S center		Outermost tube	
				δ,[b] in.	Load,[c] lb	δ,[d] in.	Load,[e] lb
MSLB	235	30.76	0.168096	-0.156090	35	0.026928	562
LOCA	248	30.708	0.027093	-0.060296	252	0.020326	137
FWLB	625	29.05	0.197079	-0.179582	48	0.023533	601

[a] Negative of rod element deformation loading.

[b] Relative displacement between tubesheets at center.

[c] Tube load = $\frac{EA}{L}(\delta + \delta_d)$ where A = 0.063127 in.^{2} and L = 673.365 in.

[d] Relative displacement between tubesheets at outer tube.

Table 5-6. Accident Condition Total Tube Loads, Mechanical + Thermal

Accident condition	Temp, F	ΔT,[a] F	E, 10^6 psi	α, $10^6/°F$	δ_d,[b] in.	δ,[c] in.	Load,[d] lb	δ,[e] in.	Load,[d] lb
MSLB	235	165	30.76	7.456	0.168096	1.14863	1408	1.74938	3140
LOCA	248	178	30.708	7.477	0.027093	1.41954	1585	1.78655	2641
FWLB	625	555	29.05	7.925	0.197079	2.53706	-620	2.55524	-570

(a) Temperature increase above 70F.

(b) Negative of rod element deformation loading.

(c) Relative displacement between tubesheets at center.

(d) Tube load = $EA\left(\frac{\delta+\delta_d}{L} - \alpha\Delta T\right)$ where A = 0.063127 $in.^2$ and L = 673.375 in.

(e) Relative displacement between tubesheets at outer tube.

Table 5-7. Summary of OTSG Tube Loads

Transient	Pressure, psi			Tube Axial Loads, lb		Moment, in.-lb
	Primary	Secondary	Δp	Mechanical[a]	Total	
1A	2200	900	1300	419	-775	NA
1B	0	0	0	65	1107	NA
2A	2250	900	1350	429	-525	NA
2B	2200	900	1300	421	143	NA
3	2225	885	1340	426	-419	53
4	2200	900	1300	420	-100	NA
MSLB	2500	0	2500	562	3140	104
LOCA	0	925	-925	252	2641	NA
FWLB	2566[b]	24	2542	601	-620	NA
LOCA+SSE	NA	NA	NA	337	NA	18

[a] Excludes thermal loads.

[b] Corresponds to the time of maximum axial load. The maximum primary pressure is 2696 psi.

Figure 5-1. Three-Dimensional Thermal Model, Axisymmetric View

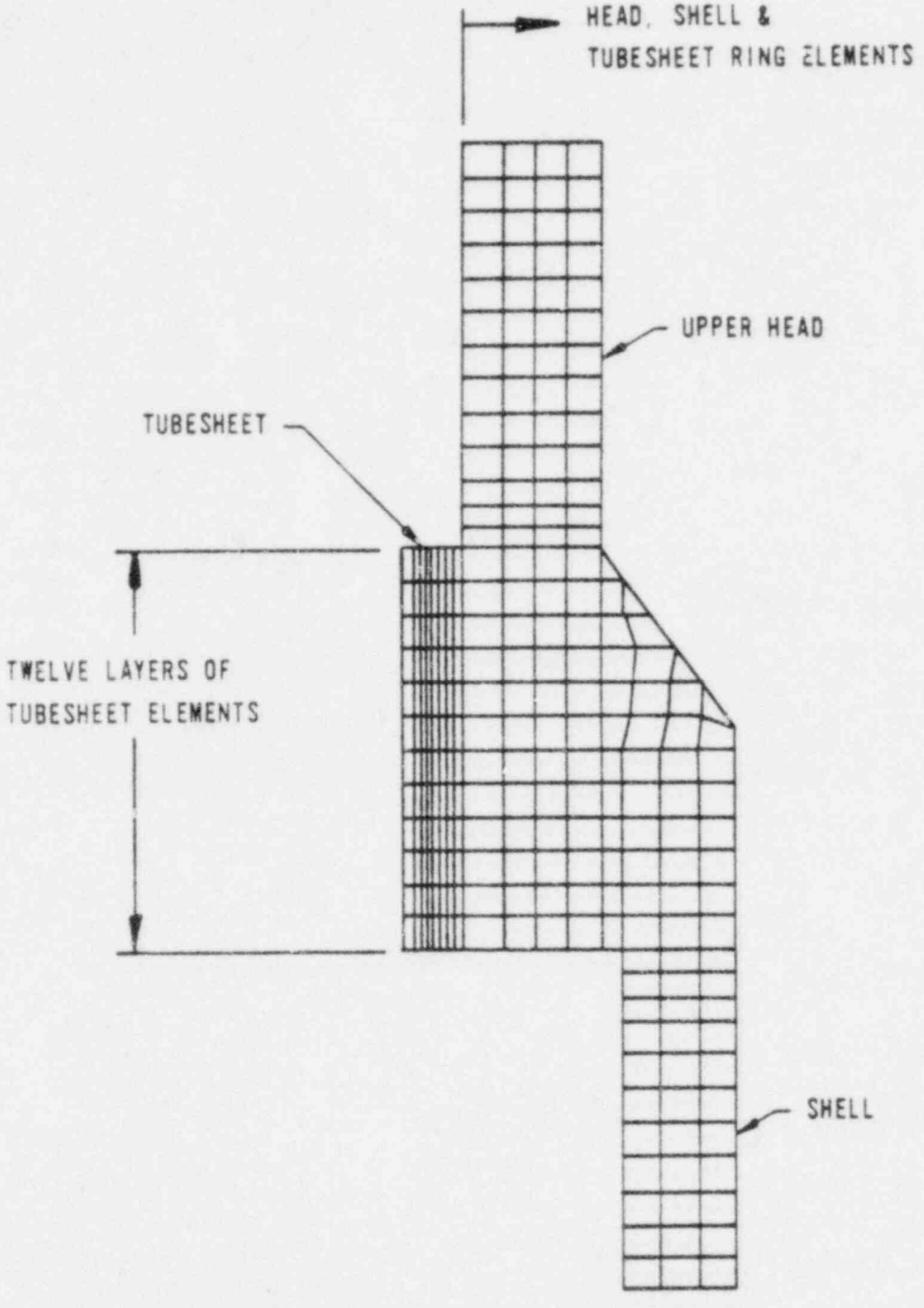

Figure 5-2. Three-Dimensional Thermal Model, Plan View of Typical Tubesheet Layer

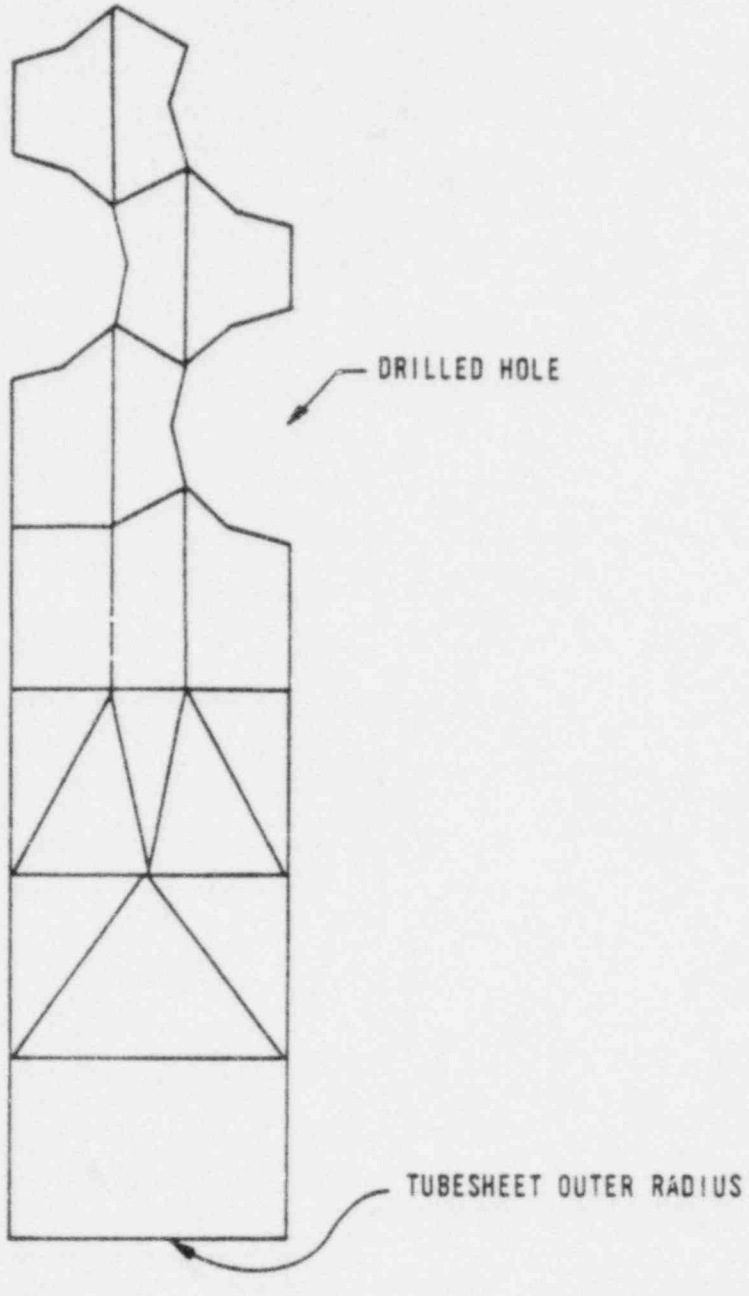

Figure 5-3. Axisymmetric OTSG Thermal Model

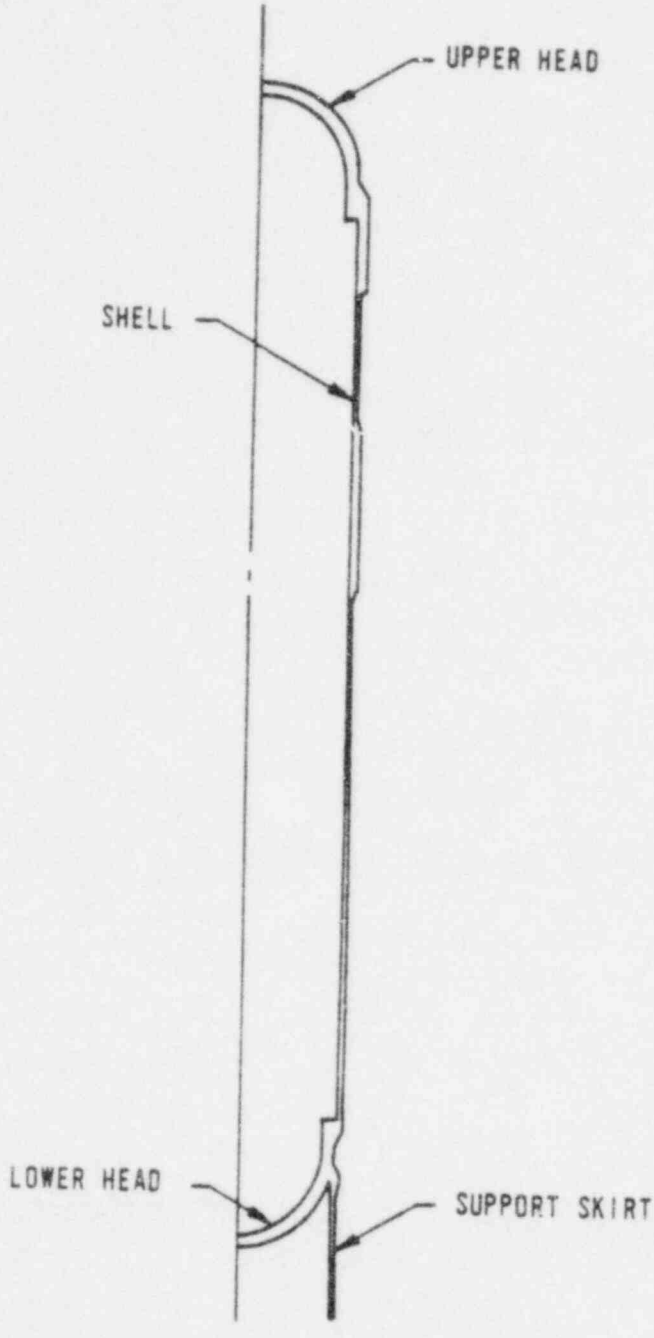

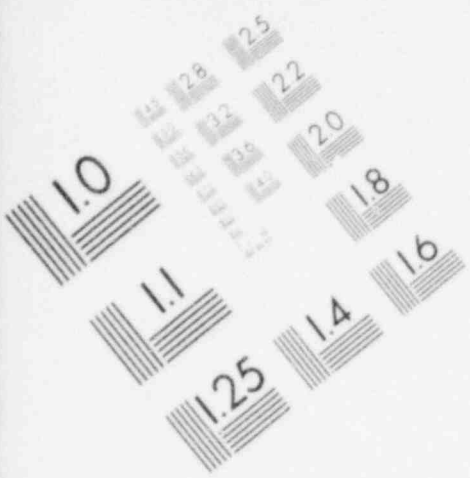

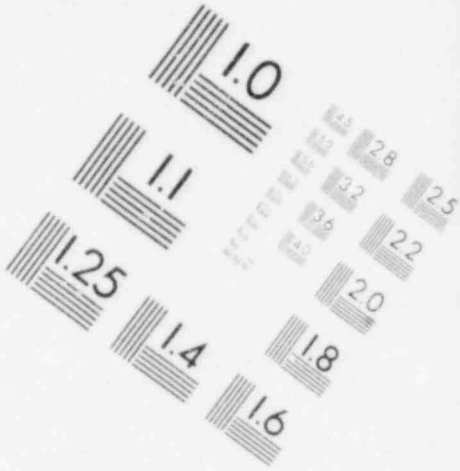

IMAGE EVALUATION
TEST TARGET (MT-3)

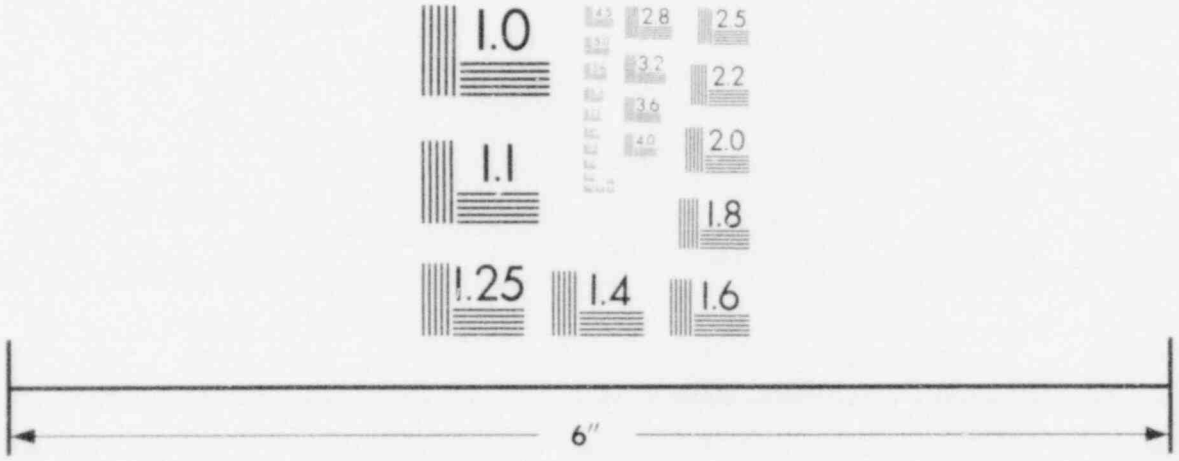

MICROCOPY RESOLUTION TEST CHART

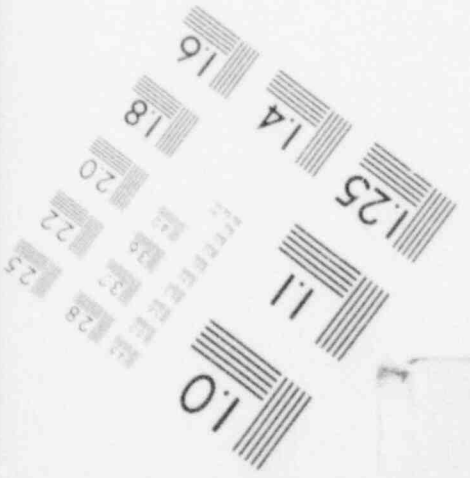

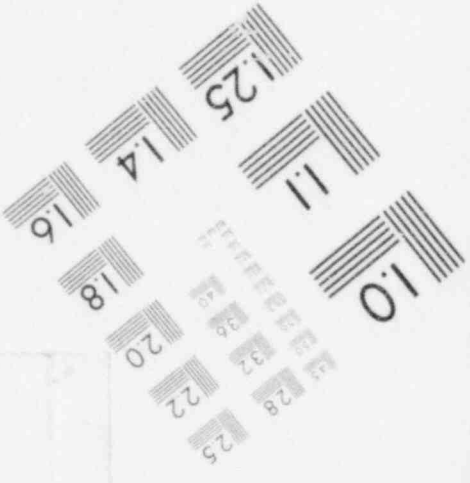

IMAGE EVALUATION
TEST TARGET (MT-3)

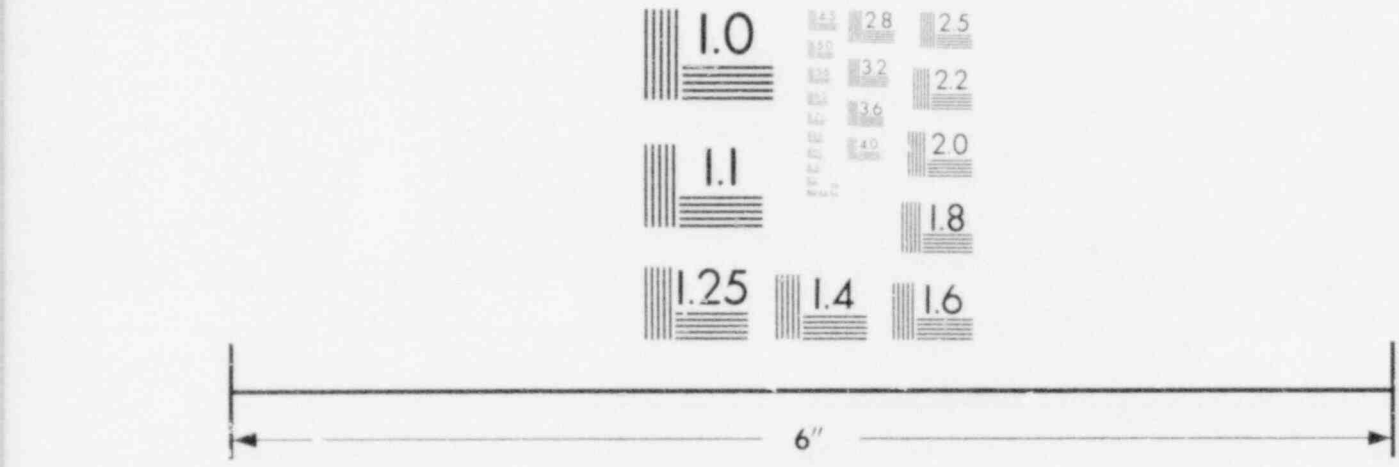

MICROCOPY RESOLUTION TEST CHART

Figure 5-4. Axisymmetric OTSG Structural Model

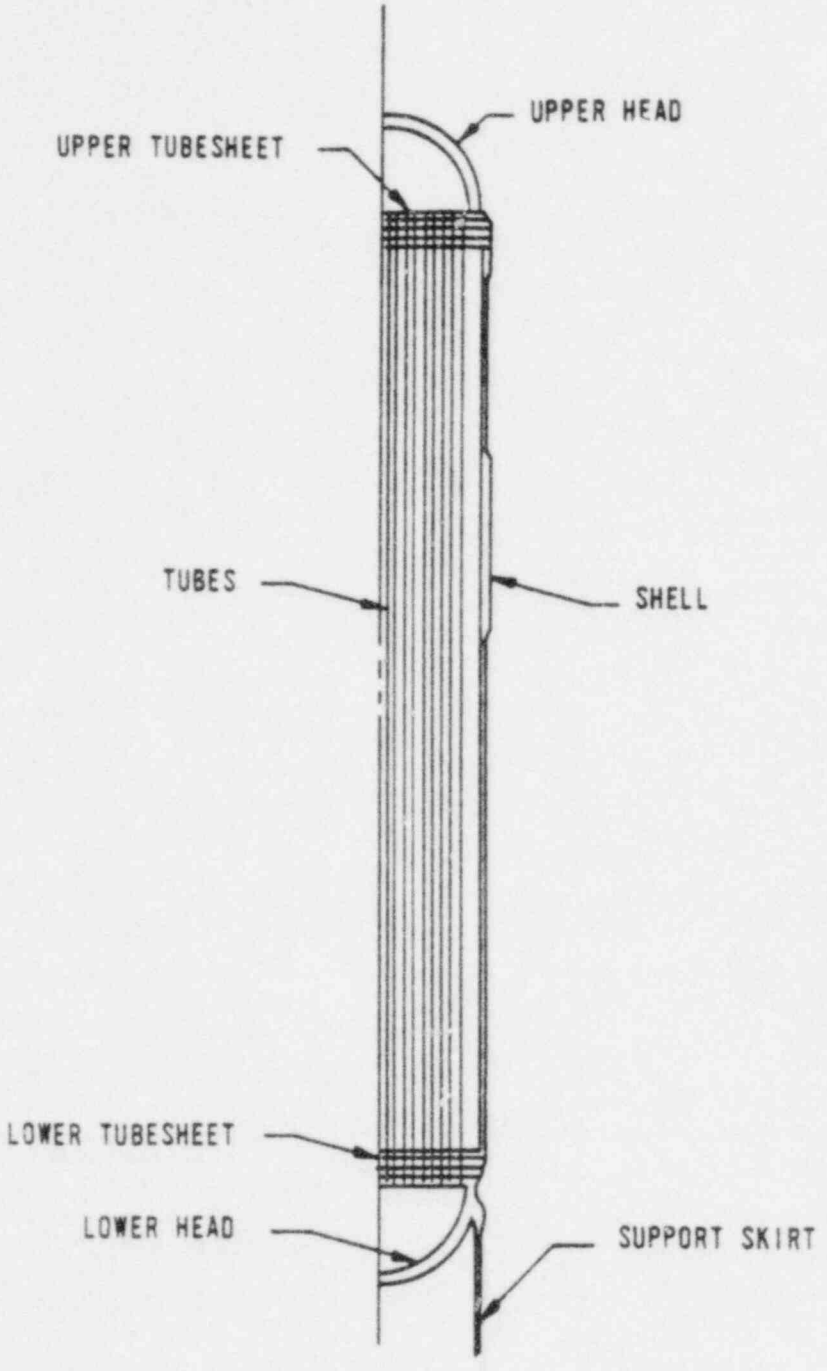

Figure 5-5. Axisymmetric Structural Model of Upper Head and Tubesheet

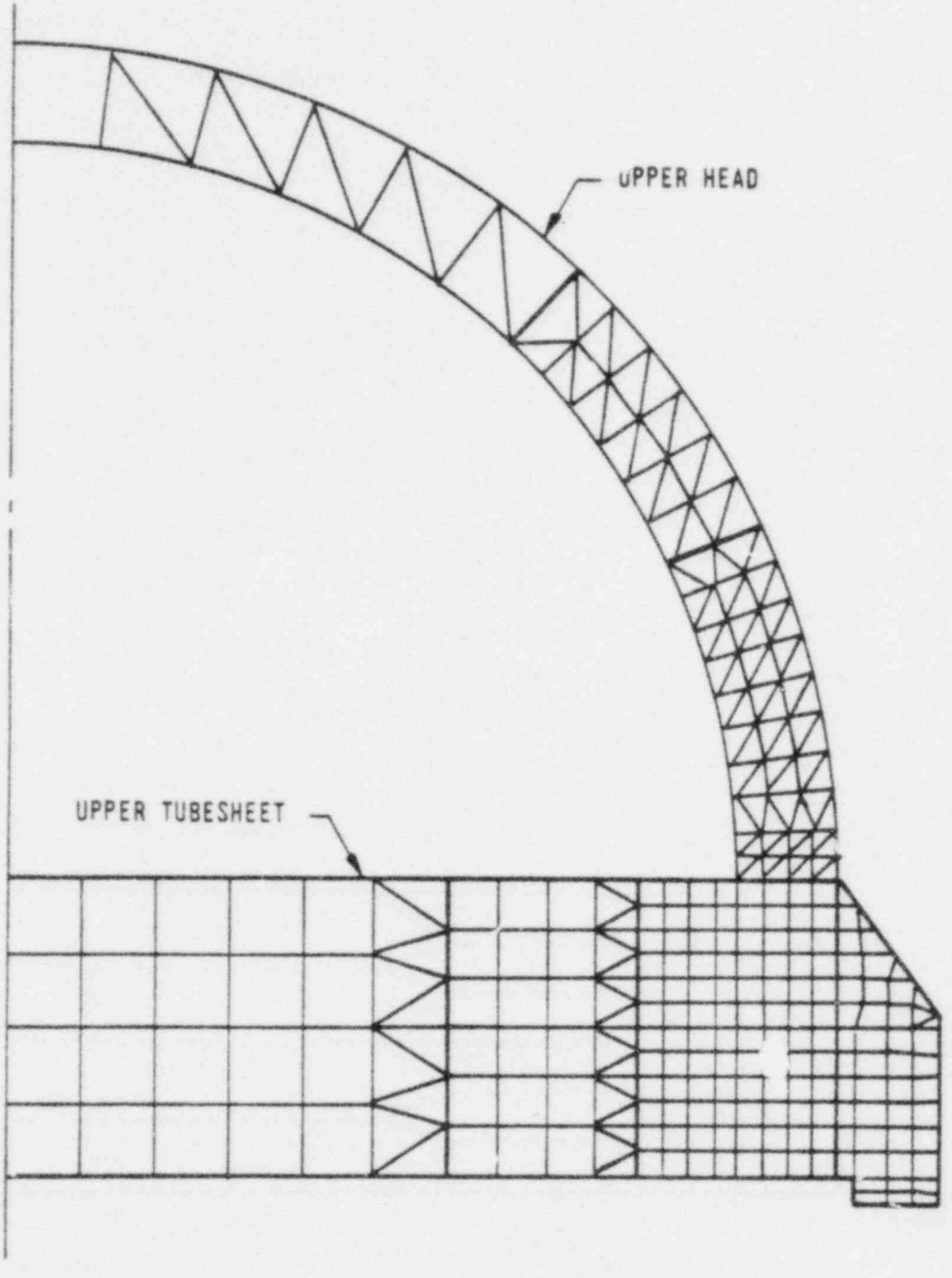

Figure 5-6. Axisymmetric Structural Model of Rod Elements for Tubes

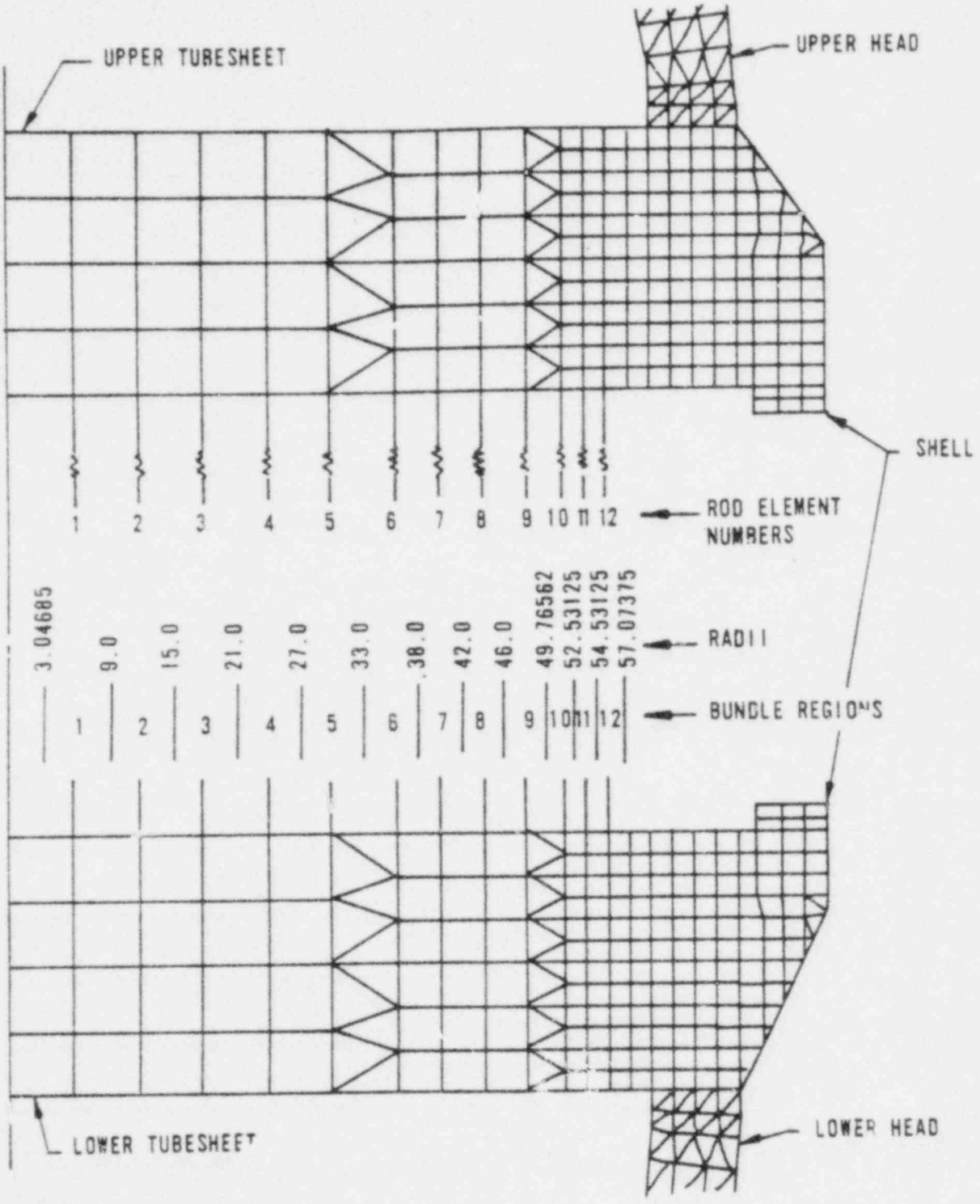

Figure 5-7. Heatup to 15% Power, Transient 1A

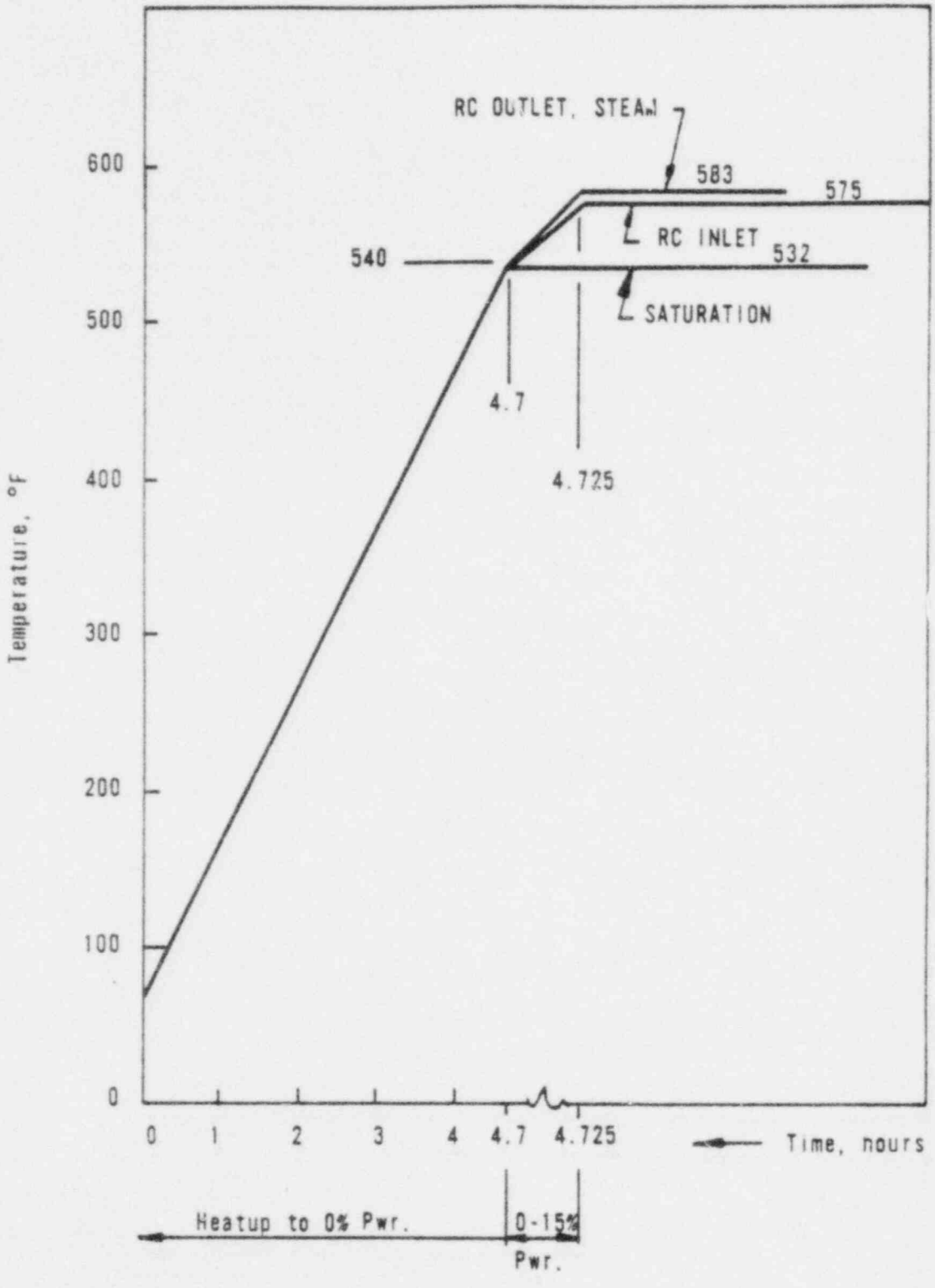

Figure 5-8. Cooldown From 15% Power, Transient 1B

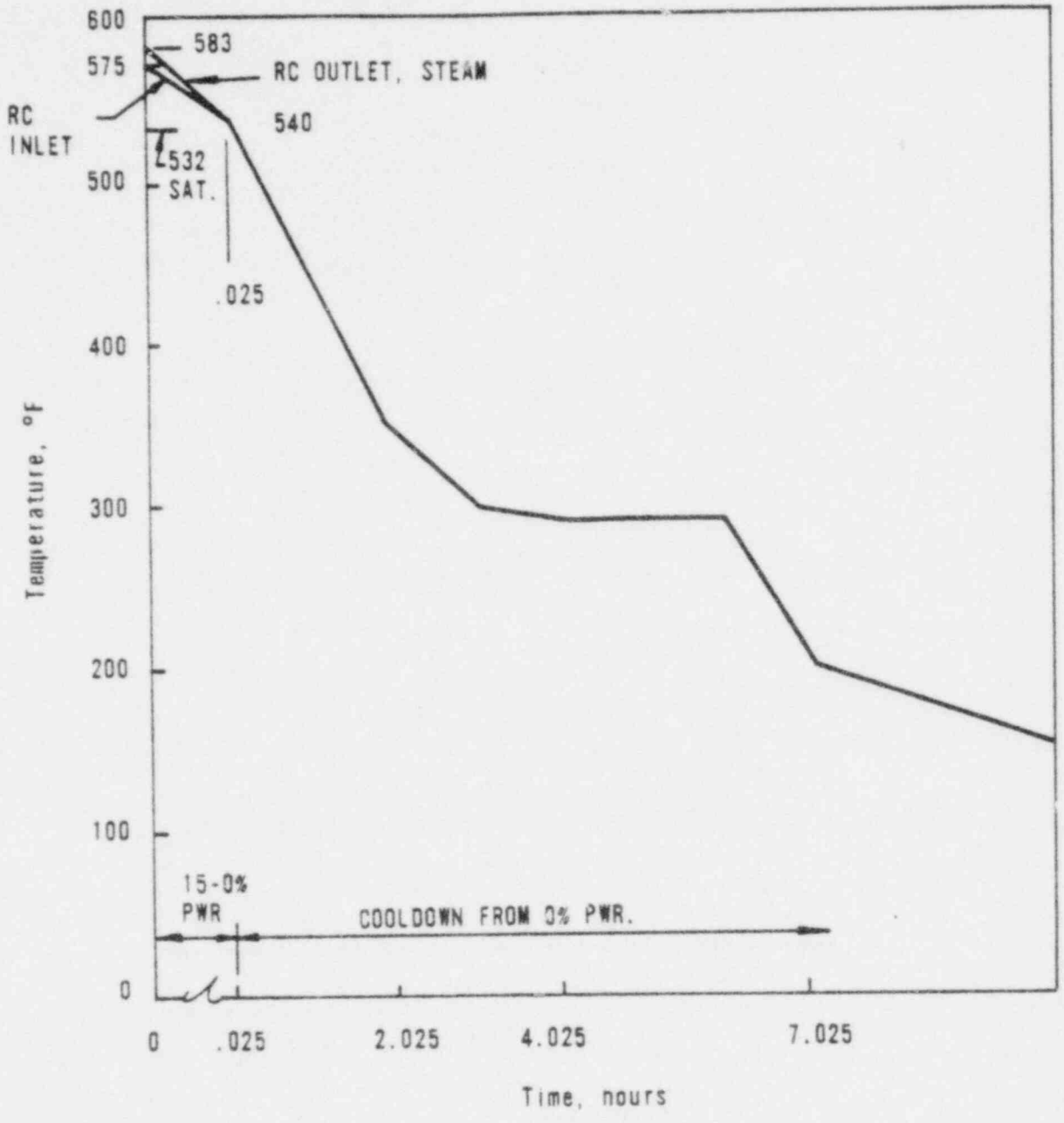

Figure 5-9. Power Change: 0 to 15% and 15 to 0% Transient 2

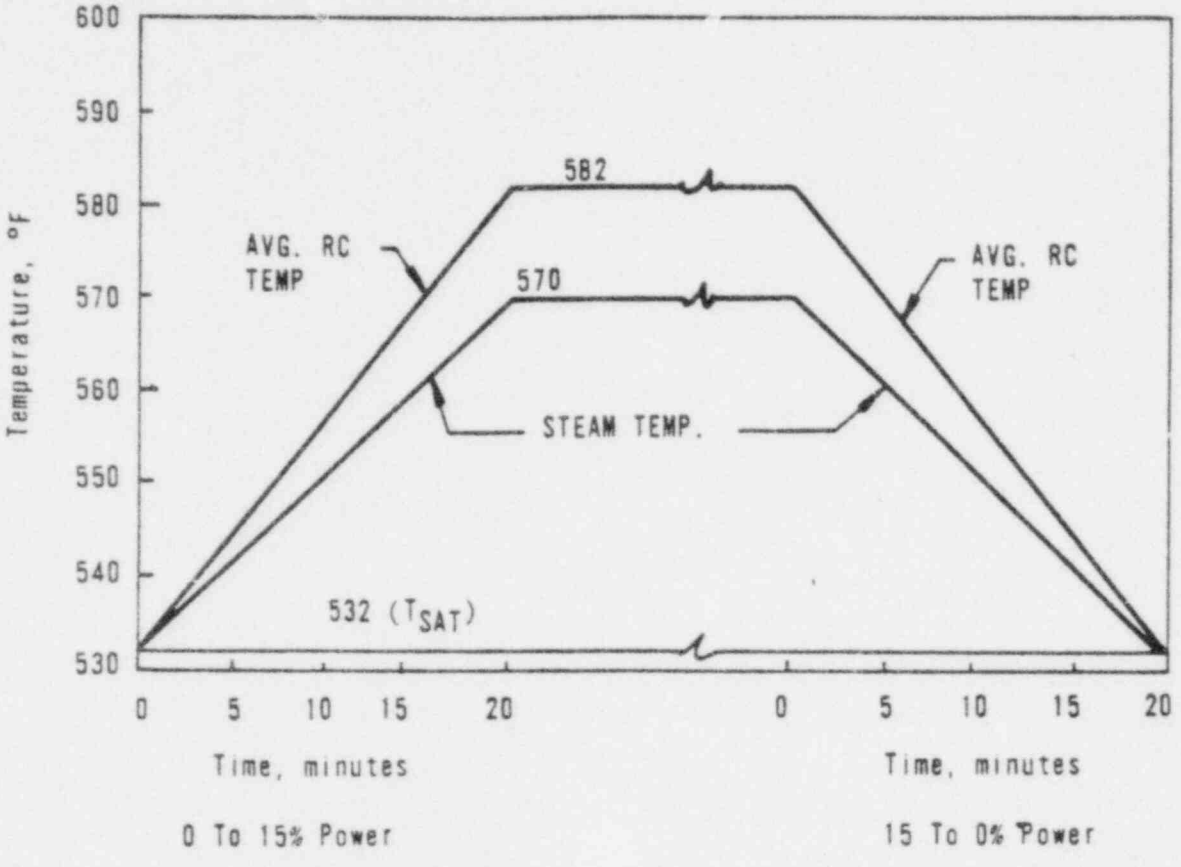

Figure 5-10. Plant Loading: 8 to 100% Power, Transient 3

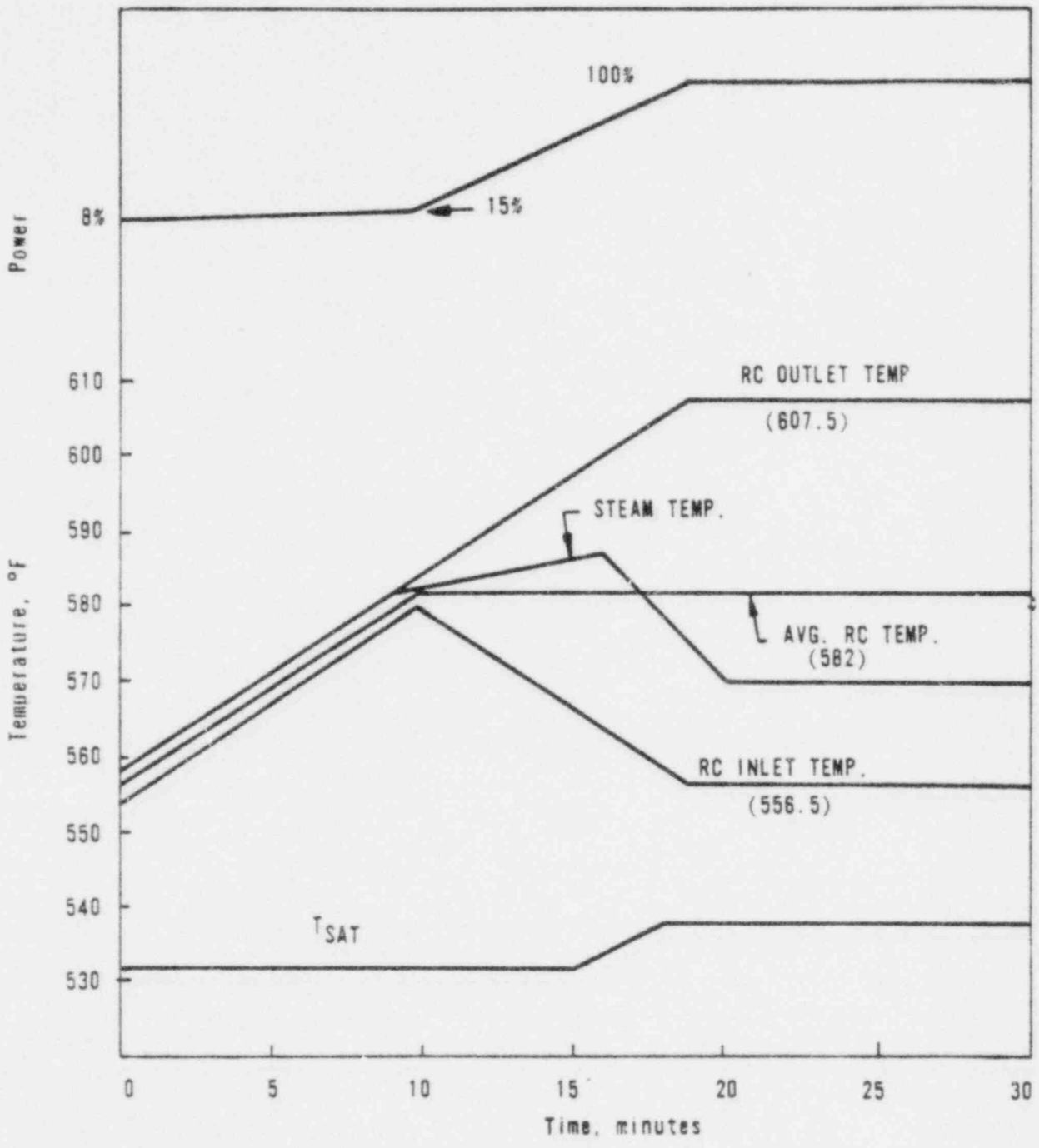

Figure 5-11. Plant Unloading: 100 to 8% Power, Transient 4

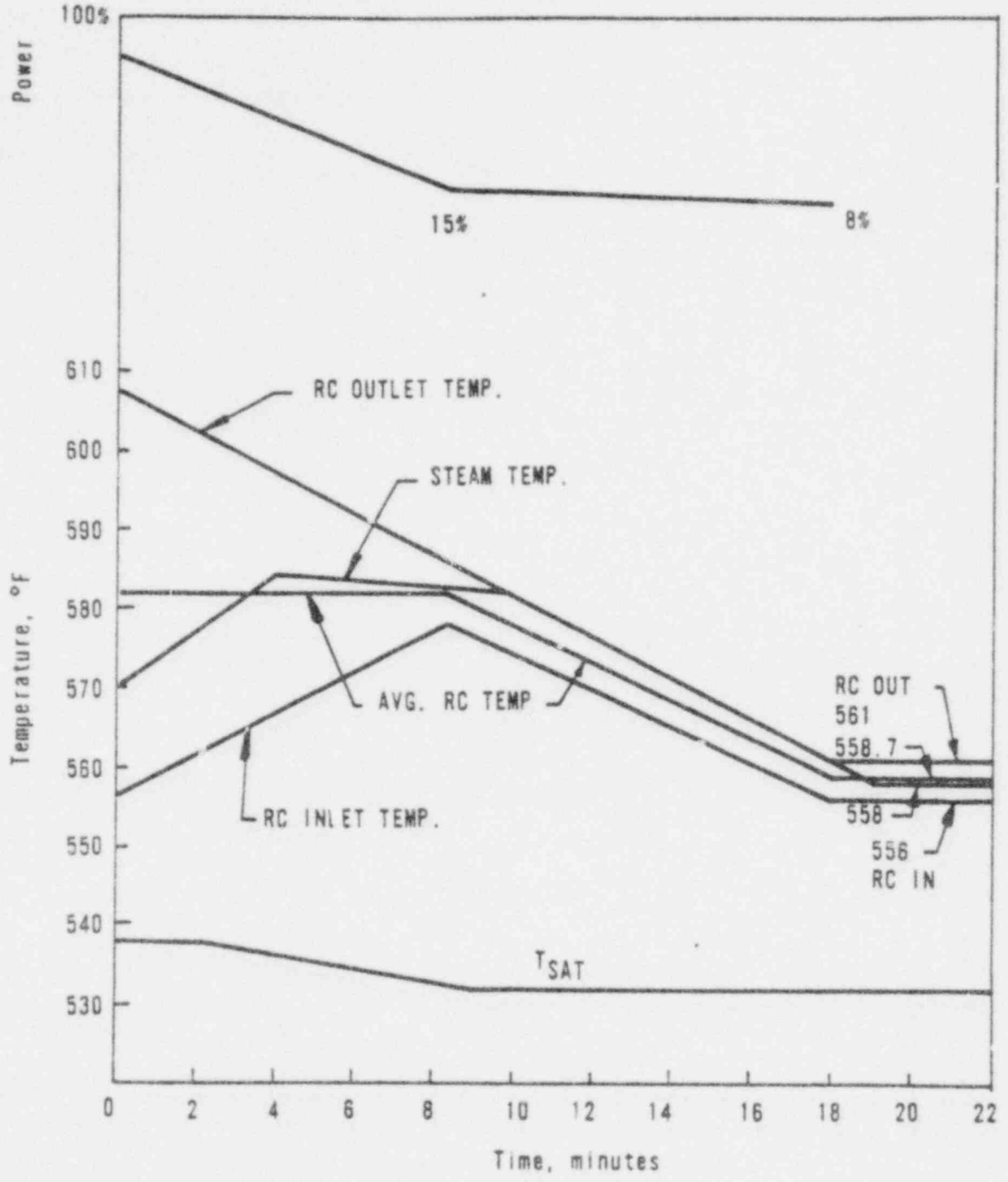

6. MINIMUM ACCEPTABLE TUBE WALL THICKNESS

This section describes the calculations performed to determine the minimum acceptable wall thickness for degraded tubes. The acceptance criteria of NRC draft Regulatory Guide 1.121[8] and the ASME Boiler and Pressure Vessel Code[11] were used to establish allowable stress and pressure limits. The actual stress or pressure applicable to each of these categories was computed as a function of wall thickness and compared to the proper limit. The objective was to determine which category was limiting and the wall thickness comparable to this limit.

The analysis uses the pressures and loads of section 5, OTSG tube failure tests results reported in references 13 through 16, statistically determined nominal tube wall thickness, and the dimensions of defects found in operating OTSGs.

6.1. Defect Types

B&W has identified four types of OD tube damage that have more than superficial wall thinning associated with them.

1. Circumferential cracks in lane tubes at the upper tubesheet (UTS) and 15th tube support plate (TSP).
2. Localized metal removal (commonly referred to as erosion/corrosion) primarily at the 14th TSP but also at other TSP locations in the upper half of the OTSG.
3. Localized wear in lane tubes at the 15th TSP caused by tube/TSP contact.
4. Manufacturing defects not related to operating service.

Types 1, 2, and 3 have been detected at some but not all of B&W's operating plants. Circumferential cracks at the UTS and 15th TSP have been found only in lane tubes at the ANO-1 and Oconee sites. Wear at the 15th TSP has been reported only in lane tubes at Rancho Seco, TMI-1, and Oconee. The 14th TSP

erosion/corrosion defects have been isolated to the Oconee I generators. Manufacturing defects have been confirmed in the TMI-2 OTSGs. Indications between TSPs have been reported in other units and are thought to be manufacturing defects.

All failures due to circumferential cracking have been confined to lane tubes. Destructive examinations of tube samples from the Oconee plants have revealed that circumferential cracks develop on the tube OD, proceed through the wall, and then propagate symmetrically around the tube. These examinations further indicated that after through-wall crack development, the circumferential crack propagation was due to low-stress, high-cycle fatigue. No tubes with partial through-wall cracks extending more than 45° around the circumference have been removed from operating plants. All those examined had either micro-cracking or a complete through-wall crack that had propagated around the circumference.

Laboratory examinations of three tubes from Oconee 1 have revealed 14th TSP tube erosion/corrosion type defects. Damaged areas are enveloped by an area approximately 0.75 inch high and 45° circumferentially around the tube. Wear marks all have the approximate dimensions of TSP land areas, 1.5 inches high and 22° around the circumference. These two types of defects will be considered together as covering an assumed bounding area 1.5 inches high and 45° around the circumference.

Various shapes and sizes of manufacturing defects have been discovered. These include tube mill "scab" defects and shallow "grind" marks. Since all reported defects of this type have been smaller than the envelope assumed in the preceding paragraph, manufacturing defects will be included as part of the assumed envelope for analysis purposes. However, these defects are inherently of a different nature than the actively growing defects. They can be characterized from eddy-current data as relatively small, with no similar defects in the area, not at a location examined previously and found to be "clean," and away from support plates and known areas of tube degradation. B&W tests on a typical pit-like defect show that a 90% through-wall defect could withstand 9,500 psi or about 3.5 times the greatest expected pressure. It is judged that these indications can be safely excluded from normal Technical Specification requirements and that a 69% plugging criteria is conservatively applicable to this type of indication.

6.2. Minimum Wall Thickness for Normal Operation

Minimum acceptable wall thicknesses for degraded OTSG tubes that satisfy the criteria of draft Ref. Guide 1.121[8] will be determined.

6.2.1. Primary Membrane Stress

Paragraph C.3.a(1) of the draft Regulatory Guide states that the primary membrane stress intensity may not exceed the yield stress of the tube material at operating temperature ($P_m \leq S_y$).

The worst-case normal operating conditions are as follows:

Primary temperature, F	600	Transient 2A*
Primary pressure, psi	2250	
Secondary pressure, psi	900	

Letting Δp = primary to secondary pressure differential, 1350 psi,

p = primary plus secondary pressure, 3150 psi,

R = inside radius, 0.275 in.,

S_y = yield strength at 600F using a 95 × 95 confidence level from material test data[8], 34,224 psi,

the minimum wall thickness is

$$t_{min} = \frac{\Delta p R}{S_y - 0.5p} = 0.0114 \text{ inches.}$$

This corresponds to a 70% defect in a tube with a wall thickness of 37.5 mils.

6.2.2. Burst Pressure

Paragraph C.2.a(4) of draft Reg. Guide 1.121[8] states that the margin of safety against tube rupture under normal operating conditions should not be less than three ($p_b \geq 3\Delta p = 4050$ psi). B&W has obtained burst pressures for 0.628 OD × 0.038-inch-wall test specimens. In addition, the Batelle Pacific Northwest Laboratories (PNL) has tested 0.625 OD × 0.034-inch-wall test specimens under burst conditions. The results are reported in references 13 and 15, respectively. The types of defects described in section 6.1 correspond most closely to the

---

*From Table 5-7; see Figure 5-1 for description of transient.

flat spot defect in the B&W tests and the elliptical wastage defects in the PNL tests. Therefore, these types of defects in the respective test reports will be used to establish the burst pressure limit.

From reference 13, the B&W test specimens burst pressures were above 4050 psi for 70% wall thinning. For tubing 0.038 inch thick the remaining wall thickness for 70% thinning is 0.0114 inch. This also corresponds to 70% thinning for 0.0375-inch-thick tubing. From reference 15, a burst pressure of 4780 psi corresponds to a remaining wall thickness of 0.0133 inch, while a burst pressure of 2390 psi corresponds to a remaining wall thickness of 0.0034 inch. Interpolating these data, a wall thickness of 0.0103 inches is allowable for 4050 psi. This is equivalent to a 73% defect in a 0.0375-inch-thick tube. Figure 6-1 presents the results of the burst tests graphically; the B&W and PNL data show good correlation.

6.2.3. Fatigue Analysis

Paragraph C.3.b (2) of draft Reg. Guide 1.121[8] states that fatigue effects of cyclic loading forces are to be considered in determining the minimum wall thickness. Cyclic loads on a tube have been determined in section 5.2 for normal operation. The number of cycles to be considered is based on a maximum expected inservice inspection interval of 2 years. It will be shown that tube alternating stresses for the non-crack defects described in section 6.1 extending 79% through the tube wall satisfy the fatigue requirements of reference 11.

The primary plus secondary stress intensity range is calculated in Table 6-1 for a 79% defect. The maximum range, 83, 909 psi, is less than the $3S_m$ limit of 85,986 psi. In preparation for the fatigue analysis, the transients of Table 5-1 were reviewed and conservatively combined as shown in Table 6-2. Table 6-3 presents calculations of the cumulative usage factor for fatigue. Assuming a strength reduction factor of 5, the usage factor of 0.097 is far below the reference 11 allowable value of 1.0. (Reg Guide 1.83 may allow an inspection interval of up to 40 months. The calculated usage factor of 0.097 for a 24-month interval indicates that the fatigue requirement would also be satisfied for a 40-month interval.)

Laboratory examinations of lane tube samples from the Oconee plants have revealed that circumferential cracks develop on the tube OD, proceed through the

wall, and then propagate symmetrically around the tube. These examinations further indicated that after through-wall crack development the circumferential crack propagation was due to low-stress, high-cycle fatigue. The most propable high-cycle fatigue mechanism is flow-induced vibration (FIV). If a crack large enough for FIV propagation should occur, a primary-to-secondary leak would probably develop rather quickly. Therefore, any lane tube with a detectable circumferential crack in the upper span should be removed from service.

6.3. Minimum Wall Thicknesses for Faulted Conditions

The acceptance criteria of paragraph C.3.a(3) of draft Reg. Guide 1.121[8] will be used to establish minimum wall thicknesses for postulated accident conditions. In addition, an independent acceptance criterion will be developed to consider faulted condition thermal stresses not addressed in Appendix F of reference 11.

6.3.1. Primary Membrane Stress

The primary membrane stress intensity is limited to the lesser of $2.4S_m$ or $0.7S_u$. Using 95 × 95 confidence level statistics for OTSG tube material, S_m = 28,662 psi and S_u = 92,923.[17] Therefore, the limiting stress allowable is $0.7S_u$ = 65,046 psi. The worst-case accident conditions for primary membrane stress occur for an FWLB at 40 seconds into the transient (Δp = 2672 psi). For a pressure differential of 2672 psi, the operating conditions are 2696 psi primary pressure and 24 psi secondary pressure. Then

p = primary plus secondary pressure, 2720 psi,

R = inside radius, 0.275 in.,

and the minimum wall thickness is

$$t_{min} = \frac{\Delta pR}{0.7S - 0.5p}$$

$$= 0.0115 \text{ in.}$$

This represents 31% of a tube 0.0375 inch thick, so a 69% through-wall defect would be acceptable.

6.3.2. Burst Pressure

Draft Reg. Guide 1.121[8] states that the ultimate burst strength should not be exceeded by any accident condition pressure loading ($p_b \geq \Delta p = 2672$ for an FWLBA). B&W tests showed that 70% thinning could withstand 4050 psi burst pressure (see section 6.2.2). From reference 15, the PNL data for the elliptical wastage defects in an 0.034-inch-wall tube indicate the burst pressure to be 4780 psi for a 0.0133-inch wall and 2390 psi for a 0.0034-inch wall. Interpolating, an 88% through-wall defect is allowable for a 0.0375-inch tube.

6.3.3. Collapse Pressure

Reference 11 states that during a LOCA where there is external pressure loading on the tube, the pressure differential must not exceed 90% of the collapse pressure ($0.9p_c \geq \Delta p = 925$ psi). Collapse pressures have been obtained by B&W for 0.628 OD × 0.038-inch wall test specimens. In addition, PNL has tested 0.625 OD × 0.034-inch wall test specimens under collapse conditions. From Table 4 of reference 14, a collapse pressure of 2000 psi can be withstood by a 0.038-inch tube with 70% thinning, which is equivalent to 70% thinning in a 0.0375-inch wall tube. Preliminary PNL data[16] indicate a 0.625 × 0.034-inch wall tube with an 85.4% defect could withstand a 1980 psi collapse pressure.

6.3.4. Primary Membrane Plus Bending Stresses

From comparison of the OTSG tube loads for faulted conditions (see Table 5-7), it is concluded that the maximum loads occur during FWLB & SSE accident conditions. The maximum primary pressure of 2696 psi and maximum axial mechanical tube load of 601 rounds are assumed to occur simultaneously. This assumption results in conservative stresses. It will be shown that a tube with 79% thinning will satisfy the primary membrane plus bending acceptance criterion ($P_m + P_b < 3.6S_m$). The loadings to be considered are as follows:

Primary pressure = 2,696 psi.

Secondary pressure = 24 psi.

Primary-to-secondary pressure differential Δp = 2672 psi.

"Initial condition" axial tube load from pressure and preload = 419 lb.

FWLB&SSE axial tube load = 664 lb.

FWLB&SSE bending moment = 18 in-lb.

Tube stresses for a 79% through-wall defect are:

$$\text{Axial} = \frac{F}{A} + (\bar{y} - \bar{y}p)\frac{C}{I} = 24,527 \text{ psi.}$$

$$\text{Hoop} = \frac{\Delta pR}{t} = 93,308 \text{ psi}$$

Radial = -0.5 (primary + secondary pressure) = -1360 psi.

The maximum stress intensity is 94, 668 psi < $3.6S_m$ = 103,183 psi.

6.3.5. Primary Plus Thermal Stresses

Draft Reg. Guide 1.121[8] states that pressure and thermal loads must be considered in determining tube plugging limits for postulated accident conditions. It further states that these loads be accommodated within the faulted condition stress limits of Appendix F to the ASME Code.[11] Appendix F prescribes stress limits only for primary stresses; general thermal stresses, the type imposed on an OTSG tube due to end constraints and considered herein, are defined by reference 11 [paragraph NB-3213.13(a)] as secondary stresses and thus do not lend themselves to scrutiny under the rules for faulted conditions. Indeed, reference 11 states (paragraph NB-3213.9) that one application of a secondary stress is not expected to cause failure.

To account for these thermal loads, tube defect limits were based on B&W tensile tests[11] in which tube specimens with machined defects are pulled to failure by tensile fracture. The following has been extracted from Table 4 of reference 11 and is limiting for the defects described in section 6.1.

Defect geometry	Percent thinning 0.038-in. wall	Ultimate tensile force, lb
Flat spot 0.75-inch long	70	6320

Before comparing the limit to the calculated axial load, it should be adjusted to account for the effects of internal pressure. From Table 3 of reference 13, 5000 psi will be used as the burst pressure for 70% through-wall defects of the types described in section 6.1. The effects of external pressure need not be considered since they would only tend to increase the ultimate tube load at fracture.

In order to analytically combine the results of the separate burst and tensile tests, an elliptical failure curve is assumed:

$$\left(\frac{\Delta p}{P_b}\right)^2 + \left(\frac{P_{ax}}{P_u}\right)^2 \leq 1$$

where

Δp = primary to secondary pressure differential (from Table 5-7),

P_b = burst pressure,

P_{ax} = calculated tube axial load (from Table 5-7),

P_u = ultimate tensile load.

Applying this acceptance criterion to tubes with thinning extending 70% through the wall:

For a MSLB,

$$\left(\frac{2500}{5000}\right)^2 + \left(\frac{3140}{6320}\right)^2 = 0.50 < 1.0.$$

For a LOCA,

2641 lb < 6320 lb.

Acceptable wall thinning for primary plus thermal stresses is therefore greater than 70%. Using the PNL burst data, a wall thinning of 85% could be justified.

6.4. Limiting Tube Wall Thickness

Minimum wall thicknesses have been calculated for normal operation and faulted conditions considering a total of eight different acceptance criteria. The minimum wall thickness for the type defects described in section 6.1 other than tubes with cracks in the upper span is 0.01156 inch, or 31% of the original tube wall; it comes from limiting the accident condition primary membrane stresses during a feedwater line break (FWLB) to 0.7 of the ultimate stress of the material.

As a means of summarizing the results of the minimum wall thickness calculations, Table 6-4 lists minimum allowable wall thicknesses and allowable depths for which the defects described in section 6.1 satisfy the various acceptance criteria. These depths do not include allowances for defect growth rate or inspection technique inaccuracies.

Defect depths will therefore be limited to 69% of the tube wall. Furthermore, any lane tube with a detectable circumferential crack in the upper span should be removed from service as discussed in sections 6.1 and 6.2.3.

Table 6-1. Primary Plus Secondary Stress Intensity Range Based on 79% Through-Wall Defect

Transient No.	P	Δp	σ_1	σ_2	S_{12}
1A	-775	1300	-15,859	45,397	-61,256
1B	1107	0	22,653	0	22,653
2A	-525	1350	-10,743	47,143	-57,886
2B	143	1300	2,926	45,397	-42,471
3	-419	1340	-8,574	46,794	-55,368
4	-100	1300	-2,046	45,397	-47,443
Range					83,909

P = tube load from Table 4-1 for outermost tube, lb

Δp = pressure differential from Table 4-1, psi

σ_1 = axial stress, $P/A - \bar{y}Pc/I$, psi

σ_2 = hoop stress, $\Delta p\ R/t$ psi

S_{12} = stress intensity $(\sigma_1 - \sigma_2)$, psi

Table 6-2. Transients Used in Fatigue Analysis

Transient groups	No. of occurrences	Transients used	Cycles in 40 yr	Cycles in 2 yr	S_{12} stress differences
1A	240	1A	330	17	-61,256
1B	240	1B	350	18	22,653
2A	1,440	2A	1,510	76	-57,886
2B	1,440	2B	1,480	74	-42,471
3	48,000	3	56,070	2,804	-55,368
4	48,000	4	56,598	2,830	-47,443
5	8,000	3	--	--	--
5	8,000	4	--	--	--
7	310	4	--	--	--
8	288	4	--	--	--
9	40	1B	--	--	--
1A	40	1A	--	--	--
11	40	1B	--	--	--
2A	30	2A	--	--	--
1A	10	1A	--	--	--
14	40	2B	--	--	--
3	40	3	--	--	--
15	40	1A	--	--	--
4	40	2A	--	--	--
17A, B	30	1B	--	--	--
3	30	3	--	--	--

Table 6-3. Calculation of Fatigue Usage Factor Based on 79% Through-Wall Defect

Stress cycle	n	S_{12} stress differences		S_{alt} [a]	N [b]	n/N
		Maximum	Minimum			
1	17	22,653	-61,256	186,781	190	0.0895
2	1	22,653	-57,886	179,280	220	0.0045
3	74	-42,471	-57,886	34,314	2.2×10^5	0.0003
4	1	-47,443	-57,886	23,240	$>10^6$	0.0
5	2804	-47,443	-55,368	17,641	$>10^6$	0.0028
6	12.5	-47,443	-47,443	0	∞	0.0
					Usage =	0.097

(a) $S_{alt} = \frac{26.0 \times 10^6}{29.2 \times 10^6}(5)(\frac{1}{2})$ (stress difference range).

(b) From Figure I-9.2 of reference 11.

Table 6-4. Allowable Depths for OTSG Defects

Criterion	Minimum thickness, in.	Defect depth, % of wall in 0.0375-in. tube	Critical accident condition
Normal Operation			
$P_m \leq S_y$	0.0114	70	--
$3\Delta p \leq P_b$	0.0103	73	--
$\left\{\begin{array}{l}\Delta(P_m + P_b + Q) \leq 3S_m \\ \text{usage factor} \leq 1.0\end{array}\right\}$	<0.0079	>79	--
Faulted Conditions			
$P_m \leq 2.4S_m,\ 0.7S_u$	0.0116	69	FWLB
$\Delta p \leq P_b$	0.0046	88	FWLB
$\Delta p \leq 0.9P_c$	<0.0050	>85	LOCA
$P_m + P_b \leq 3.6S_m$	<0.0079	>79	FWLB + SSE
Primary Plus Thermal			
$\left(\frac{\Delta p}{P_b}\right)^4 + \left(\frac{P_{ax}}{P_u}\right)^2 \leq 1$	<0.0114	>70	MSLB

Note: Nomenclature not specifically defined in this section is from the ASME Boiler and Pressure Vessel Code.

Figure 6-1. PNL Burst Test Data

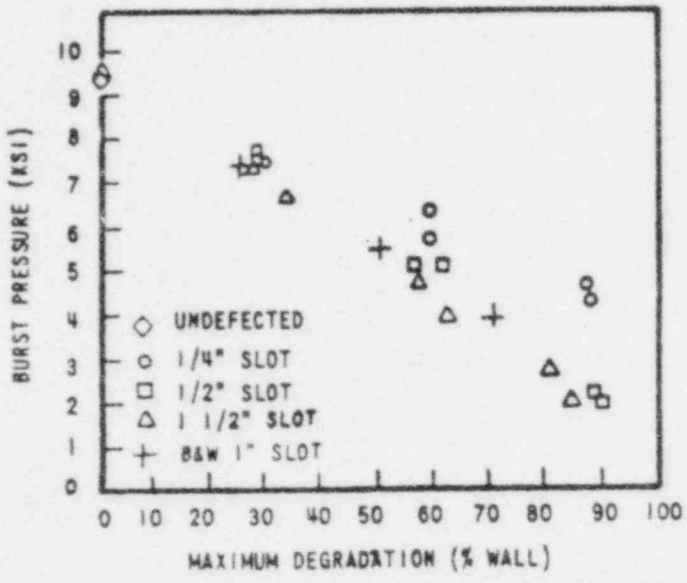

BURST PRESSURES FOR 0.625 x 0.034 IN. EDM SLOTS

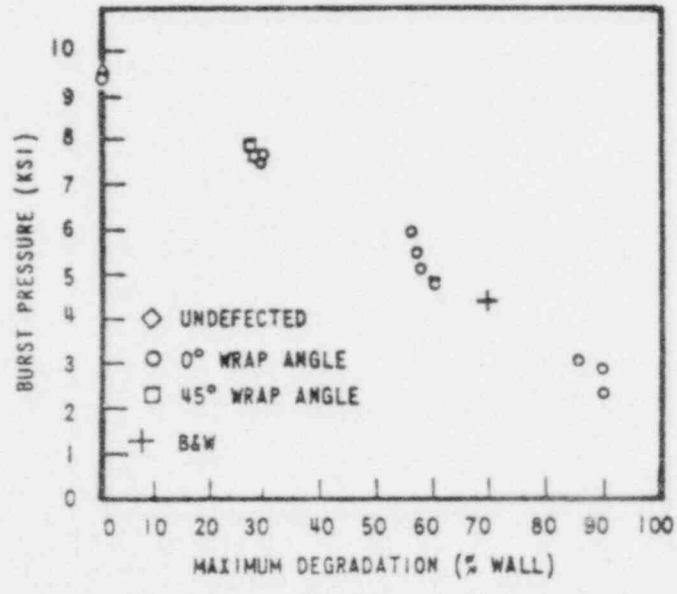

BURST PRESSURES FOR 0.625 x 0.034 IN. ELLIPTICAL WASTAGE

REFERENCES

1 J. J. Cudlin, R. A. Hedrick, and R. C. Foltz, CRAFT2 – Fortran Program for Digital Simulation of a Multinode Reactor Plant During Loss-of-Coolant, BAW-10092, Rev. 2, Babcock & Wilcox, Lynchburg, Virginia, April 1975.

2 F. Aguilar and L. M. Smalec, Analytical Methods Description Reactor Coolant System Hydrodynamic Loadings During a Loss-of-Coolant Accident, BAW-10132, Babcock & Wilcox, Lynchburg, Virginia, November 1977.

3 S. A. Varga (NRC) to J. H. Taylor (B&W), Letter, "Evaluation of BAW-10132P," October 31, 1978.

4 R. C. Jones, J. R. Biller, and B. M. Dunn, ECCS Analysis of B&W's 177-FA Lowered-Loop NSS, BAW-10103A, Rev. 3, Babcock & Wilcox, Lynchburg, Virginia, July 1977.

5 NUREG-75/087, "Standard Review Plan," Section 3.6.2, p. 3.6.2-6.

6 R. A. Brooks and H. Chang, INTFCE, TRG-78-25, Rev. 5, Babcock & Wilcox, Lynchburg, Virginia, June 1977.

7 J. J. Cudlin, TRAP2 – Fortran Program for Digital Simulation of the Transient Behavior of the Once-Through Steam Generator and Associated Reactor Coolant System, BAW-10128, Babcock & Wilcox, Lynchburg, Virginia, August 1976.

8 R.G. 1.121, "Bases for Plugging Degraded PWR Steam Generator Tubes," Draft, U.S. Nuclear Regulatory Commission, August 1976.

9 Reactor Coolant System Structural Loading Analysis, BAW-10131, Babcock & Wilcox, Lynchburg, Virginia, November 1976.

10 B-SAR-205, B&W Standard Safety Analysis Report, Babcock & Wilcox, Lynchburg, Virginia, (Preliminary Design Approval issued May 31, 1978).

11 ASME Boiler and Pressure Vessel Code, Section III, "Nuclear Vessels," 1977 Edition.

12 MSC/NASTRAN User's Manual, March 1976 With Updates, MacNeal-Schwendler Corporation.

13 Letter Report, Rupture Tests of Intentionally Damaged Alloy 600, Alliance Research Center, OTSG Tubing, LR:77:2341-71:1, Babcock & Wilcox, October 4, 1977.

14 Letter Report, Collapse Tests on Intentionally Damaged Alloy 600, Alliance Research Center, OTSG Tubing, LR:76:2341-74:1, Babcock & Wilcox, April 20, 1976.

15 Steam Generator Tube Integrity Program, Battelle Pacific Northwest Laboratories Annual Progress Report January 1 – December 31, 1977, NUREG/CR-0277, PNL-2684.

16 PWR Steam Generator Tube Integrity Program, Battelle Pacific Northwest Laboratories, April 1978 Monthly Progress Report, May 3, 1978.

17 Letter D. F. Levstek to A. G. Ware, Letter, "Mechanical Properties – OTSG Tubing," September 10, 1979.